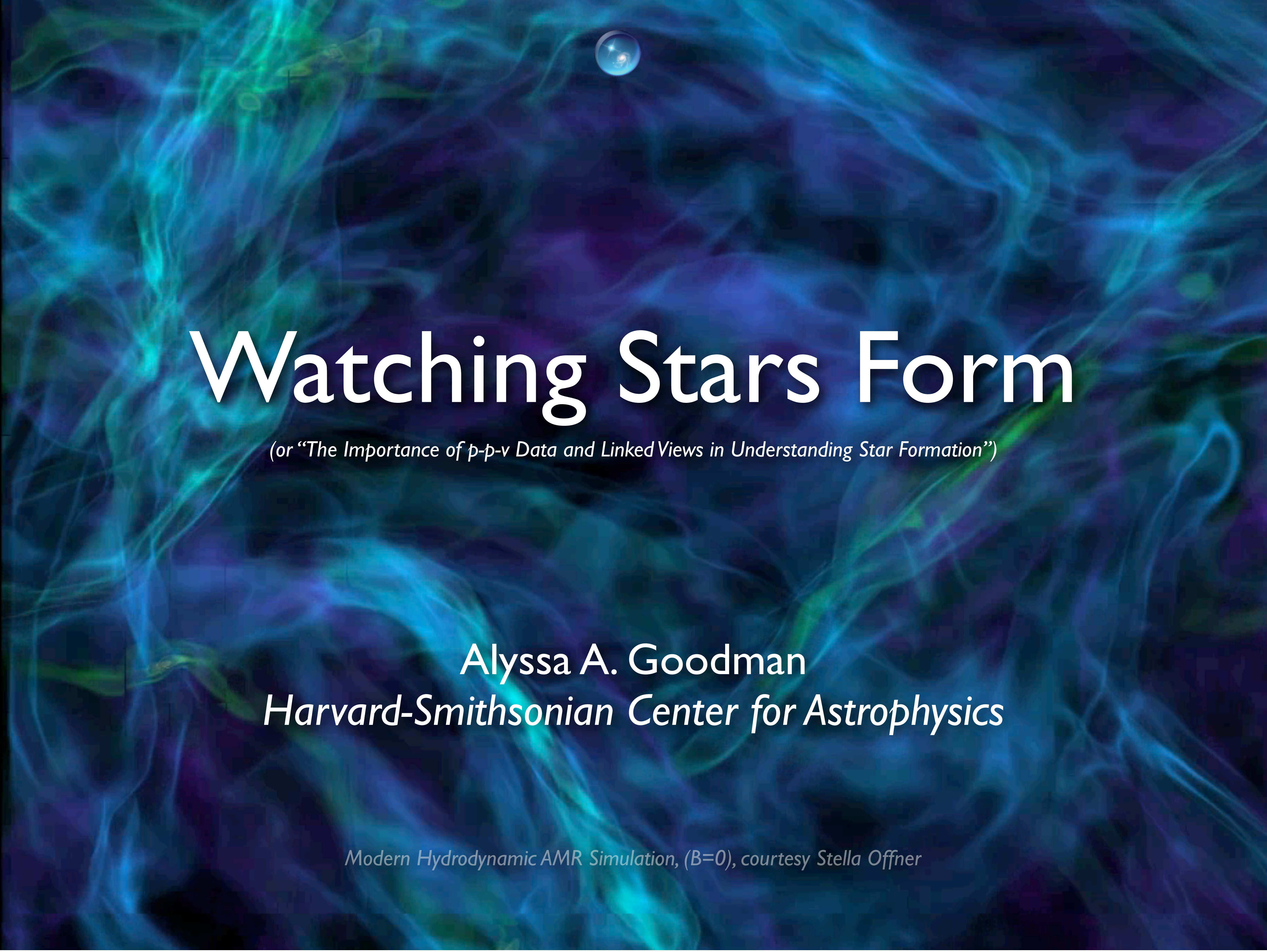

# Watching Stars Form

*(or "The Importance of p-p-v Data and Linked Views in Understanding Star Formation")*

Alyssa A. Goodman
*Harvard-Smithsonian Center for Astrophysics*

*Modern Hydrodynamic AMR Simulation, (B=0), courtesy Stella Offner*


www.flickr.com/photos/66496709@N00/6791649829/in/photostream

# Star Formation 101

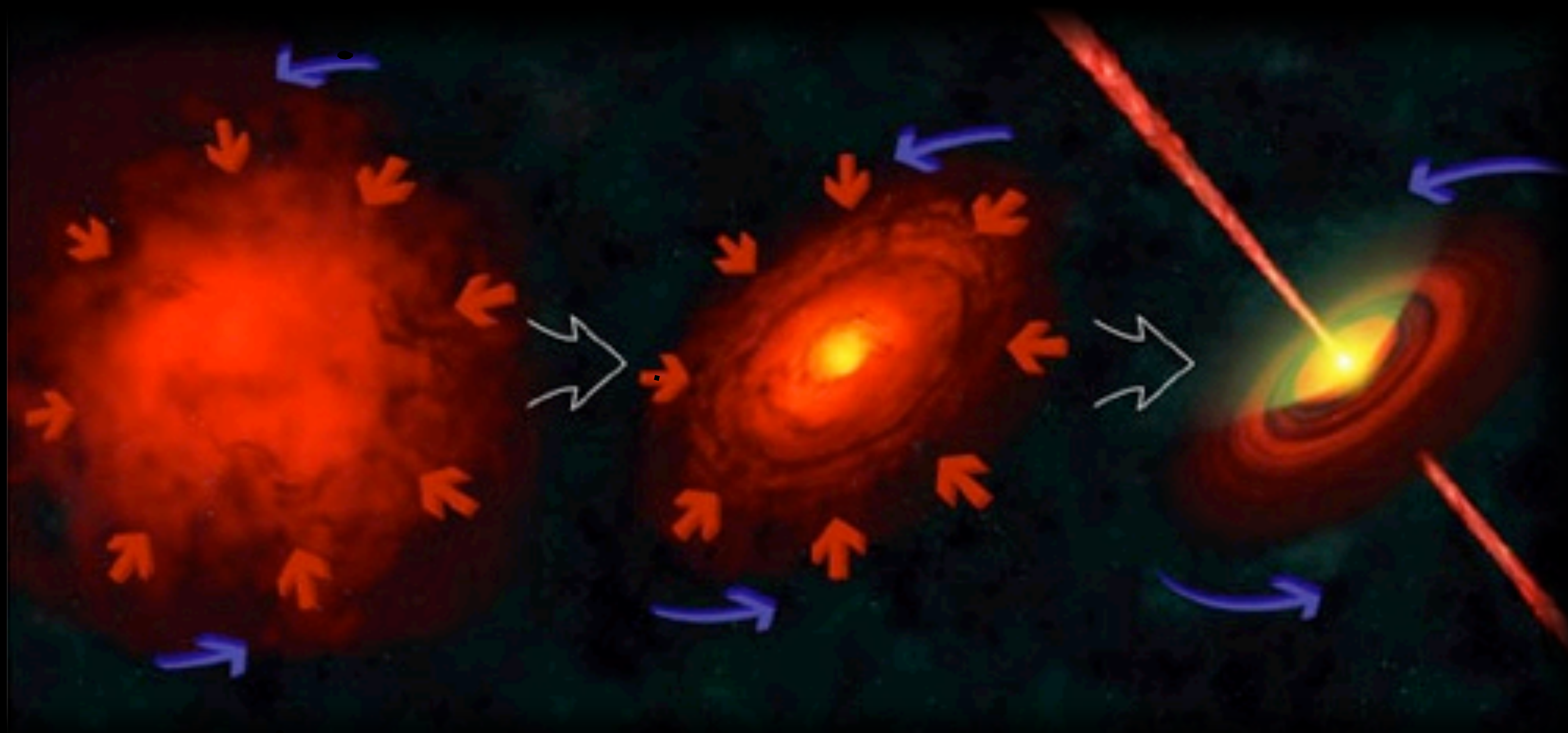

*©Adison-Wesley 2004*

ay201b.wordpress.com/2011/04/12/course-notes/#some_thoughts_on_jeans_scales

# Star Formation 201

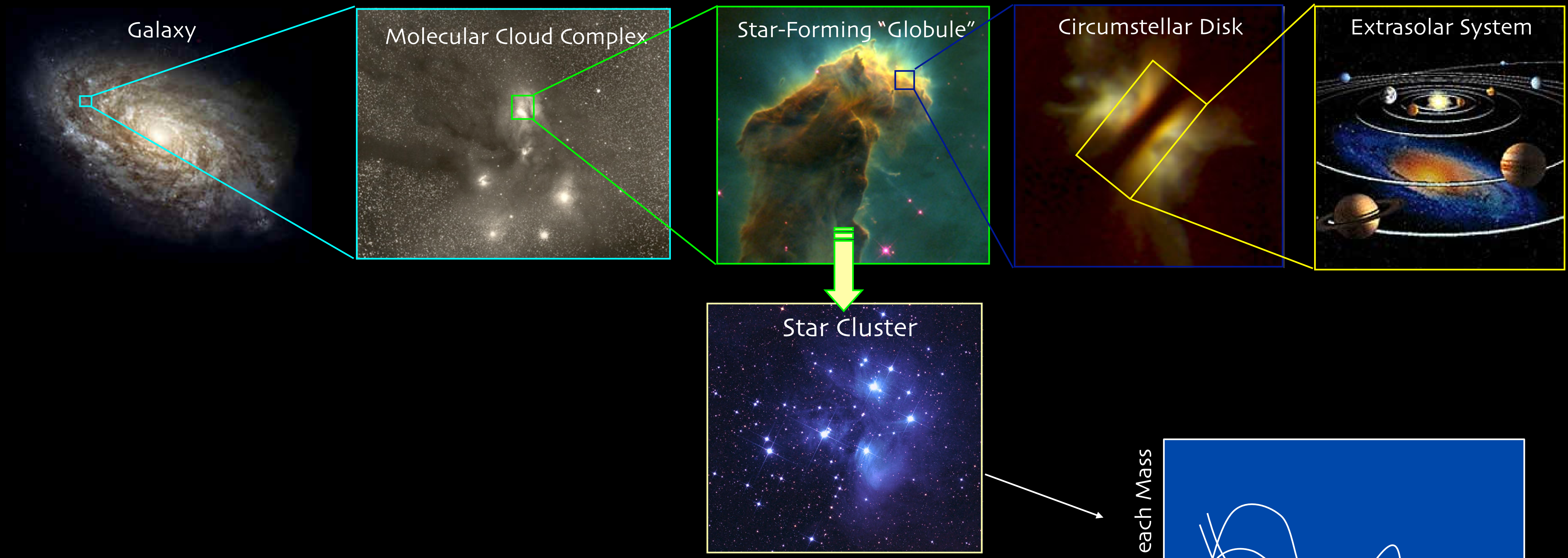


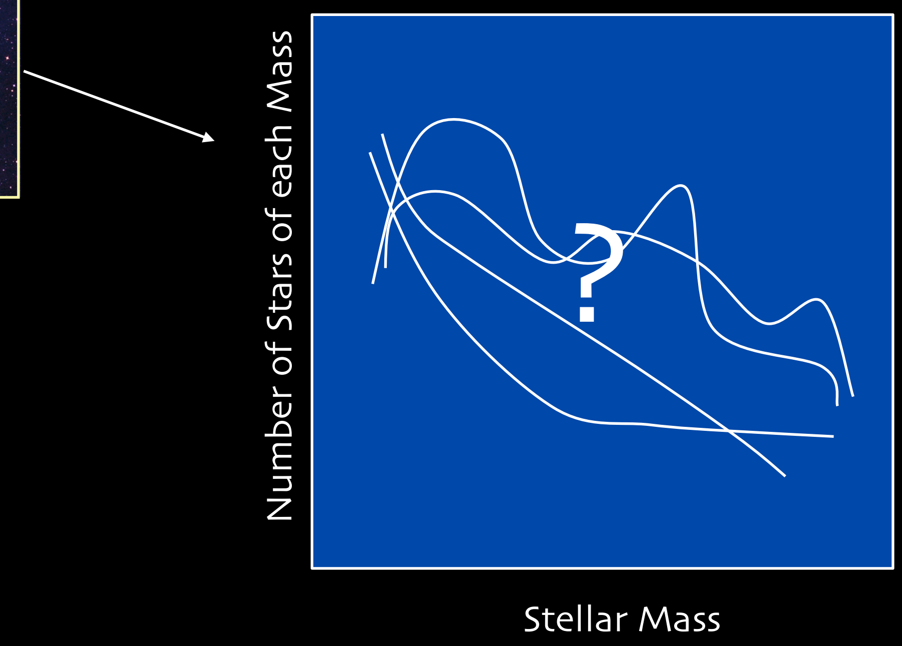

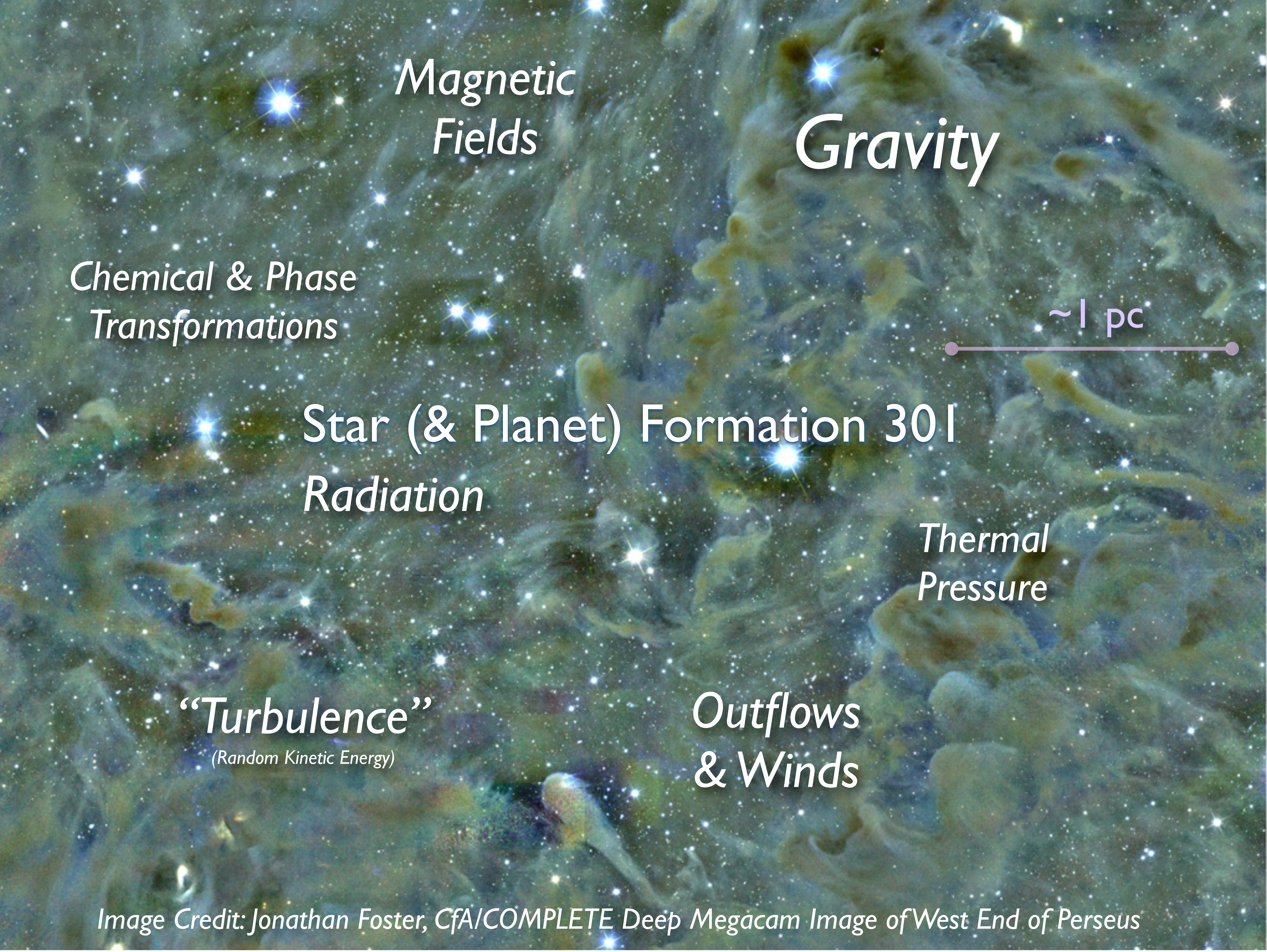
Magnetic Fields
Gravity
Chemical & Phase Transformations
~1 pc
Star (& Planet) Formation 301
Radiation
Thermal Pressure
“Turbulence”
(Random Kinetic Energy)
Outflows & Winds
Image Credit: Jonathan Foster, CfA/COMPLETE Deep Megacam Image of West End of Perseus

# What forces matter most on what scales?

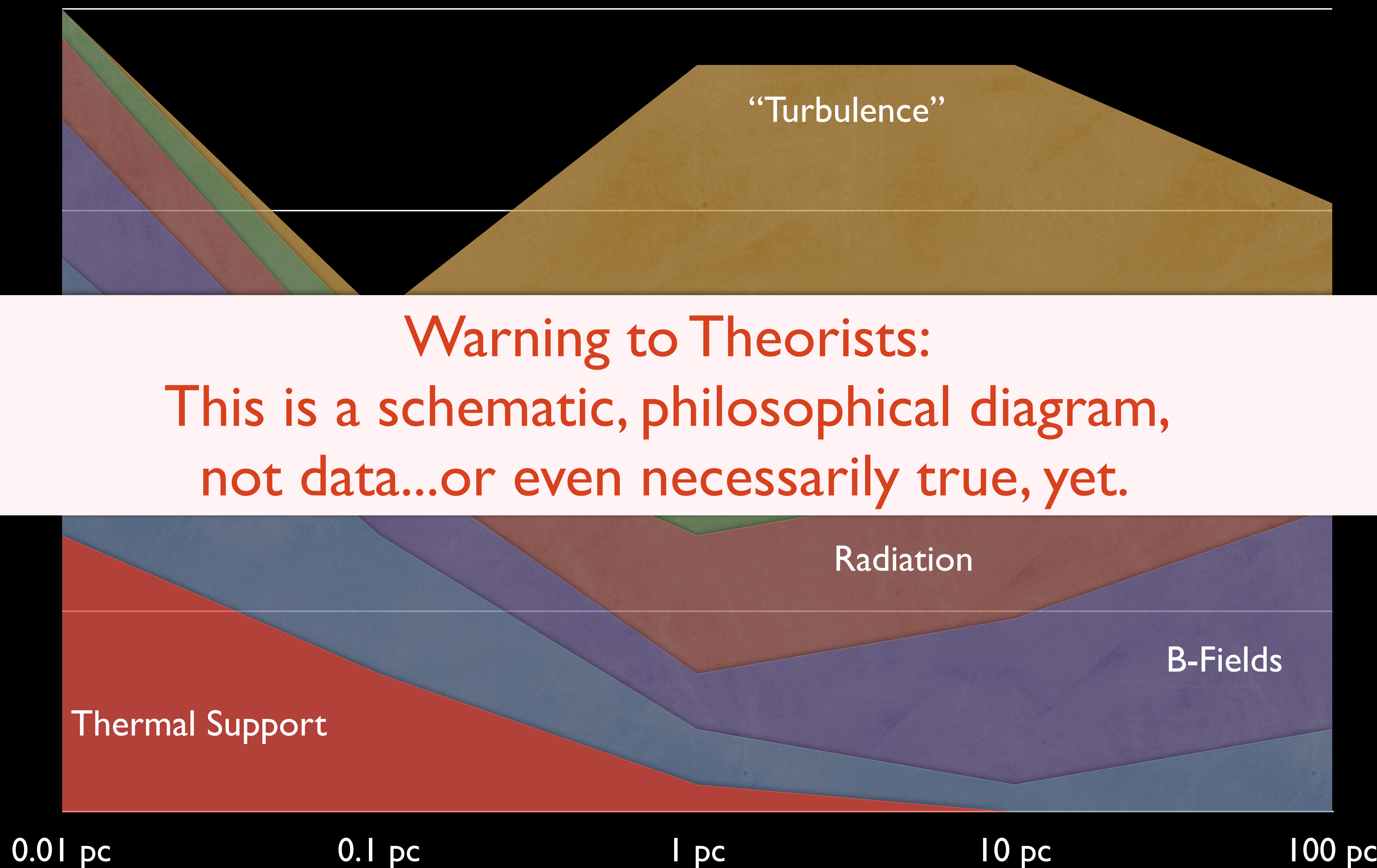


Warning to Theorists:
This is a schematic, philosophical diagram, not data...or even necessarily true, yet.

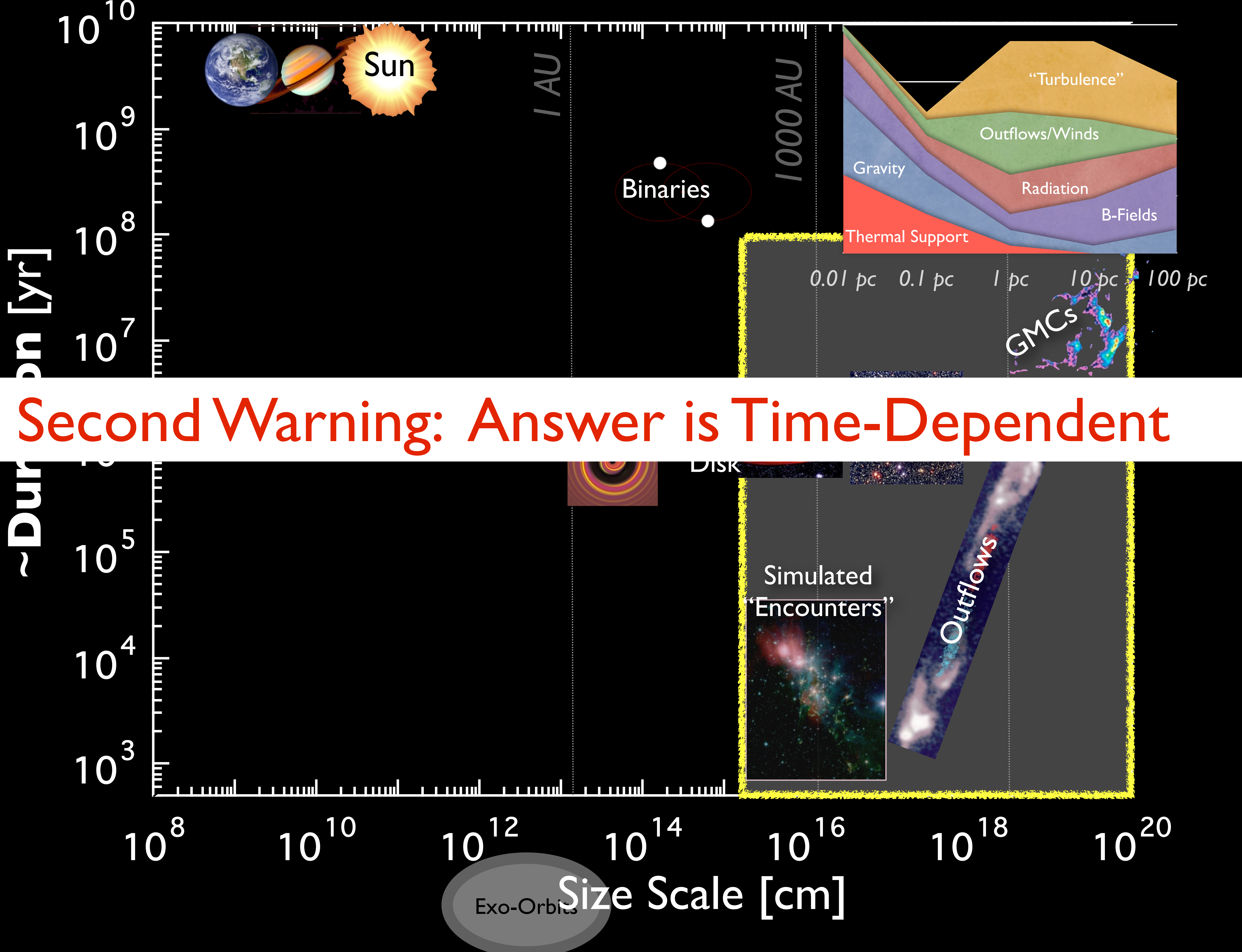


# Second Warning: Answer is Time-Dependent

# Changes of Heart, rather than in Physics...

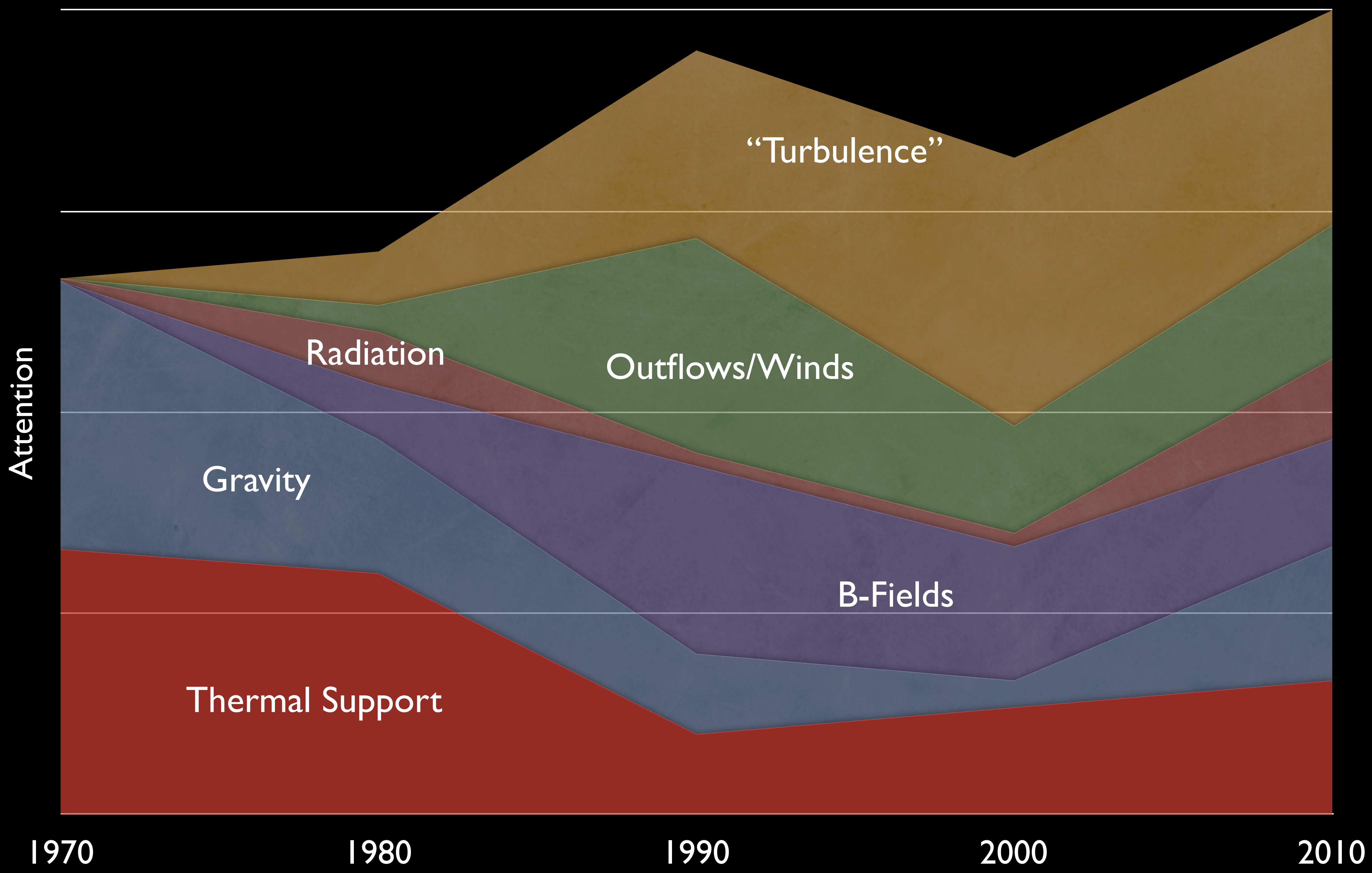

# 3 Questions

1. At what scales does **gravity** matter?

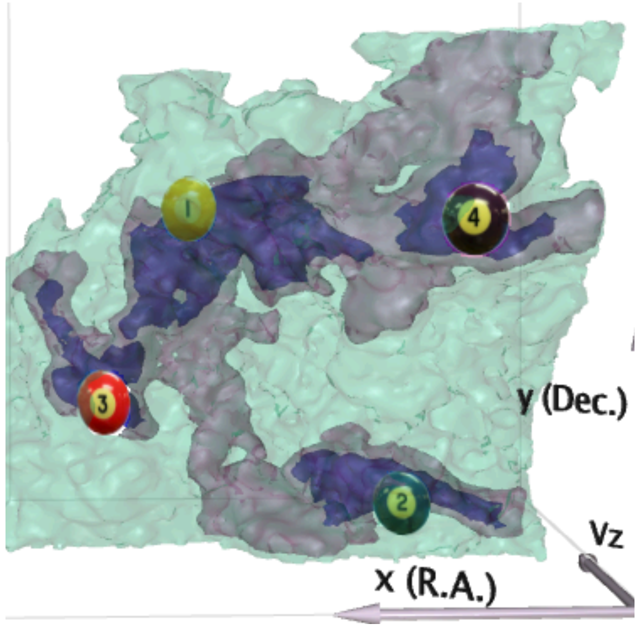


2. What do **stars** really do to clouds?

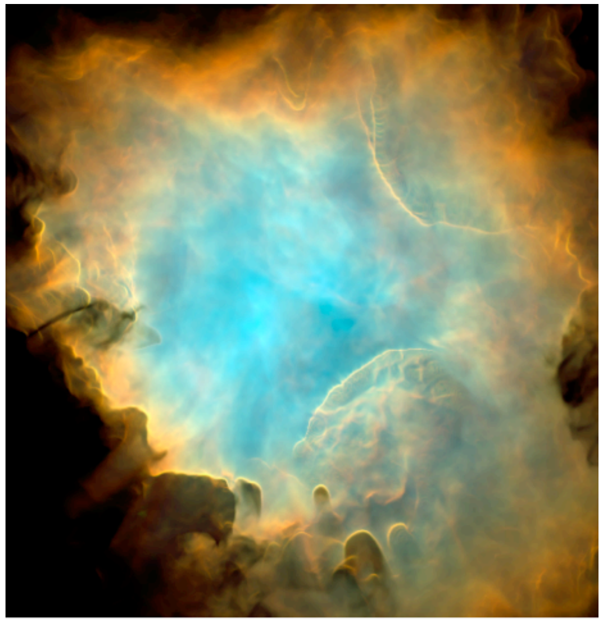

3. How can "new" statistical **visualization** tools help?

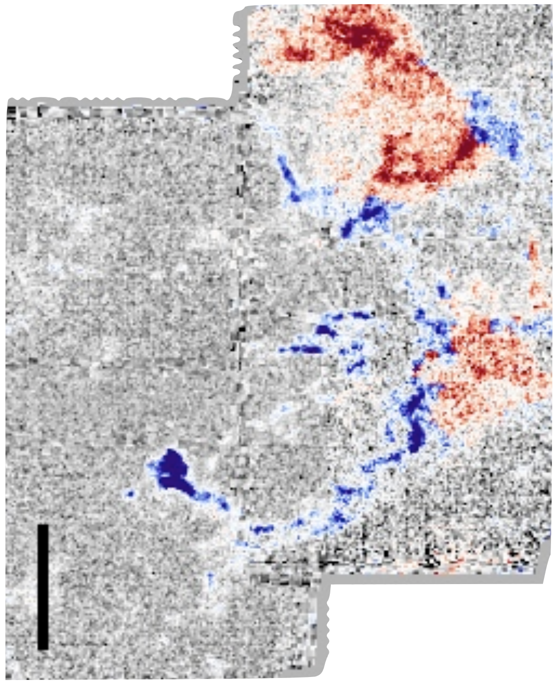

*+ "tasty" approaches to answers*

# The Taste-Testing Process

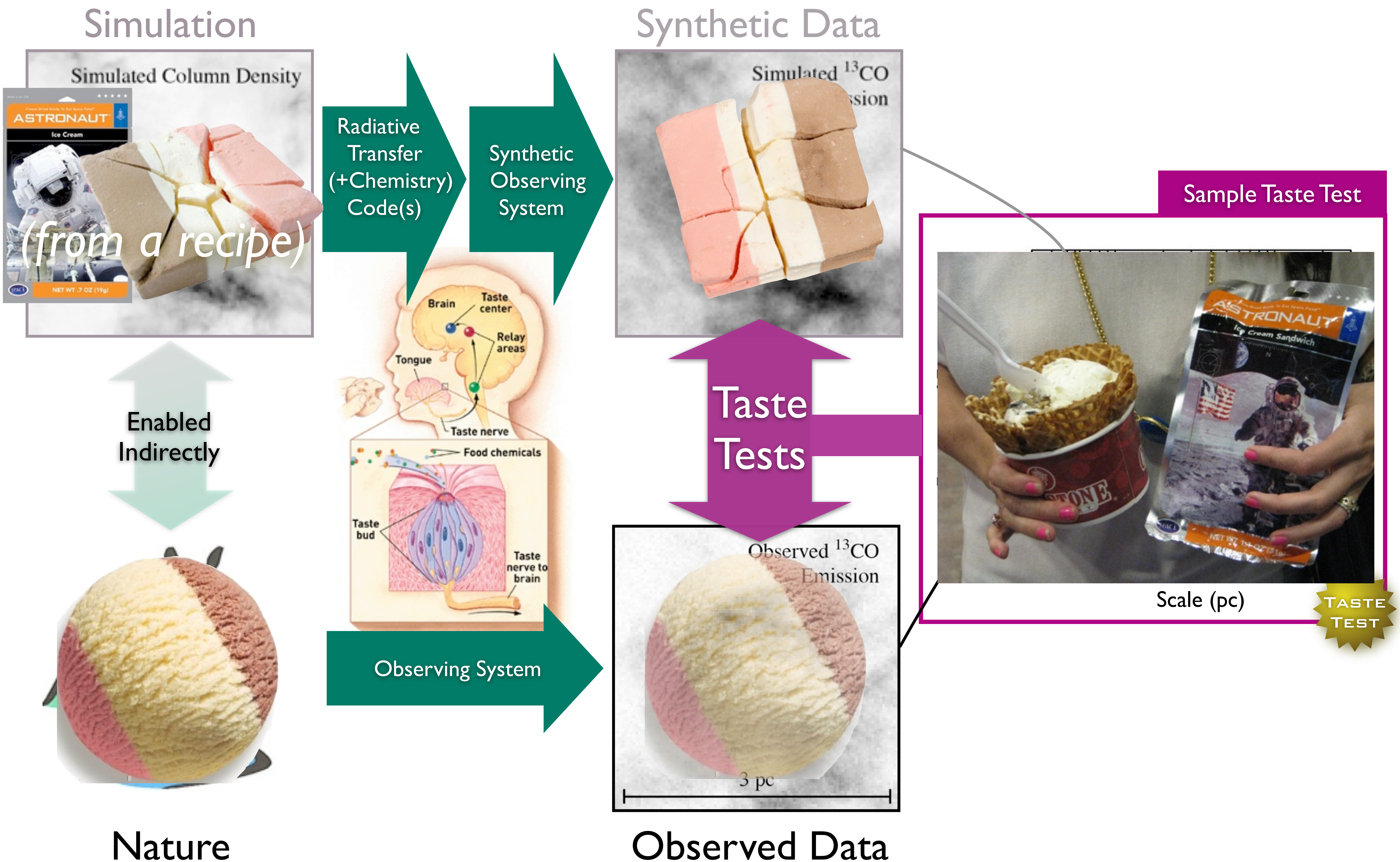

# Our Goal is to "Taste" Star Formation

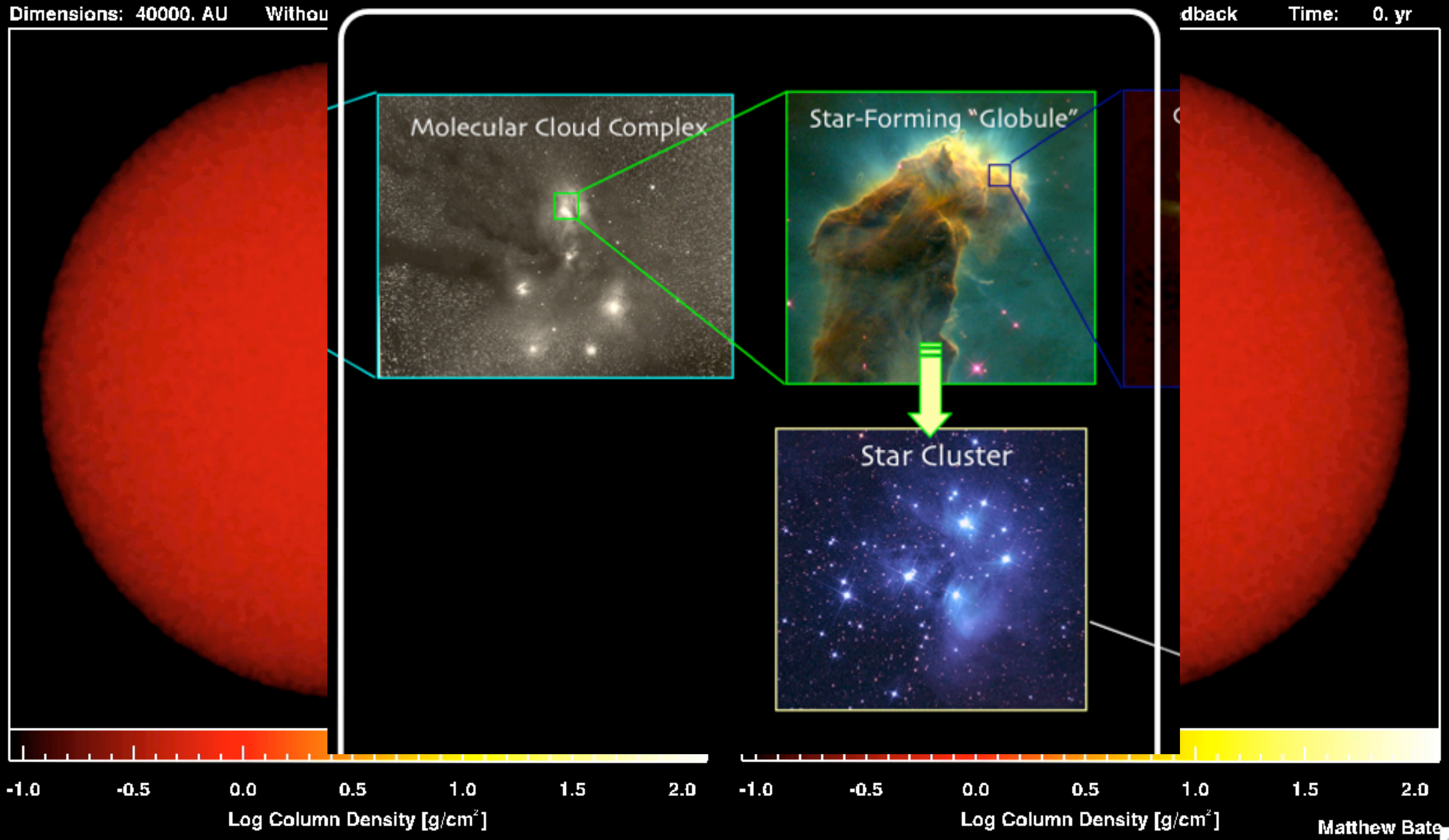


*Simulations of Bate 2009*

# "Three" Dimensions: Spectral-Line Mapping

*We wish we could measure…*

Simulations

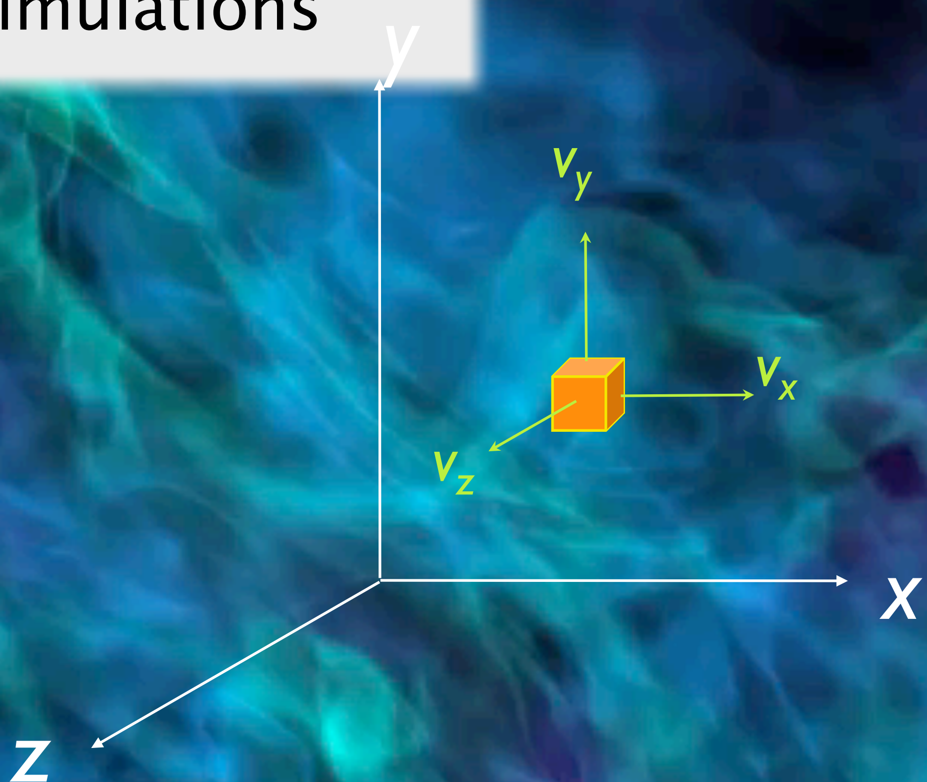


*But we can measure…*

"p-p-v" cubes

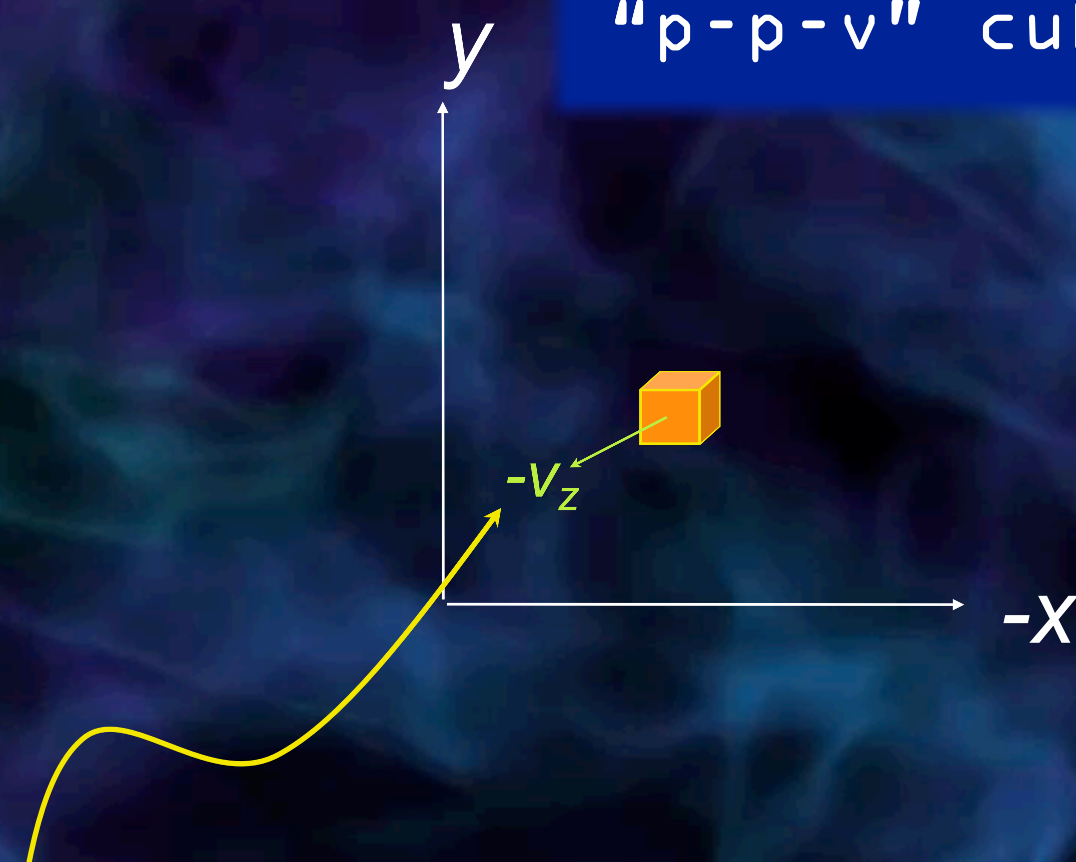


$v_z$ *only* from "spectral-line maps"

*Hydrodynamic AMR Simulation, courtesy Stella Offner*

# Velocity from Spectroscopy

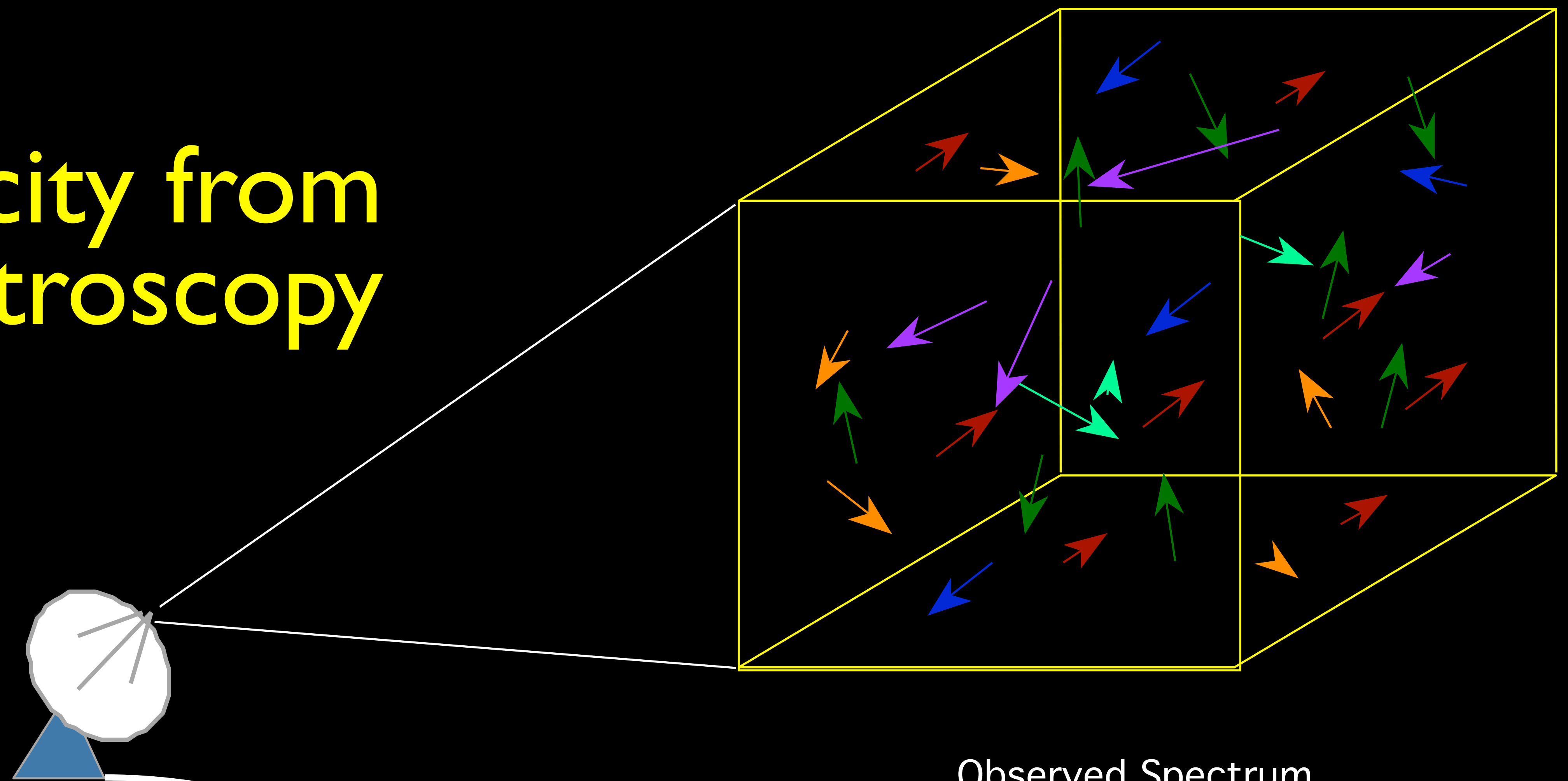


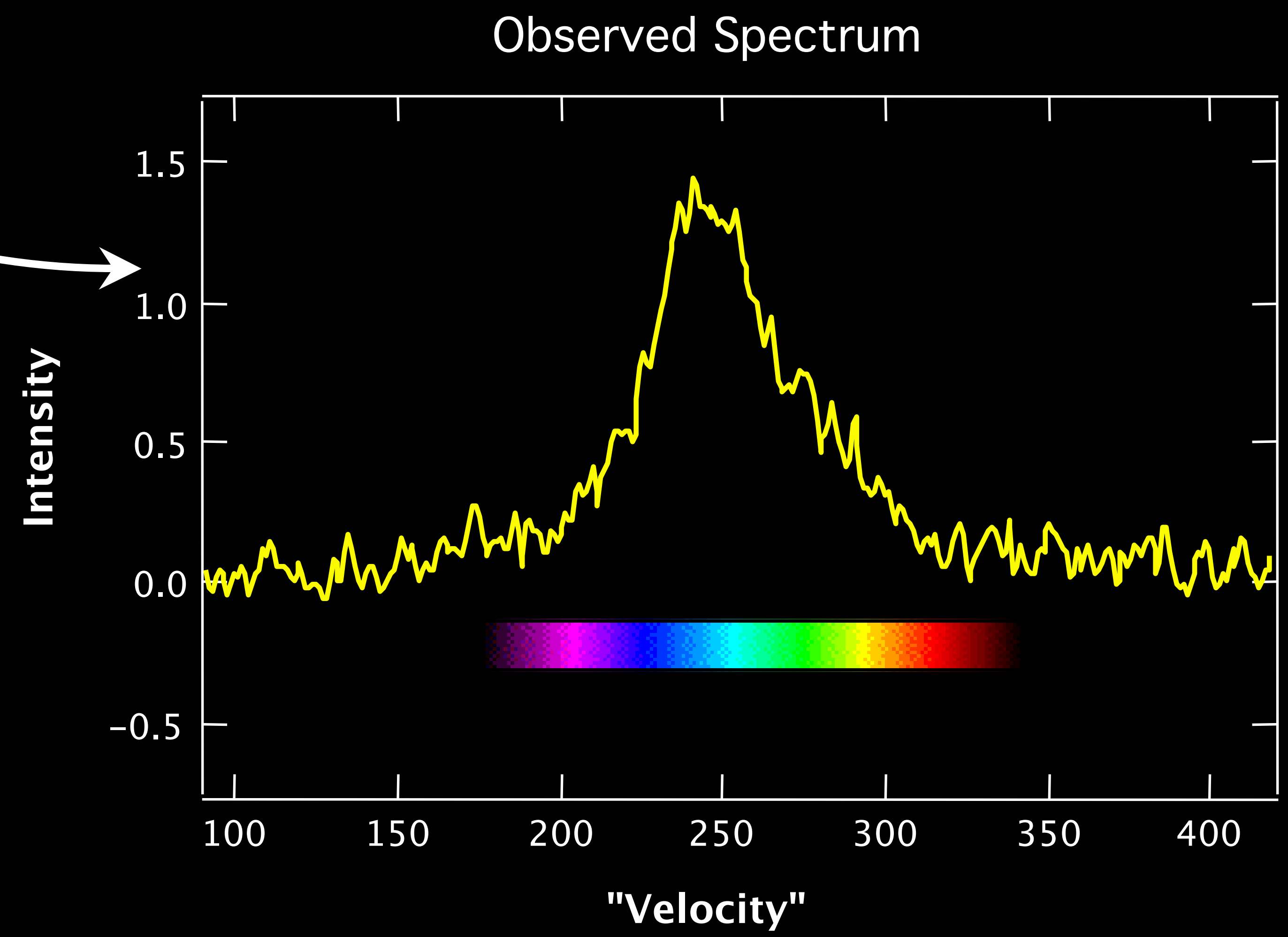


All thanks to Doppler

# Radio Spectral-line Observations of Interstellar Clouds

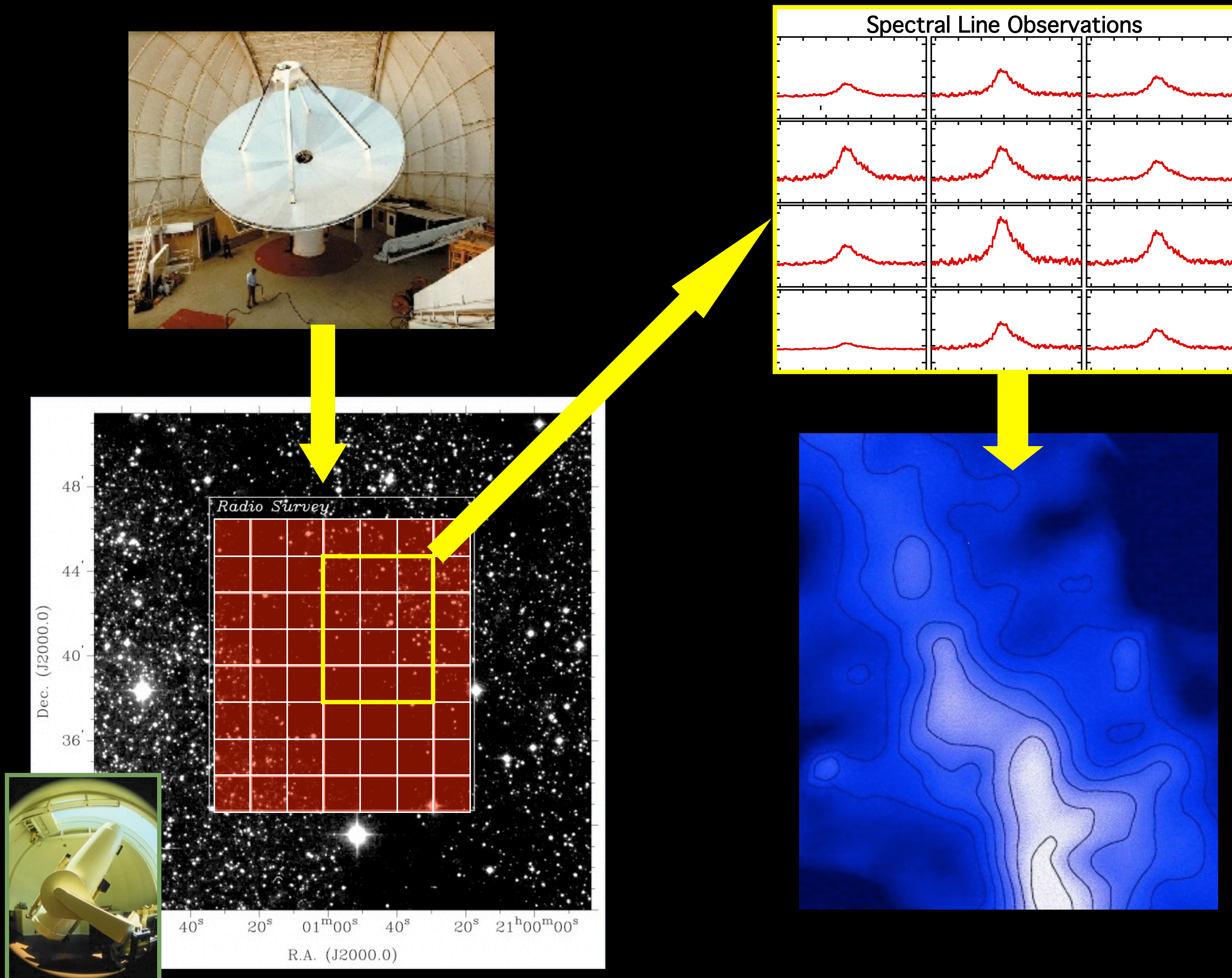

# Radio Spectral-line Observations of Interstellar Clouds

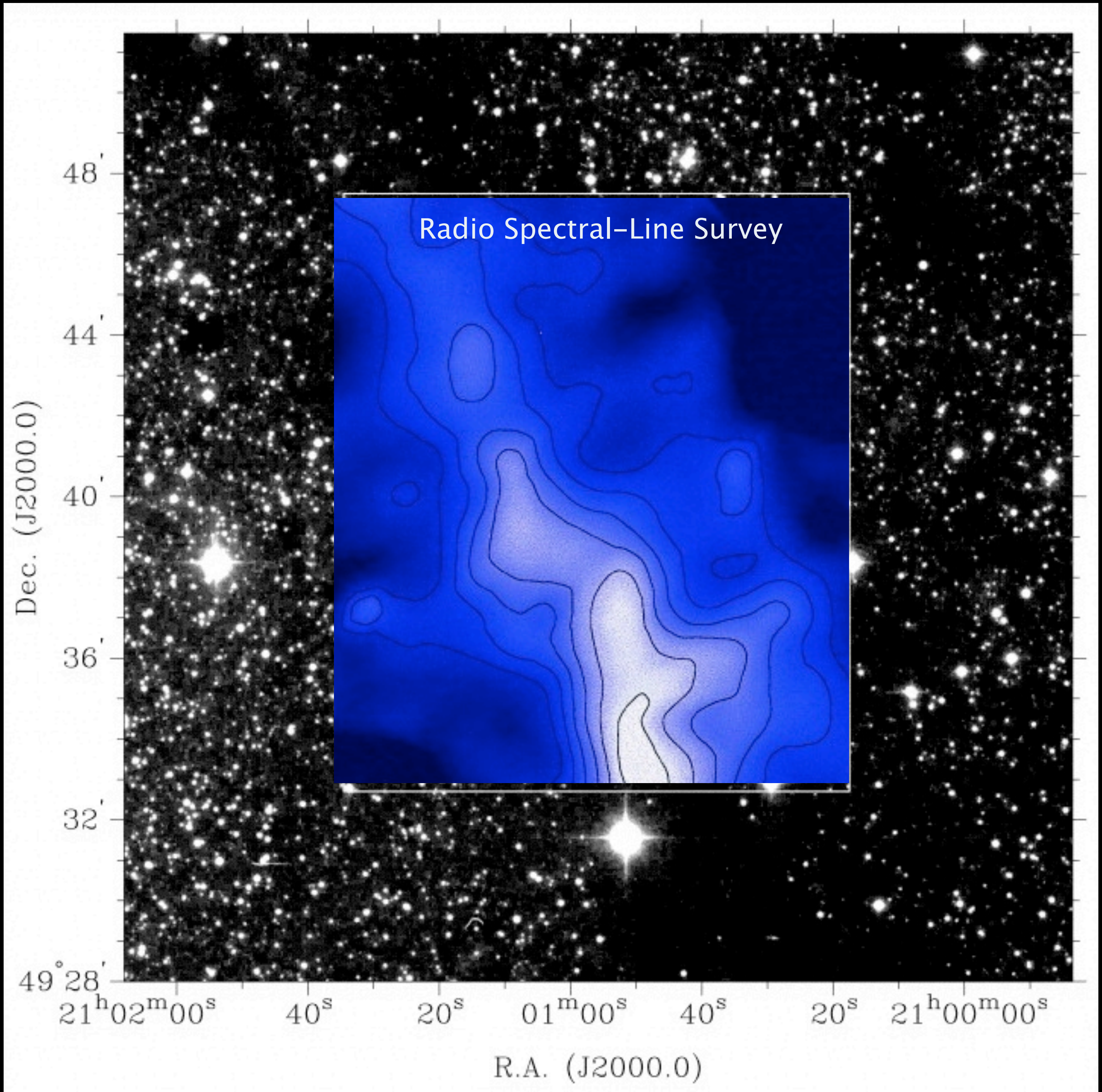


Alves, Lada & Lada 1999

# Velocity as a "Fourth" Dimension

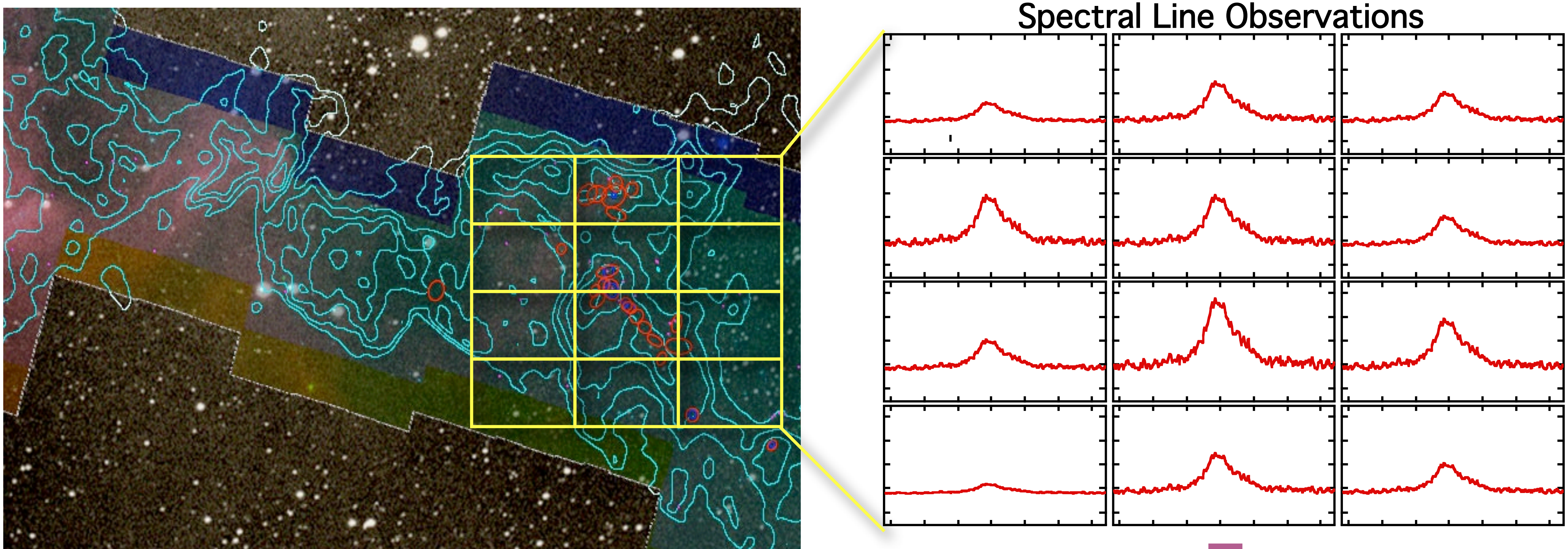


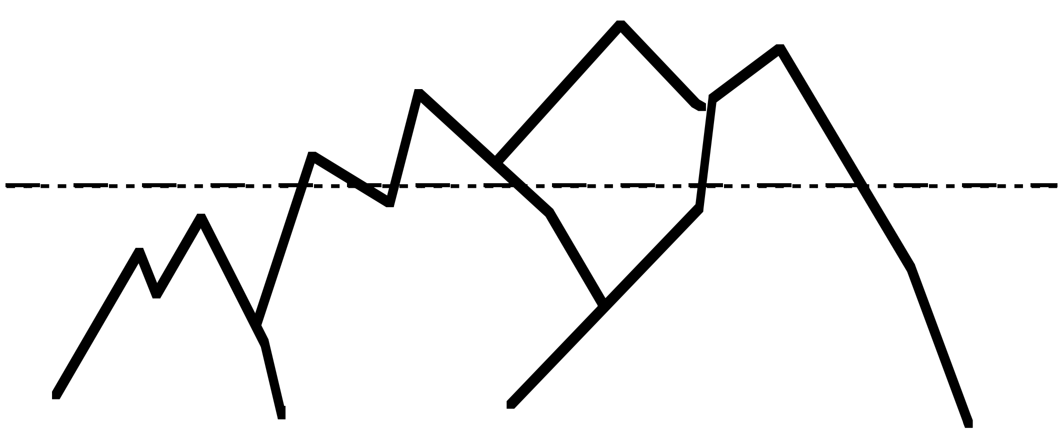

Mountain Range

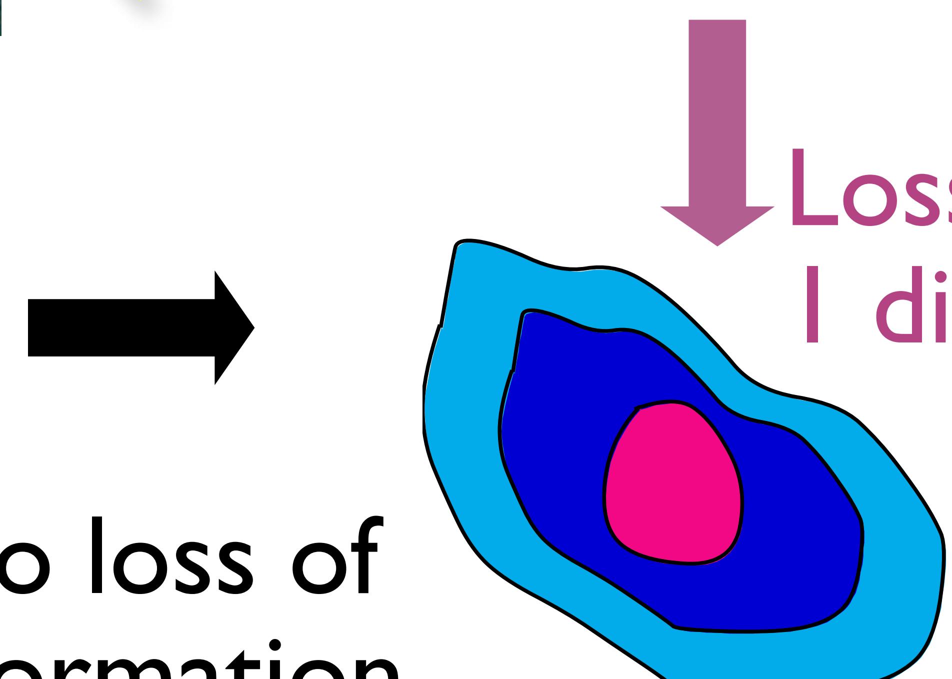

No loss of information

Loss of 1 dimension

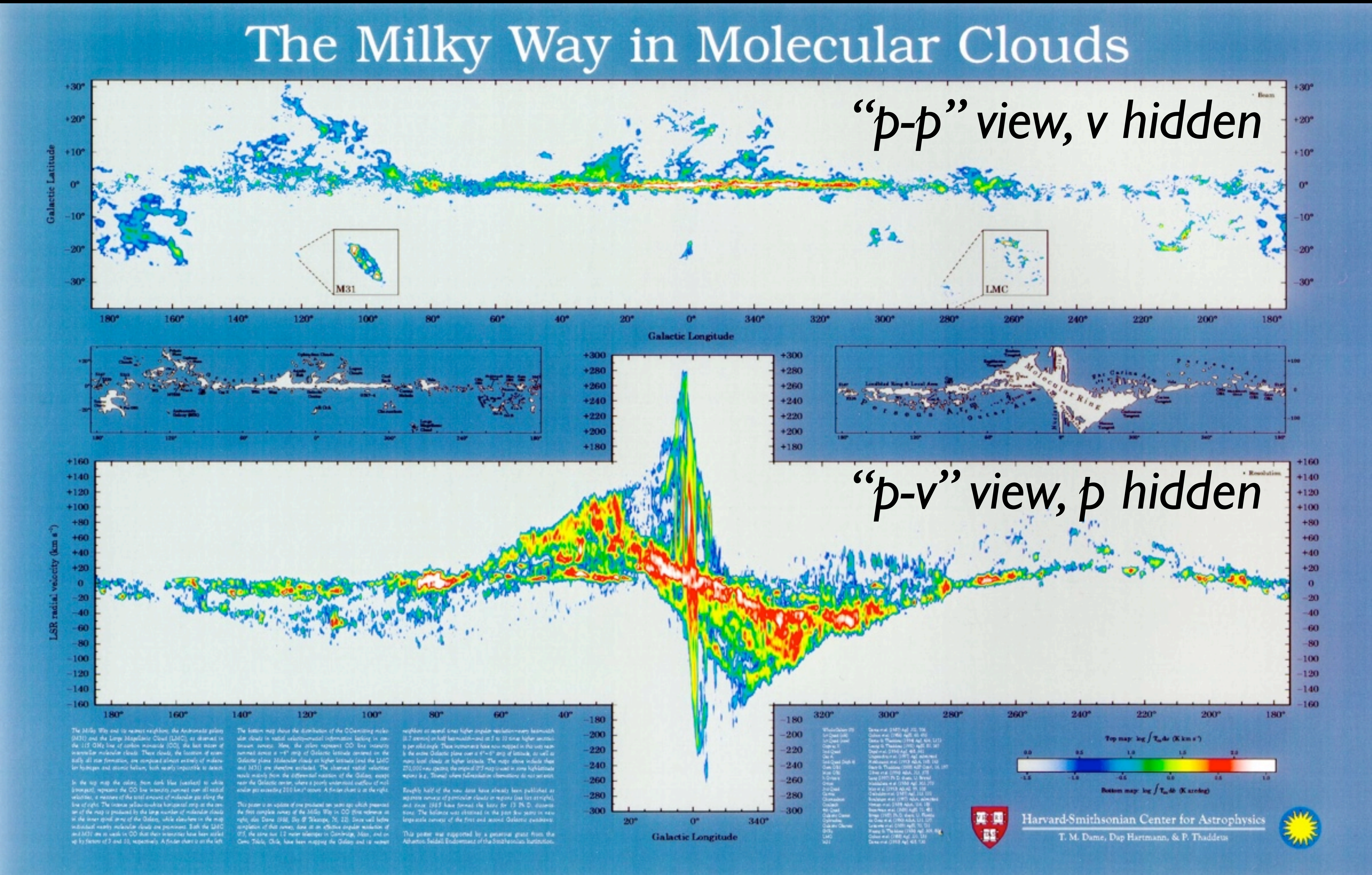


Dame et al. 2001 1.3-m “Mini” Telescope Survey of the Milky Way in CO

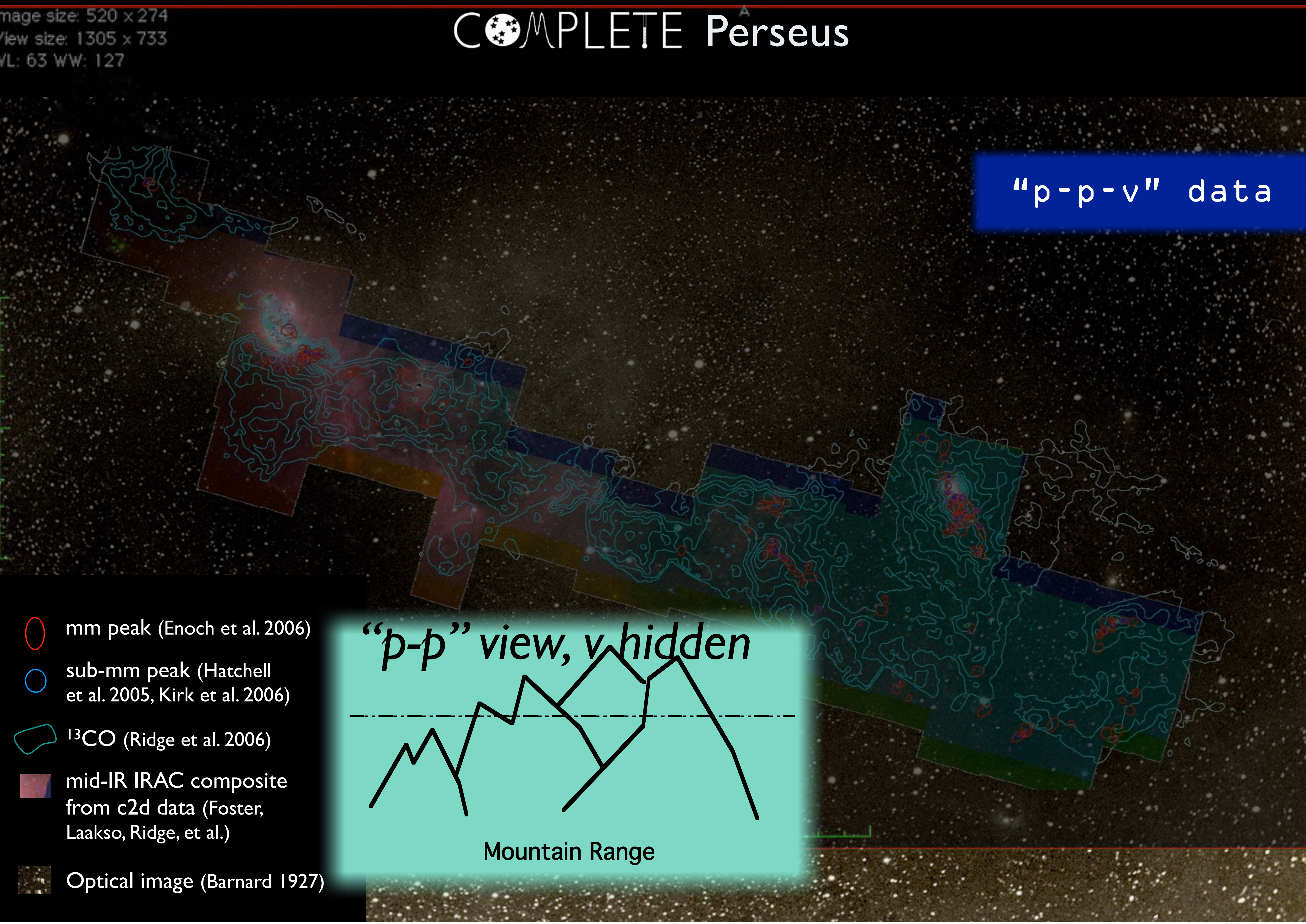
mage size: 520 x 274
/iew size: 1305 x 733
VL: 63 WW: 127
COMPLETE Perseus
"p-p-v" data
mm peak (Enoch et al. 2006)
sub-mm peak (Hatchell et al. 2005, Kirk et al. 2006)
13CO (Ridge et al. 2006)
mid-IR IRAC composite from c2d data (Foster, Laakso, Ridge, et al.)
Optical image (Barnard 1927)
"p-p" view, v hidden
Mountain Range

# “Astronomical Medicine”

“KEITH”

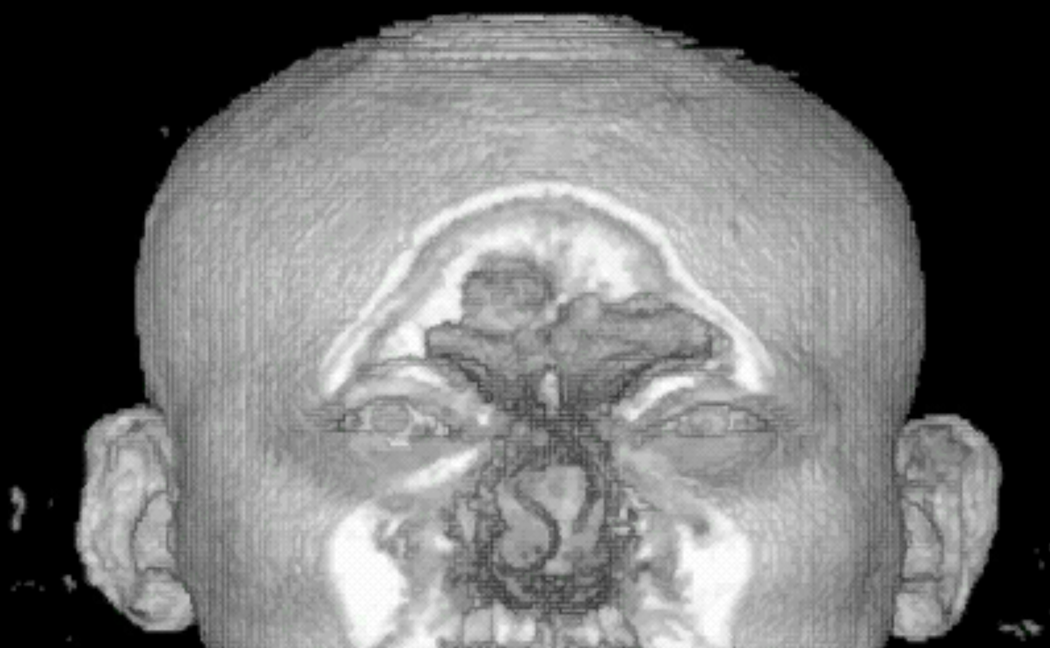

“z” is depth into head

“PERSEUS”


“z” is line-of-sight velocity

http://am.iic.harvard.edu/

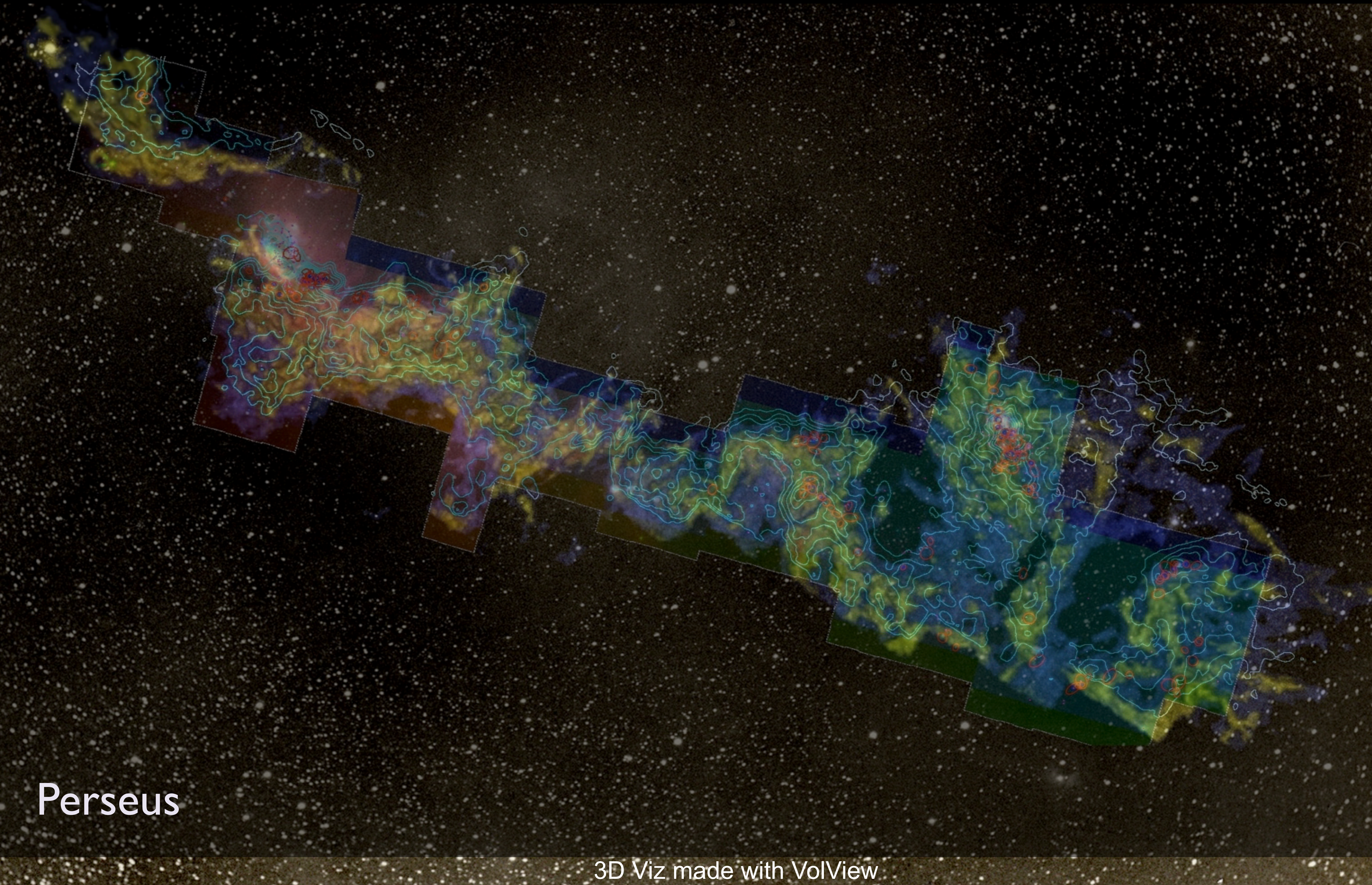


AstronomicalMedicine@IIC COMPLETE

1. At what scales does **gravity** matter?

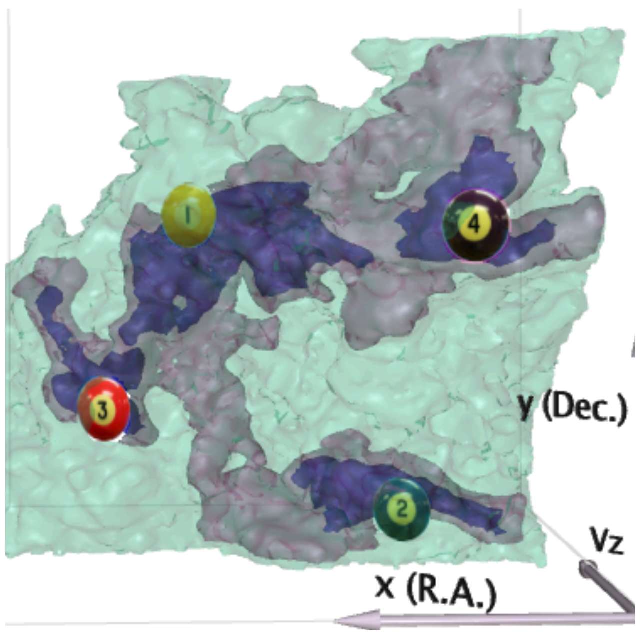


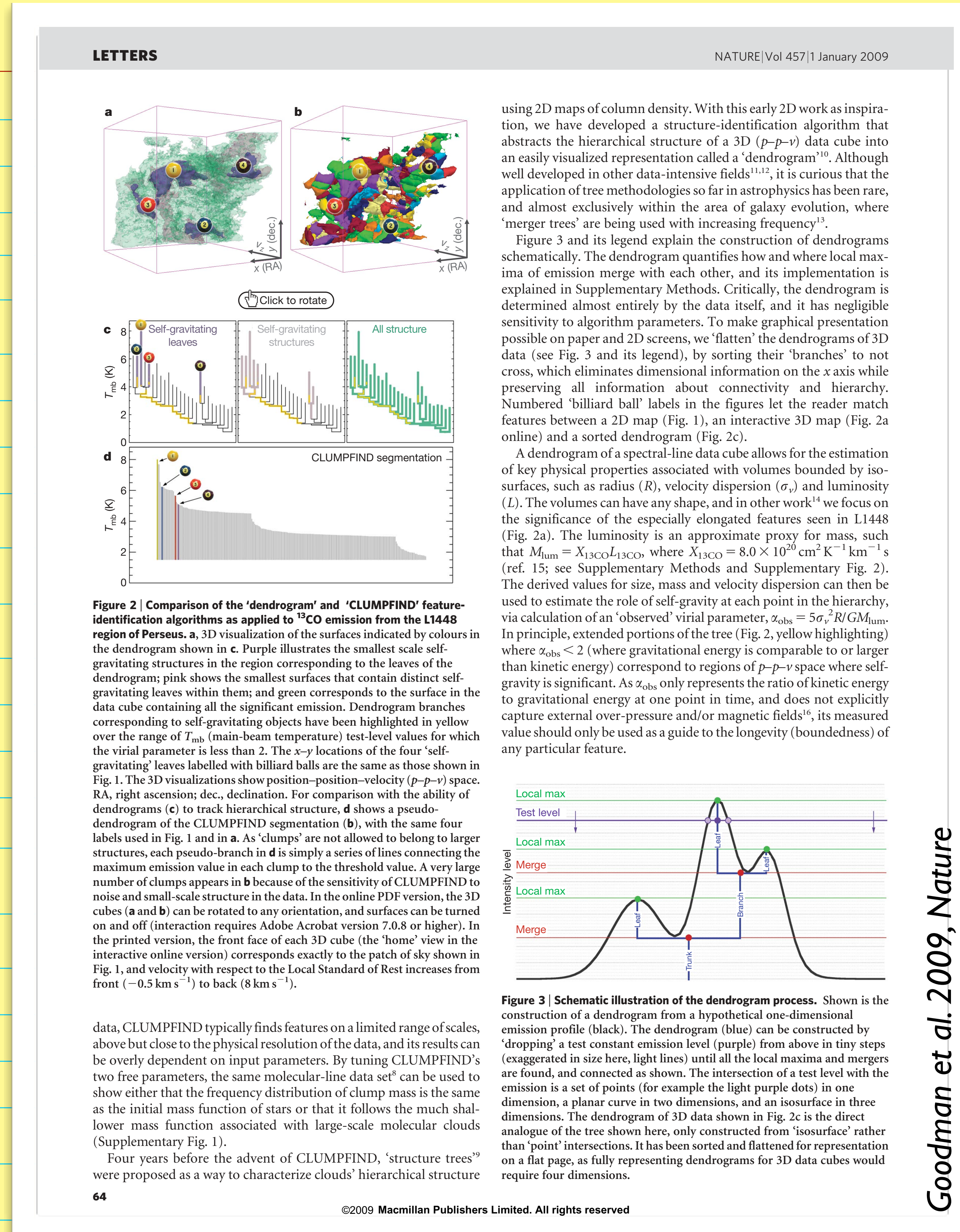




**Figure 2 | Comparison of the 'dendrogram' and 'CLUMPFIND' feature-identification algorithms as applied to $^{13}CO$ emission from the L1448 region of Perseus. a**, 3D visualization of the surfaces indicated by colours in the dendrogram shown in **c**. Purple illustrates the smallest scale self-gravitating structures in the region corresponding to the leaves of the dendrogram; pink shows the smallest surfaces that contain distinct self-gravitating leaves within them; and green corresponds to the surface in the data cube containing all the significant emission. Dendrogram branches corresponding to self-gravitating objects have been highlighted in yellow over the range of $T_{mb}$ (main-beam temperature) test-level values for which the virial parameter is less than 2. The $x$–$y$ locations of the four 'self-gravitating' leaves labelled with billiard balls are the same as those shown in Fig. 1. The 3D visualizations show position–position–velocity ($p$–$p$–$v$) space. RA, right ascension; dec., declination. For comparison with the ability of dendrograms (**c**) to track hierarchical structure, **d** shows a pseudo-dendrogram of the CLUMPFIND segmentation (**b**), with the same four labels used in Fig. 1 and in **a**. As 'clumps' are not allowed to belong to larger structures, each pseudo-branch in **d** is simply a series of lines connecting the maximum emission value in each clump to the threshold value. A very large number of clumps appears in **b** because of the sensitivity of CLUMPFIND to noise and small-scale structure in the data. In the online PDF version, the 3D cubes (**a** and **b**) can be rotated to any orientation, and surfaces can be turned on and off (interaction requires Adobe Acrobat version 7.0.8 or higher). In the printed version, the front face of each 3D cube (the 'home' view in the interactive online version) corresponds exactly to the patch of sky shown in Fig. 1, and velocity with respect to the Local Standard of Rest increases from front ($-0.5\ km\ s^{-1}$) to back ($8\ km\ s^{-1}$).

data, CLUMPFIND typically finds features on a limited range of scales, above but close to the physical resolution of the data, and its results can be overly dependent on input parameters. By tuning CLUMPFIND's two free parameters, the same molecular-line data set[8] can be used to show either that the frequency distribution of clump mass is the same as the initial mass function of stars or that it follows the much shallower mass function associated with large-scale molecular clouds (Supplementary Fig. 1).

Four years before the advent of CLUMPFIND, 'structure trees'[9] were proposed as a way to characterize clouds' hierarchical structure using 2D maps of column density. With this early 2D work as inspiration, we have developed a structure-identification algorithm that abstracts the hierarchical structure of a 3D ($p$–$p$–$v$) data cube into an easily visualized representation called a 'dendrogram'[10]. Although well developed in other data-intensive fields[11,12], it is curious that the application of tree methodologies so far in astrophysics has been rare, and almost exclusively within the area of galaxy evolution, where 'merger trees' are being used with increasing frequency[13].

Figure 3 and its legend explain the construction of dendrograms schematically. The dendrogram quantifies how and where local maxima of emission merge with each other, and its implementation is explained in Supplementary Methods. Critically, the dendrogram is determined almost entirely by the data itself, and it has negligible sensitivity to algorithm parameters. To make graphical presentation possible on paper and 2D screens, we 'flatten' the dendrograms of 3D data (see Fig. 3 and its legend), by sorting their 'branches' to not cross, which eliminates dimensional information on the $x$ axis while preserving all information about connectivity and hierarchy. Numbered 'billiard ball' labels in the figures let the reader match features between a 2D map (Fig. 1), an interactive 3D map (Fig. 2a online) and a sorted dendrogram (Fig. 2c).

A dendrogram of a spectral-line data cube allows for the estimation of key physical properties associated with volumes bounded by isosurfaces, such as radius ($R$), velocity dispersion ($\sigma_v$) and luminosity ($L$). The volumes can have any shape, and in other work[14] we focus on the significance of the especially elongated features seen in L1448 (Fig. 2a). The luminosity is an approximate proxy for mass, such that $M_{lum} = X_{13CO}L_{13CO}$, where $X_{13CO} = 8.0 \times 10^{20}\ cm^2\ K^{-1}\ km^{-1}\ s$ (ref. 15; see Supplementary Methods and Supplementary Fig. 2). The derived values for size, mass and velocity dispersion can then be used to estimate the role of self-gravity at each point in the hierarchy, via calculation of an 'observed' virial parameter, $\alpha_{obs} = 5\sigma_v^2 R/GM_{lum}$. In principle, extended portions of the tree (Fig. 2, yellow highlighting) where $\alpha_{obs} < 2$ (where gravitational energy is comparable to or larger than kinetic energy) correspond to regions of $p$–$p$–$v$ space where self-gravity is significant. As $\alpha_{obs}$ only represents the ratio of kinetic energy to gravitational energy at one point in time, and does not explicitly capture external over-pressure and/or magnetic fields[16], its measured value should only be used as a guide to the longevity (boundedness) of any particular feature.

**Figure 3 | Schematic illustration of the dendrogram process.** Shown is the construction of a dendrogram from a hypothetical one-dimensional emission profile (black). The dendrogram (blue) can be constructed by 'dropping' a test constant emission level (purple) from above in tiny steps (exaggerated in size here, light lines) until all the local maxima and mergers are found, and connected as shown. The intersection of a test level with the emission is a set of points (for example the light purple dots) in one dimension, a planar curve in two dimensions, and an isosurface in three dimensions. The dendrogram of 3D data shown in Fig. 2c is the direct analogue of the tree shown here, only constructed from 'isosurface' rather than 'point' intersections. It has been sorted and flattened for representation on a flat page, as fully representing dendrograms for 3D data cubes would require four dimensions.





*Goodman et al. 2009, Nature*

+ "tasty" approaches to answers

Monday, March 12, 2012

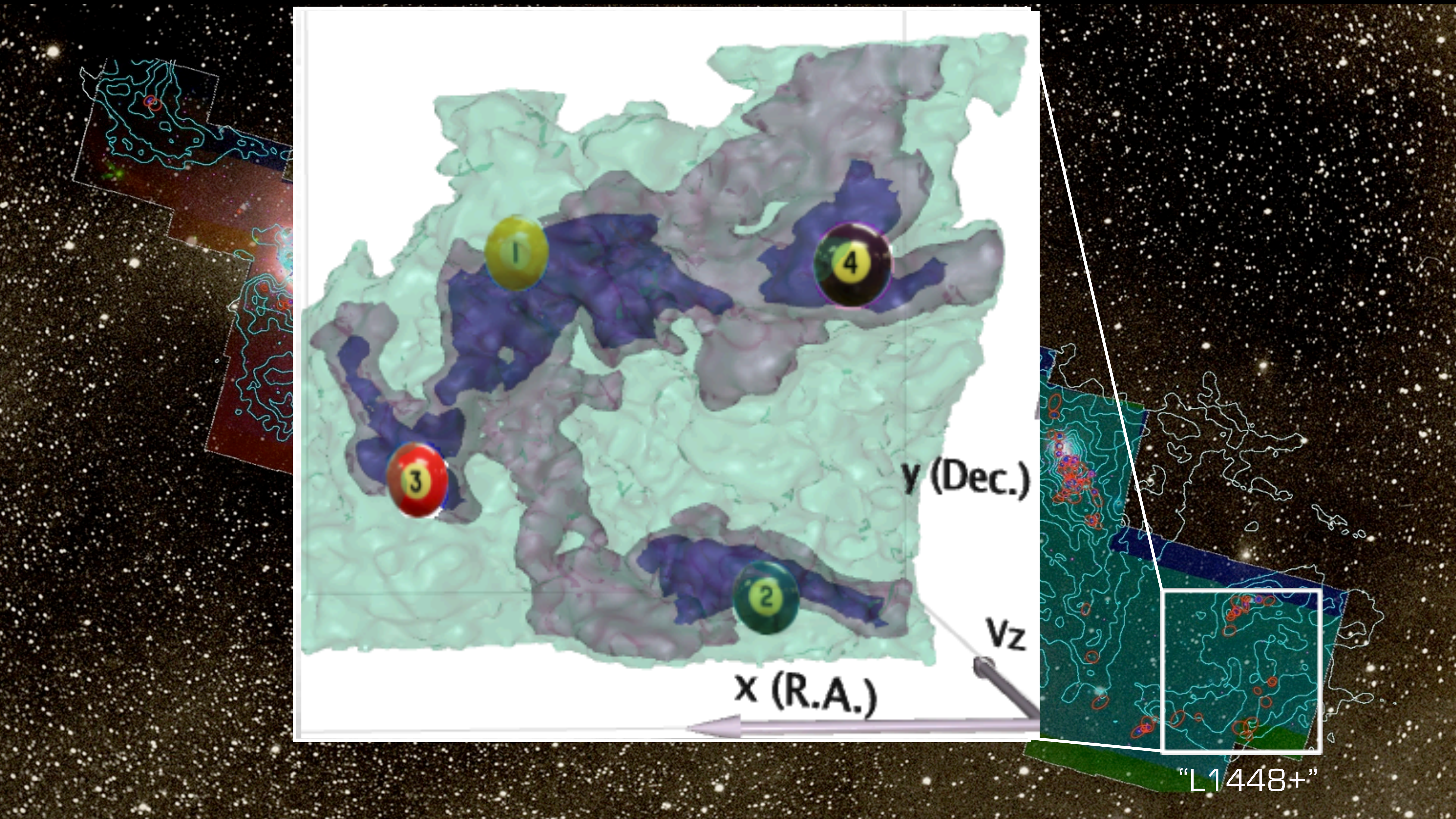


Perseus

COMPLETE

# Dendrograms

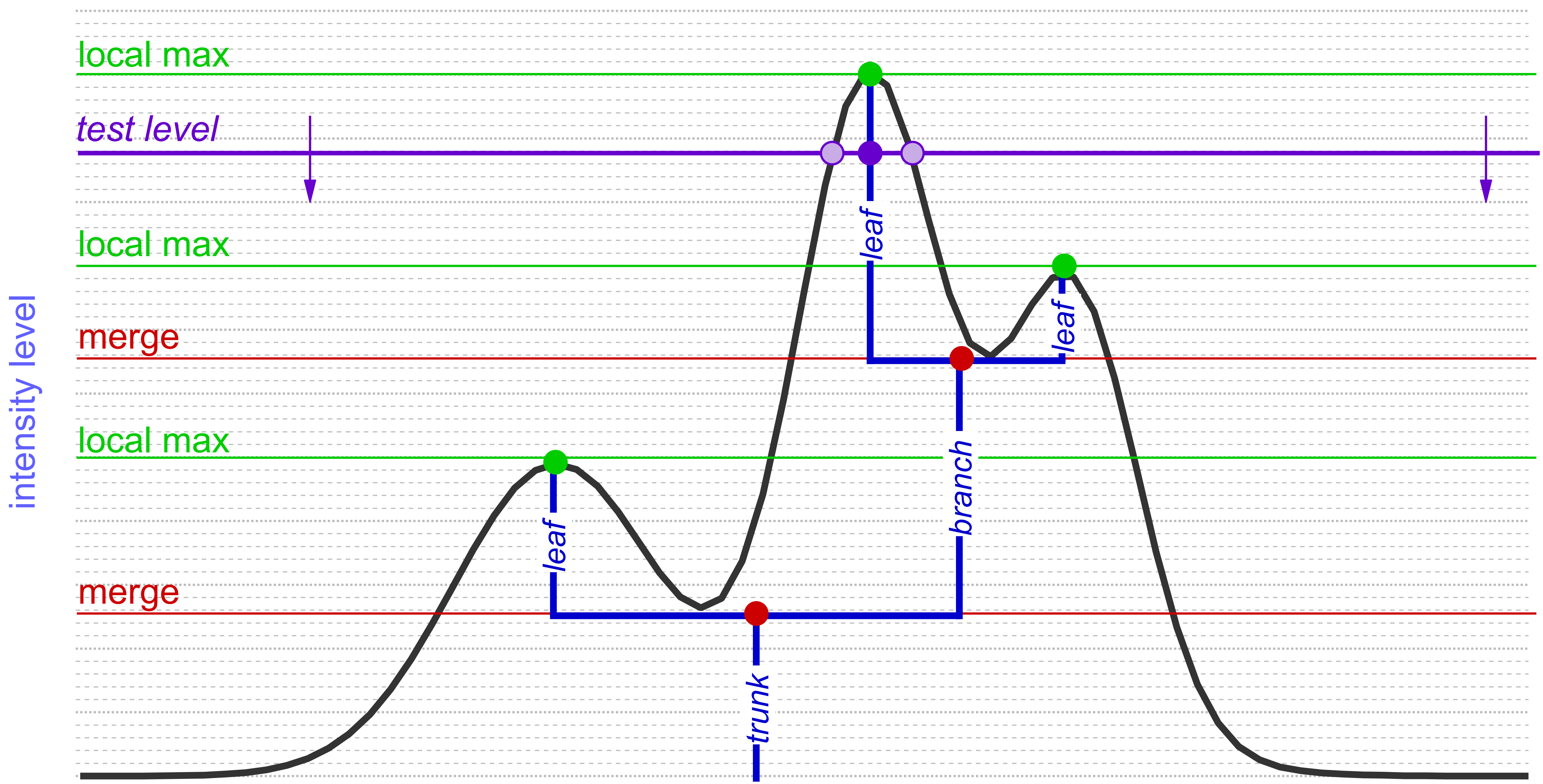


Hierarchical "Segmentation"

*Rosolowsky, Pineda, Kauffmann & Goodman 2008*

# Dendrograms

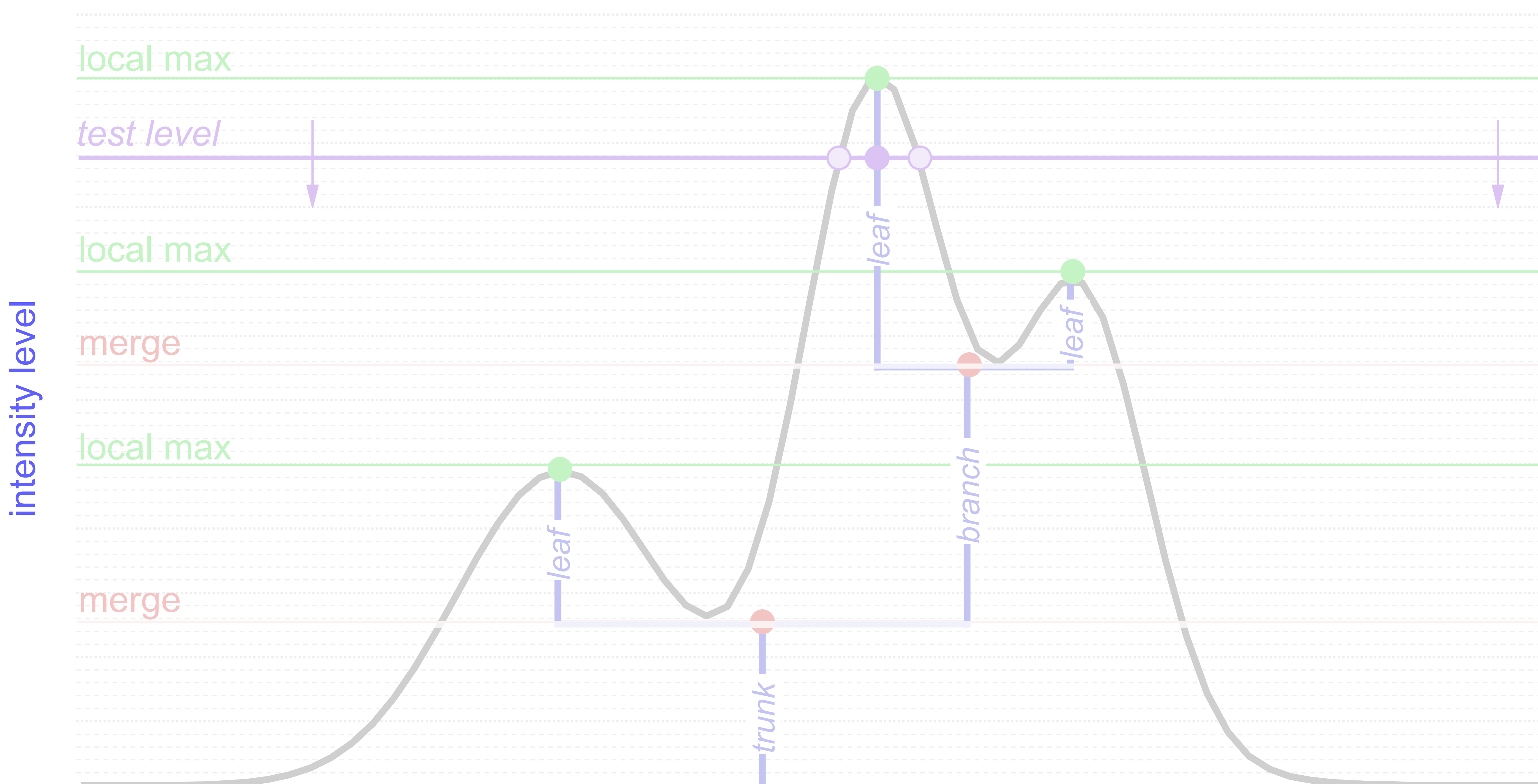


1-D: points; 2-D closed curves (contours); 3-D surfaces enclosing volumes

see 2D demo at *http://am.iic.harvard.edu/index.cgi/DendroStar/applet*

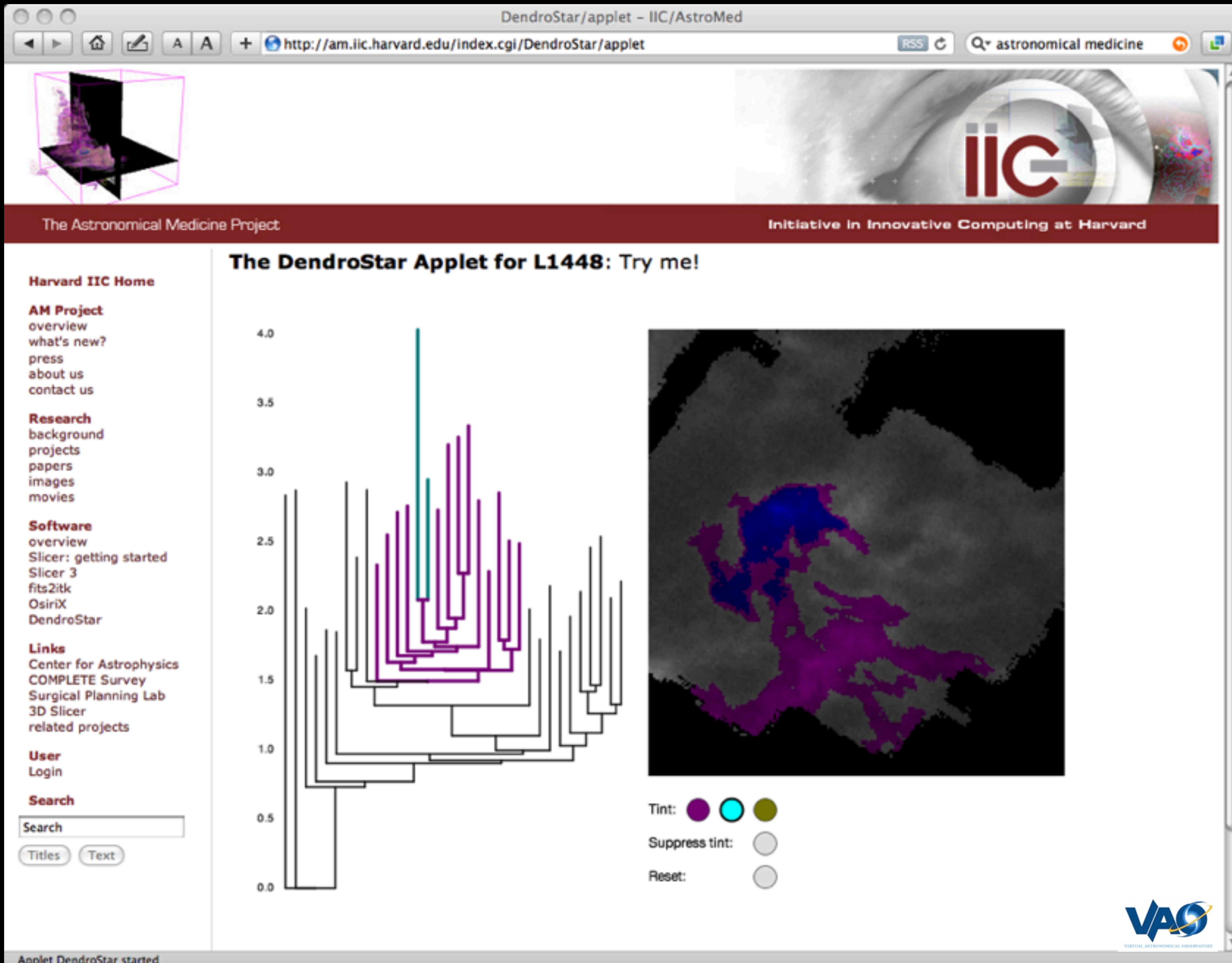


*http://am.iic.harvard.edu/index.cgi/DendroStar/applet*

*Dendrogram Algorithm by Erik Rosolwosky; Applet by Douglas Alan*

# 1. At what scales does gravity matter?

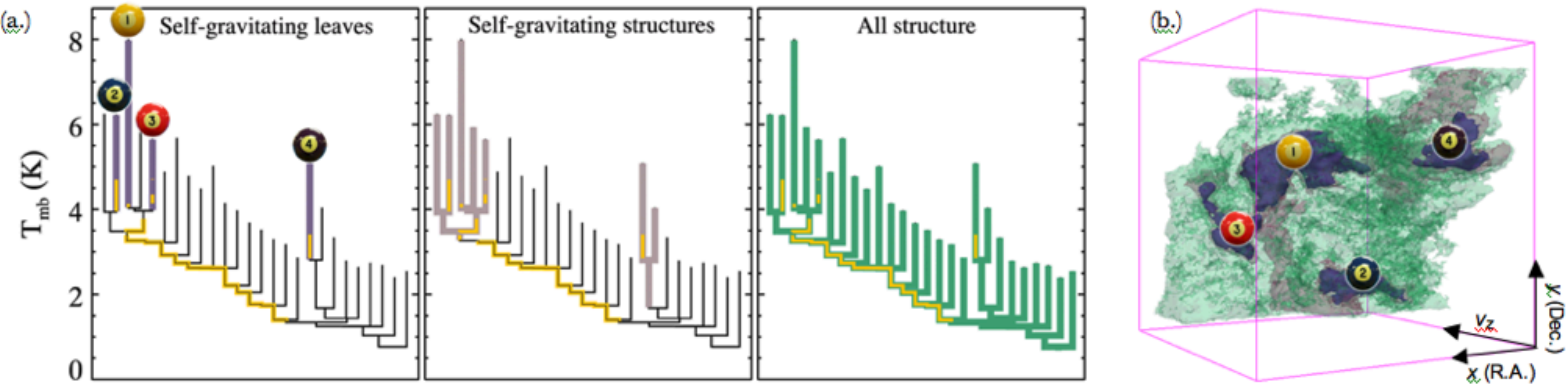


Yellow highlighting= "self-gravitating"

*(according to virial theorem!?!)*

"Self-gravitating" here just means $\alpha_{vir}$ $(=5s_v^2 R/GM_{lum}) < 2$

(à la Bertoldi & McKee 1992–*BUT*–see Shetty et al. 2010)

*Rosolowsky et al. 2008 (ApJ) &*
*Goodman et al. 2009 (Nature)*

*see PDF...*

# Real and Simulated $^{13}$CO

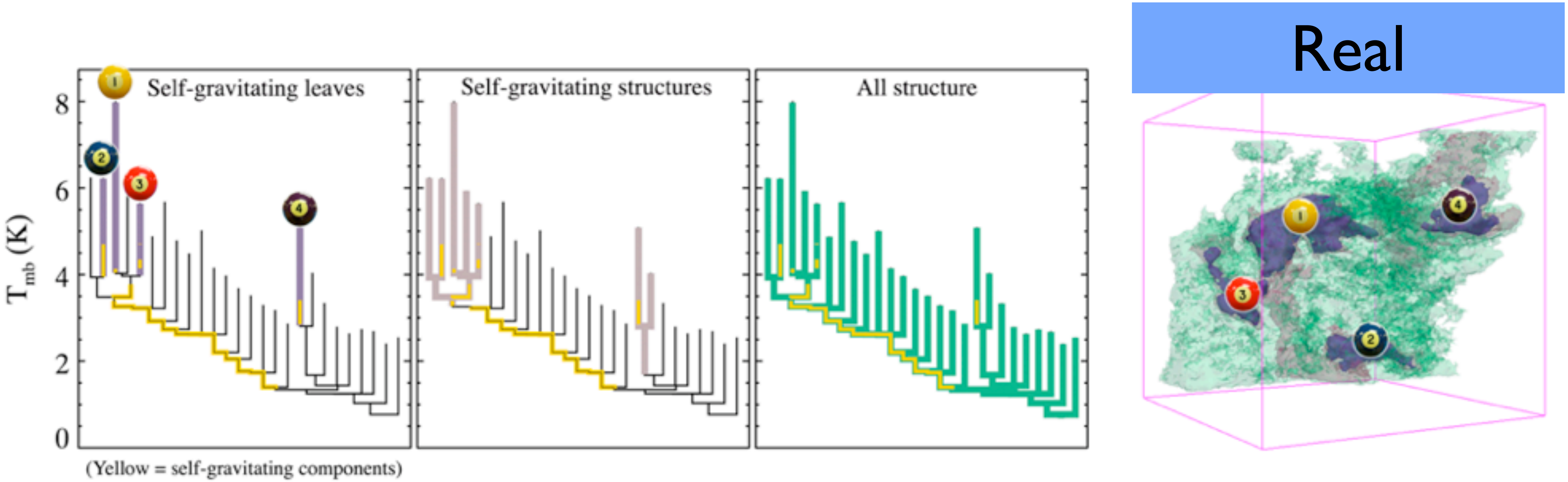


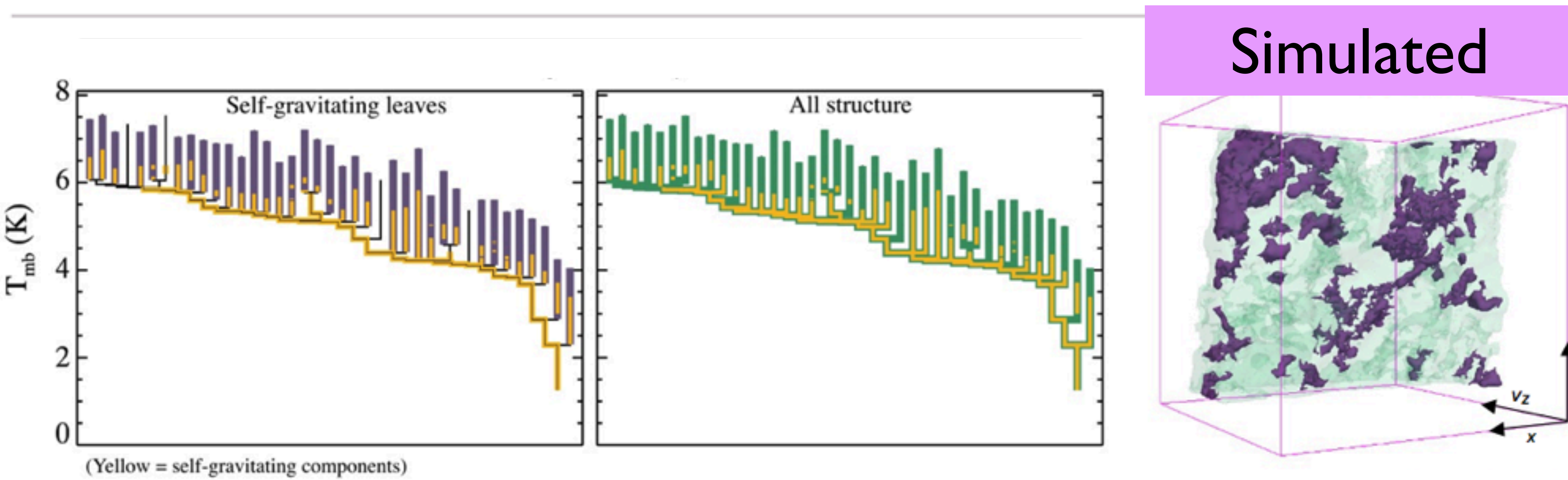

# The Taste-Testing Process

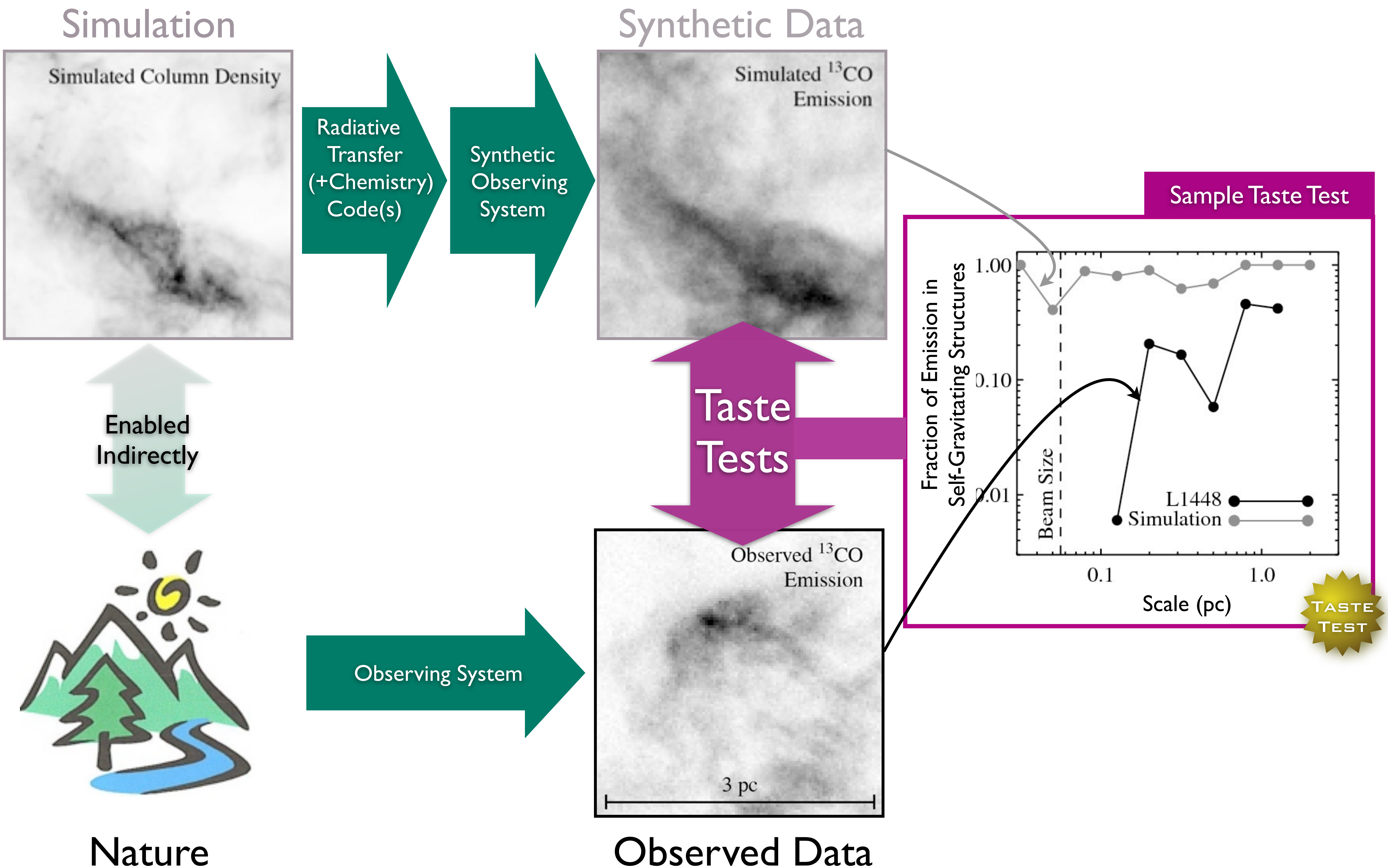

# Taste-Testing "Gravity"

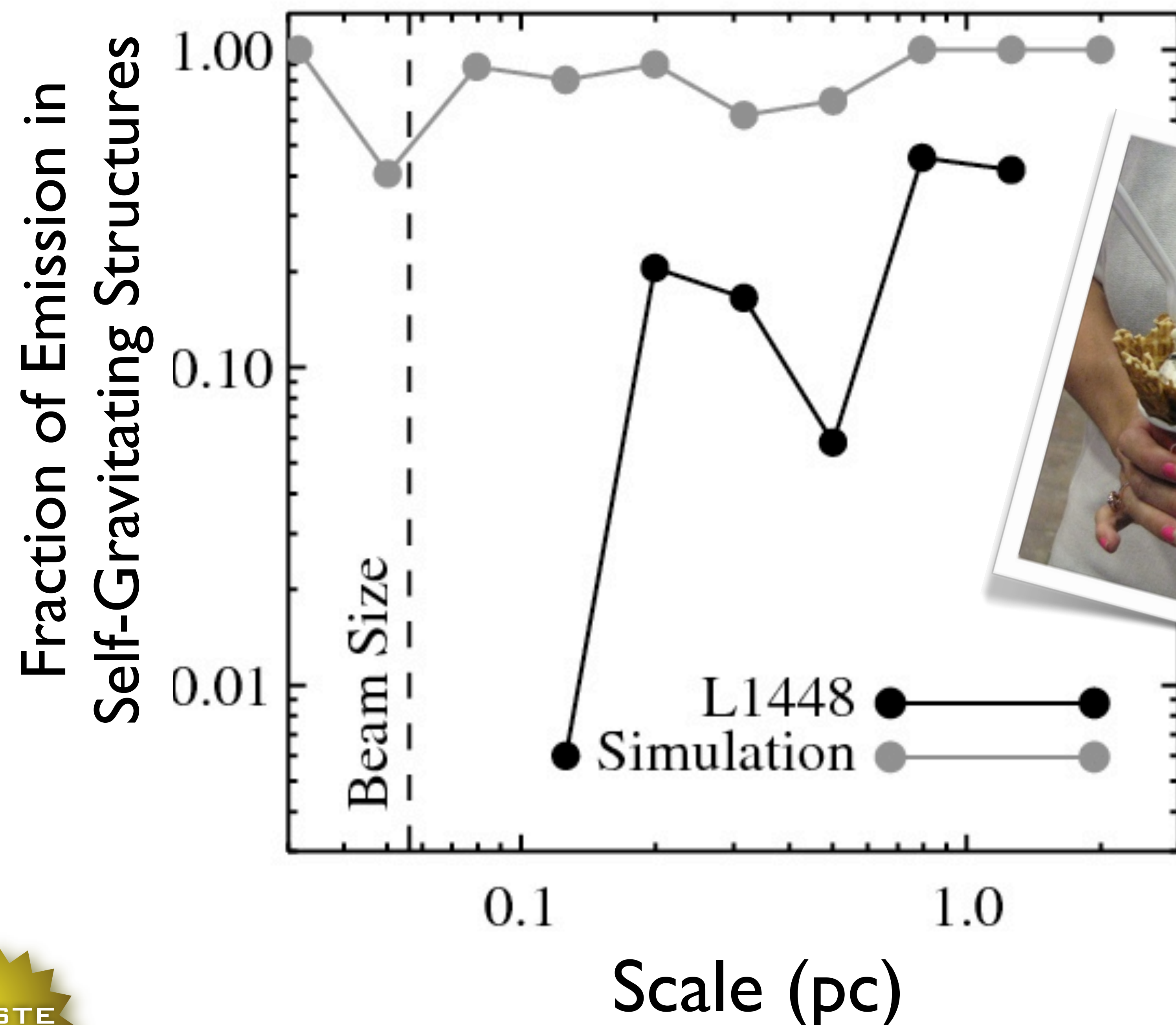



TASTE TEST

*Gravity-free HD Simulations from Padoan et al. 2006;*
*L1448 analysis from Rosolowsky et al. 2008*
both lines derived from $^{13}CO$ "observations"

# *Philosophical Interlude*  *for non-Experts*

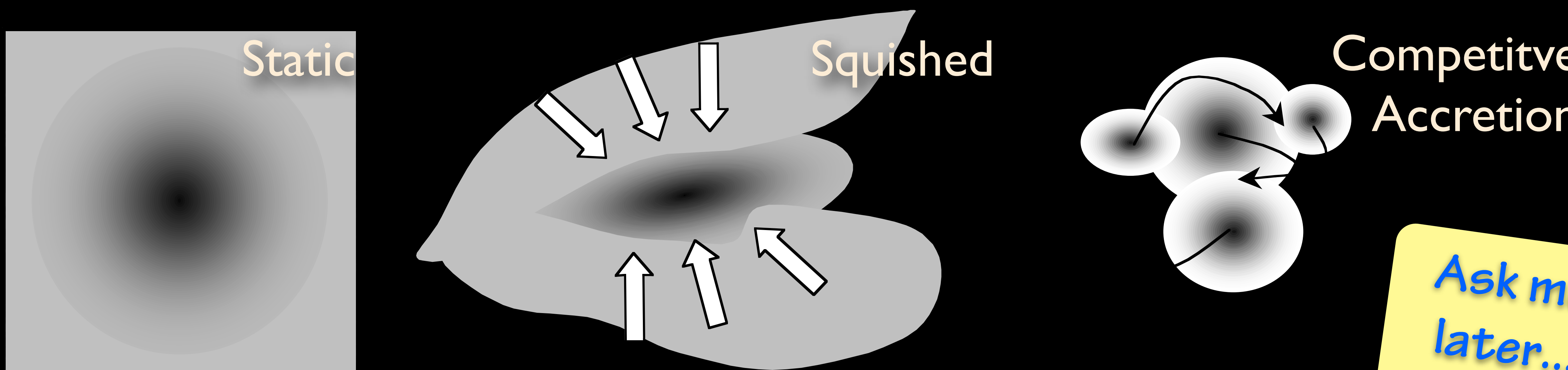


Ask me later...

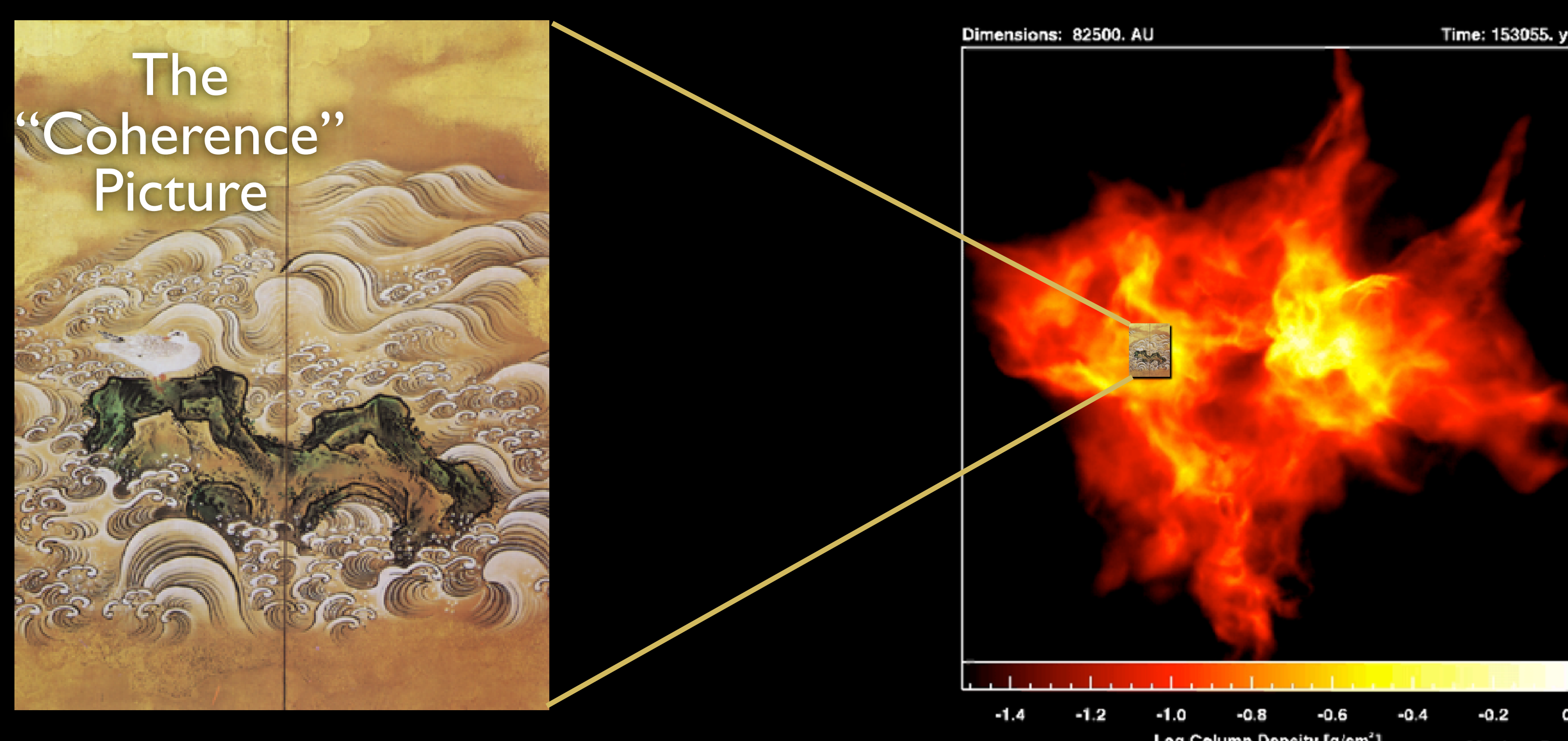

# “Islands of Calm in a Turbulent Sea”

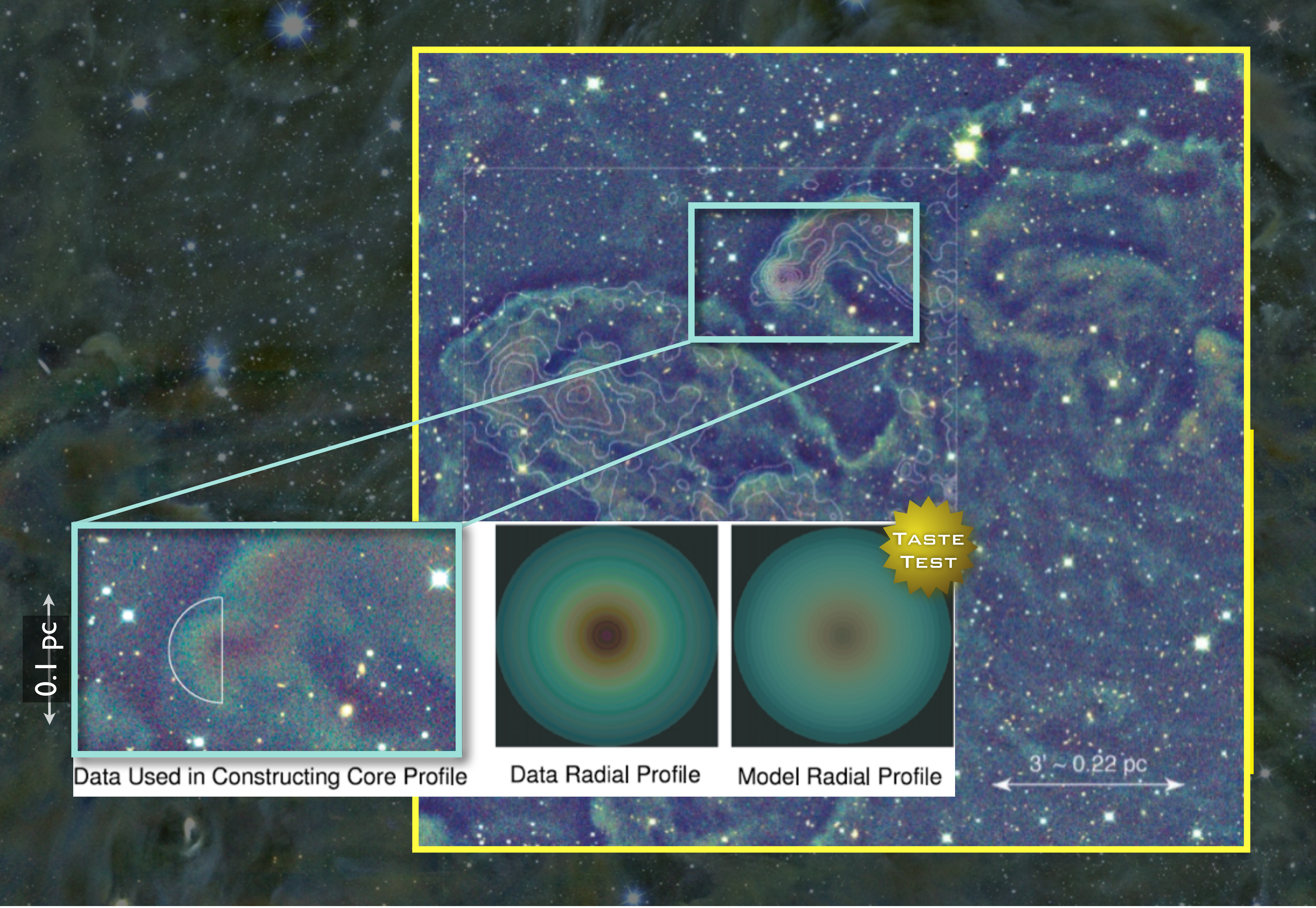

# *p-p-v* structure of the B5 region in Perseus

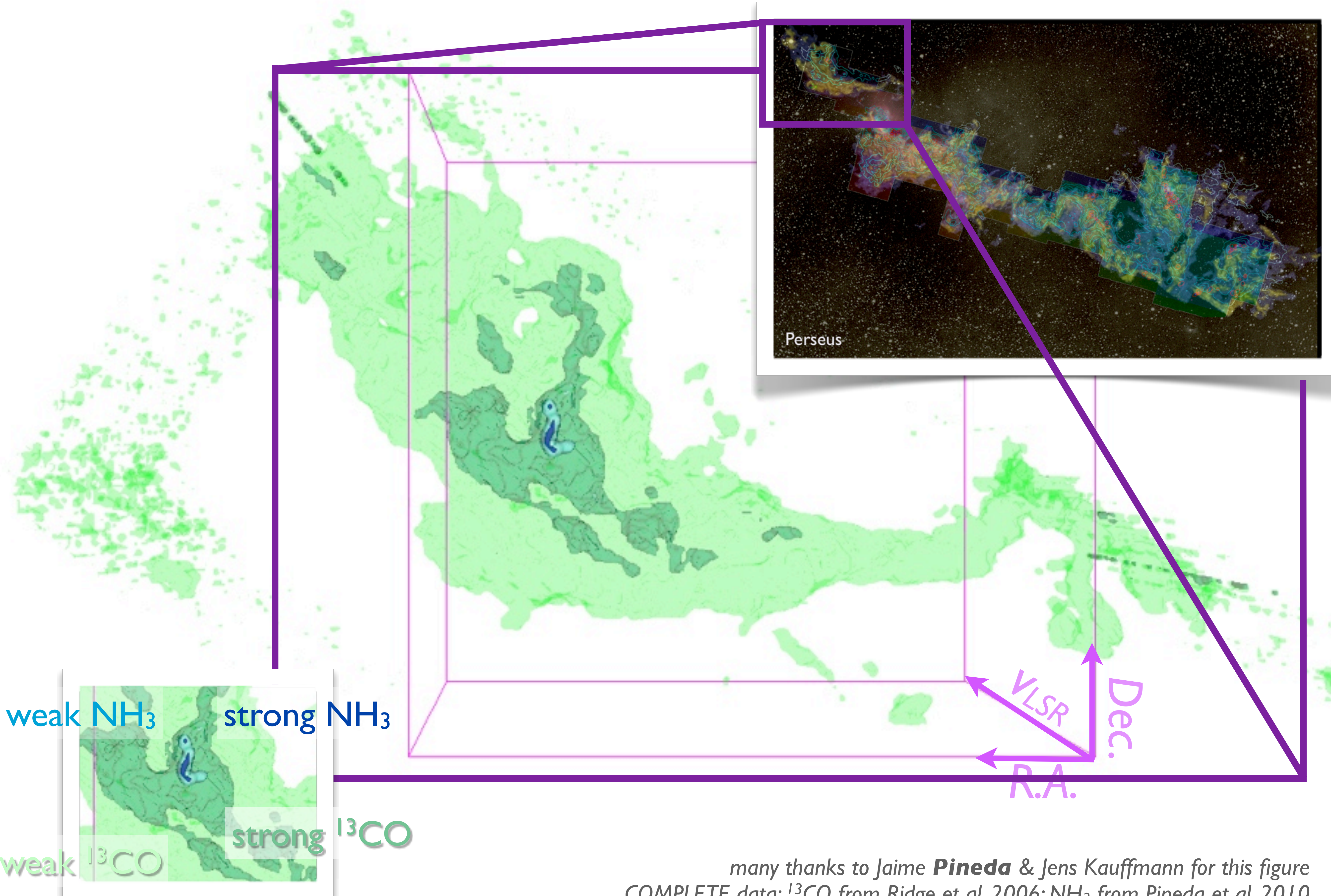


*many thanks to Jaime **Pineda** & Jens Kauffmann for this figure*
*COMPLETE data: $^{13}CO$ from Ridge et al. 2006; $NH_3$ from Pineda et al. 2010*

# STRONG Evidence for Coherence in Dense Cores

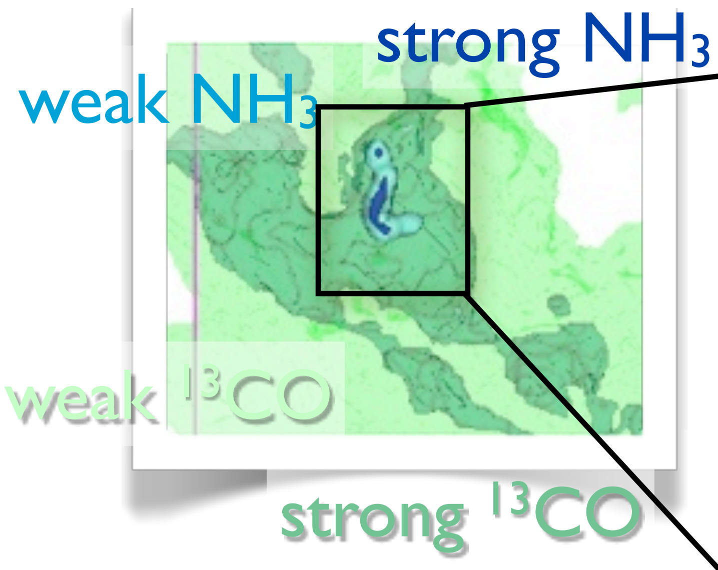


greyscale shows $NH_3$ velocity dispersion,
arrows show gradient in dispersion

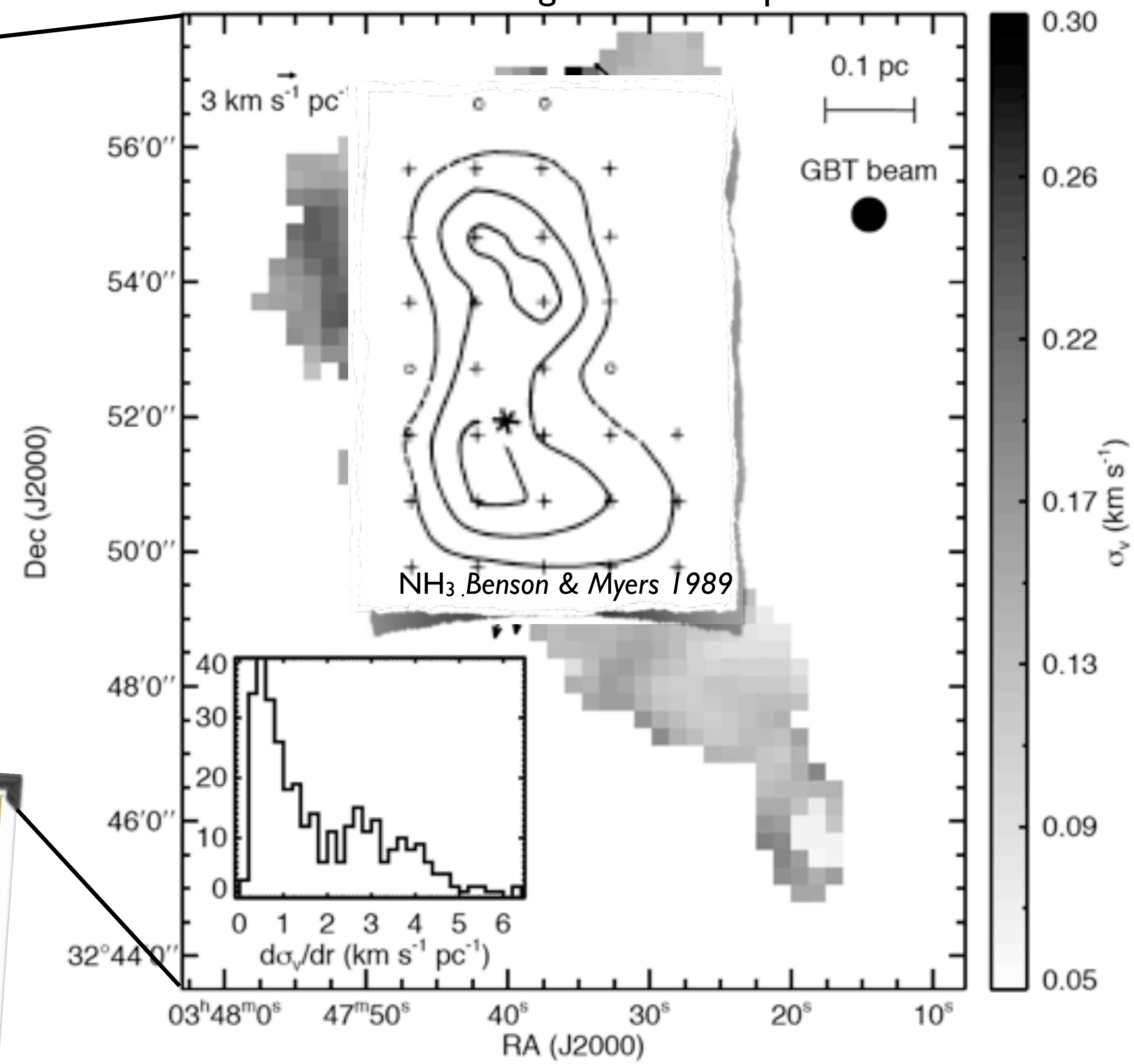


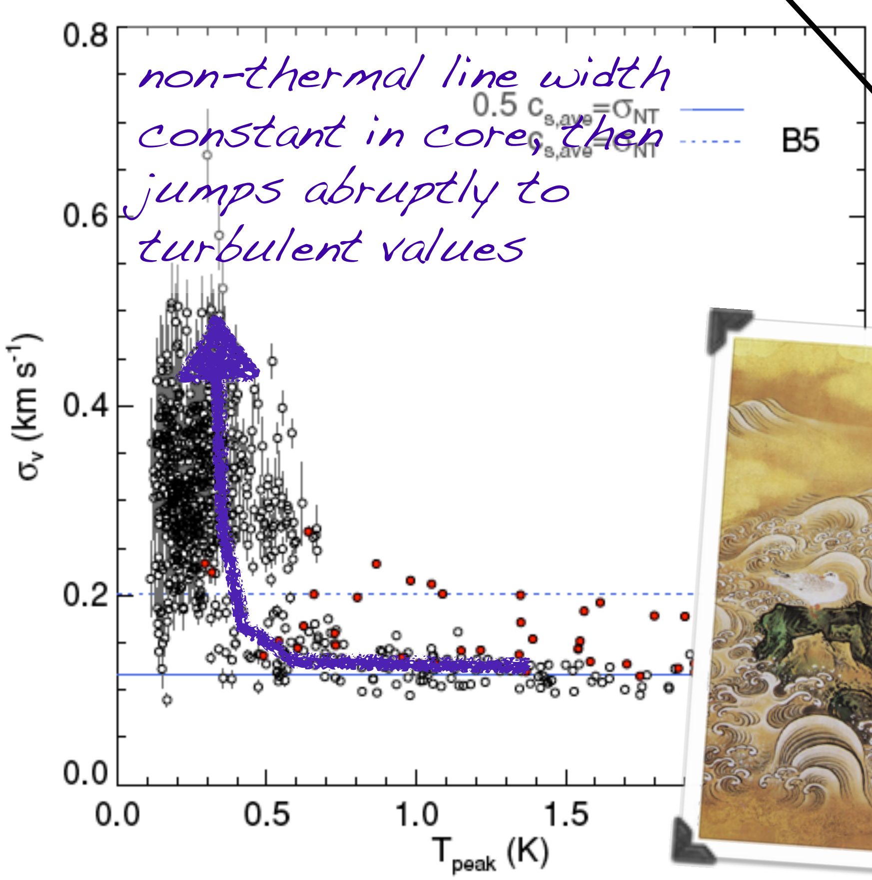


*GBT $NH_3$ observations of the B5 core (Pineda et al. 2010)*

1. At what scales does gravity matter?

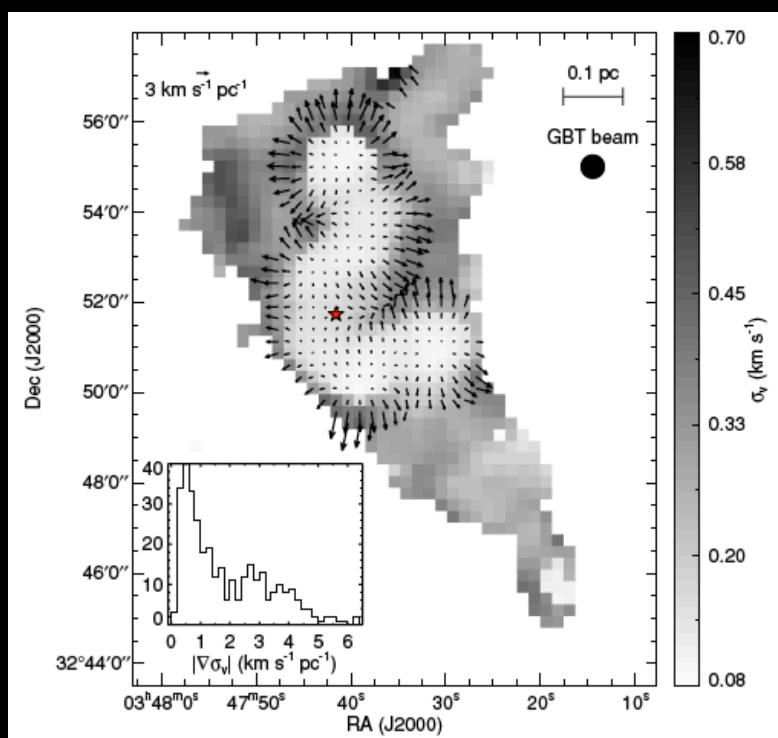


"Transition" so sharp the GBT cannot resolve it.

We need EVLA...

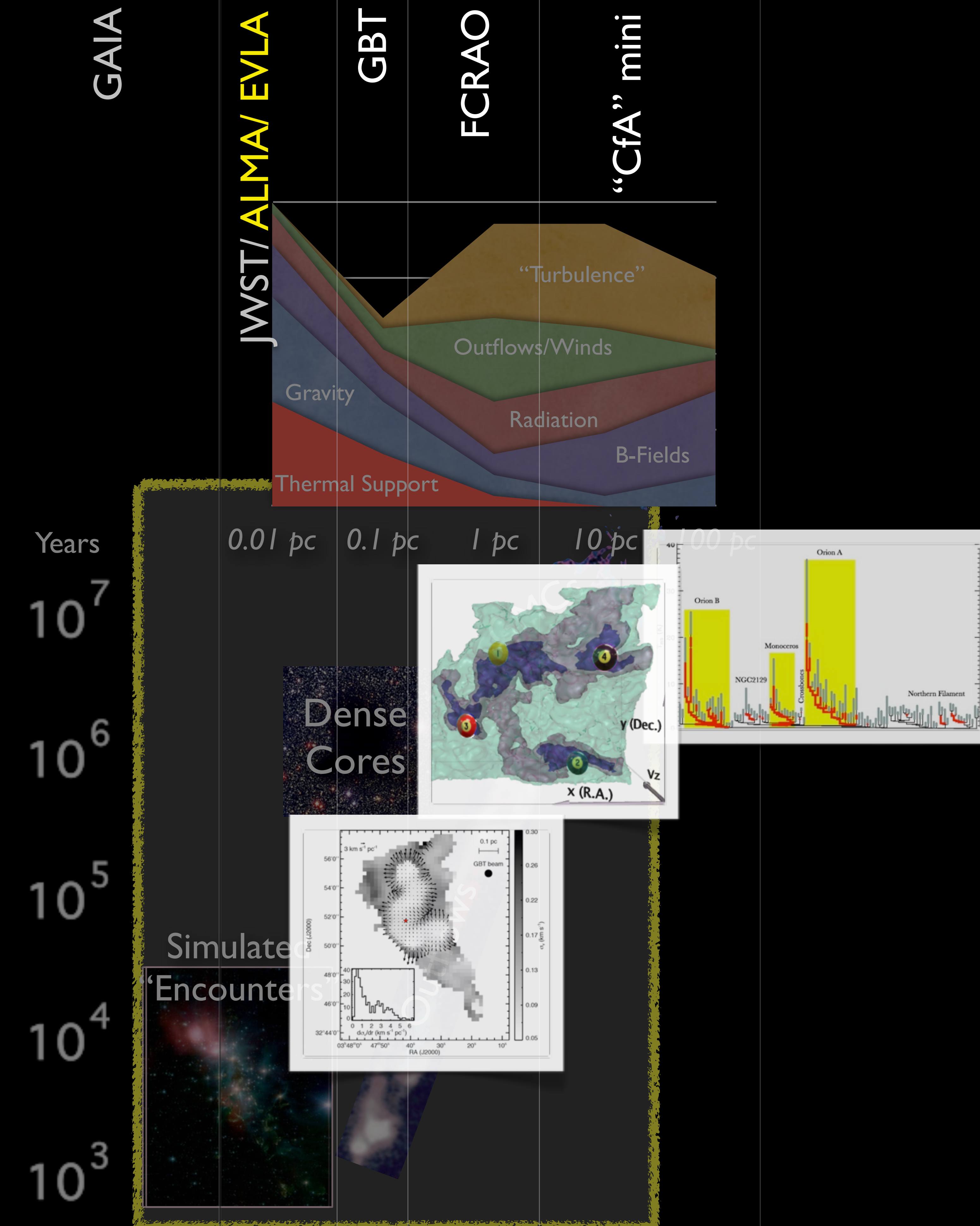

# Thermal Fragmentation *in* Bound Coherent Cores?!

*Thank you EVLA!*

The Astrophysical Journal Letters, 739:L2 (5pp), 2011 September 20

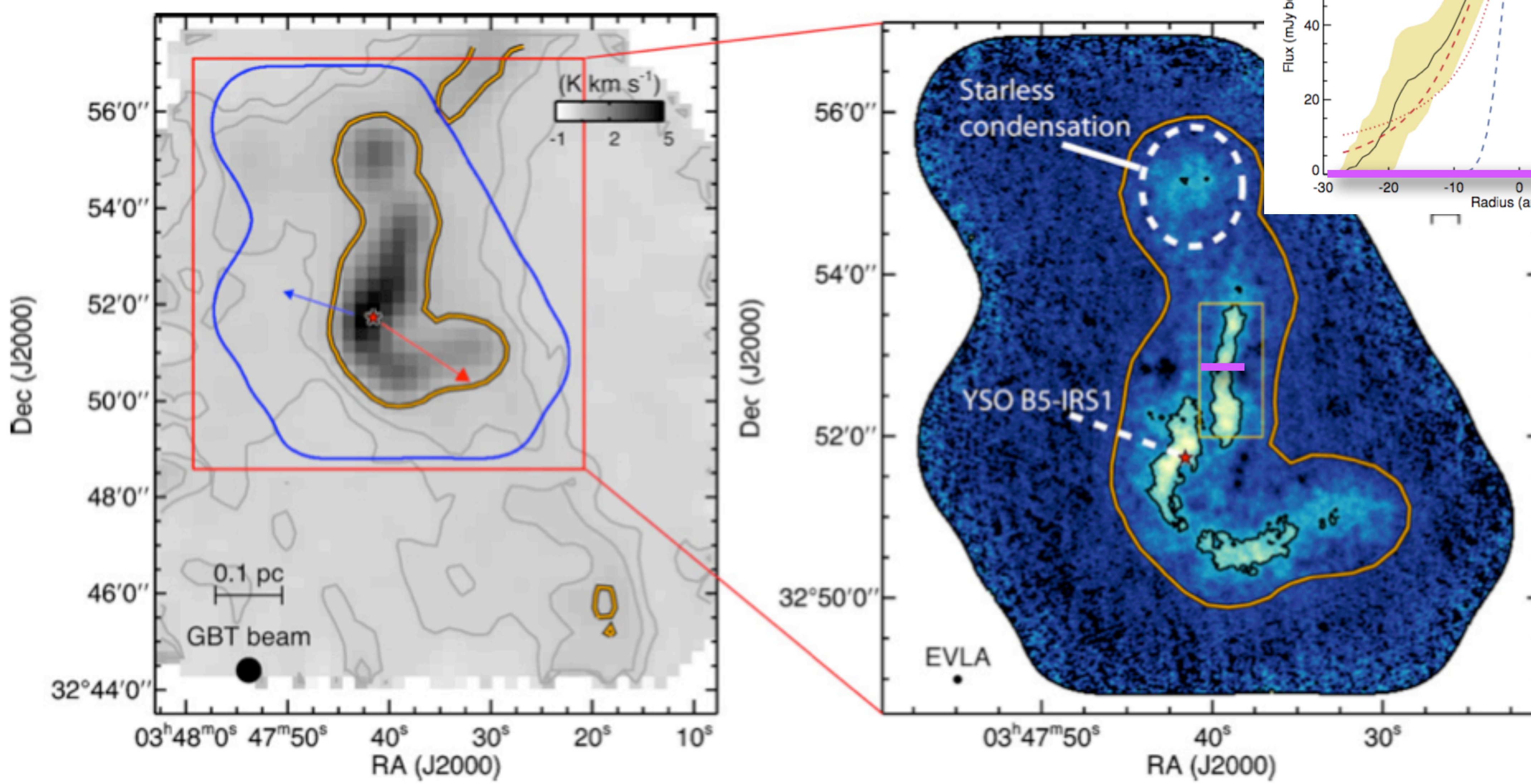


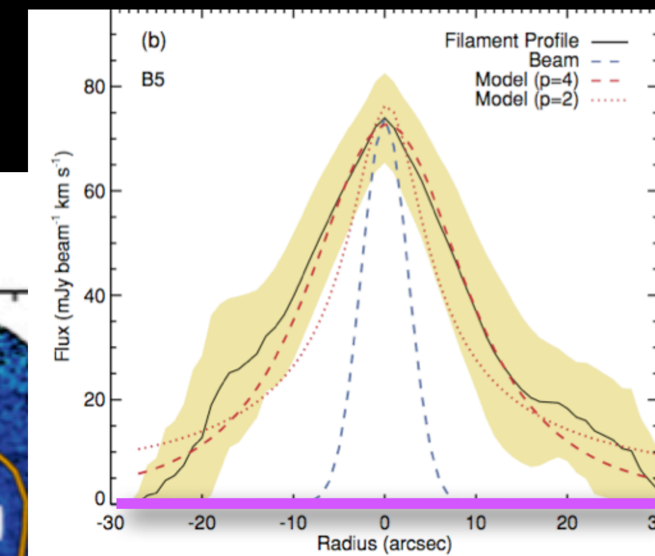


**Figure 1.** Left panel: integrated intensity map of B5 in $NH_3$ (1,1) obtained with GBT. Gray contours show the 0.15 and 0.3 K km s$^{-1}$ level in $NH_3$ (1,1) integrated intensity. The orange contours show the region in the GBT data where the non-thermal velocity dispersion is subsonic. The young star, B5–IRS1, is shown by the star in both panels. The outflow direction is shown by the arrows. The blue contour shows the area observed with the EVLA and the red box shows the area shown in the right panel. Right panel: integrated intensity map of B5 in $NH_3$ (1,1) obtained combining the EVLA and GBT data. Black contour shows the 50 mJy beam$^{-1}$ km s$^{-1}$ level in $NH_3$ (1,1) integrated intensity. The yellow box shows the region used in Figure 4. The northern starless condensation is shown by the dashed circle.

*Pineda et al. 2011*

# 3 Questions

2. What
**star**
do to

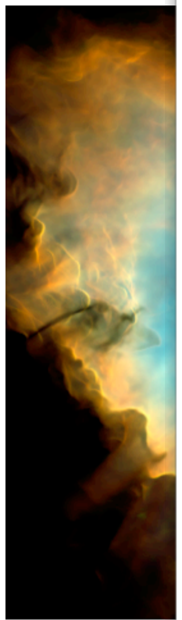

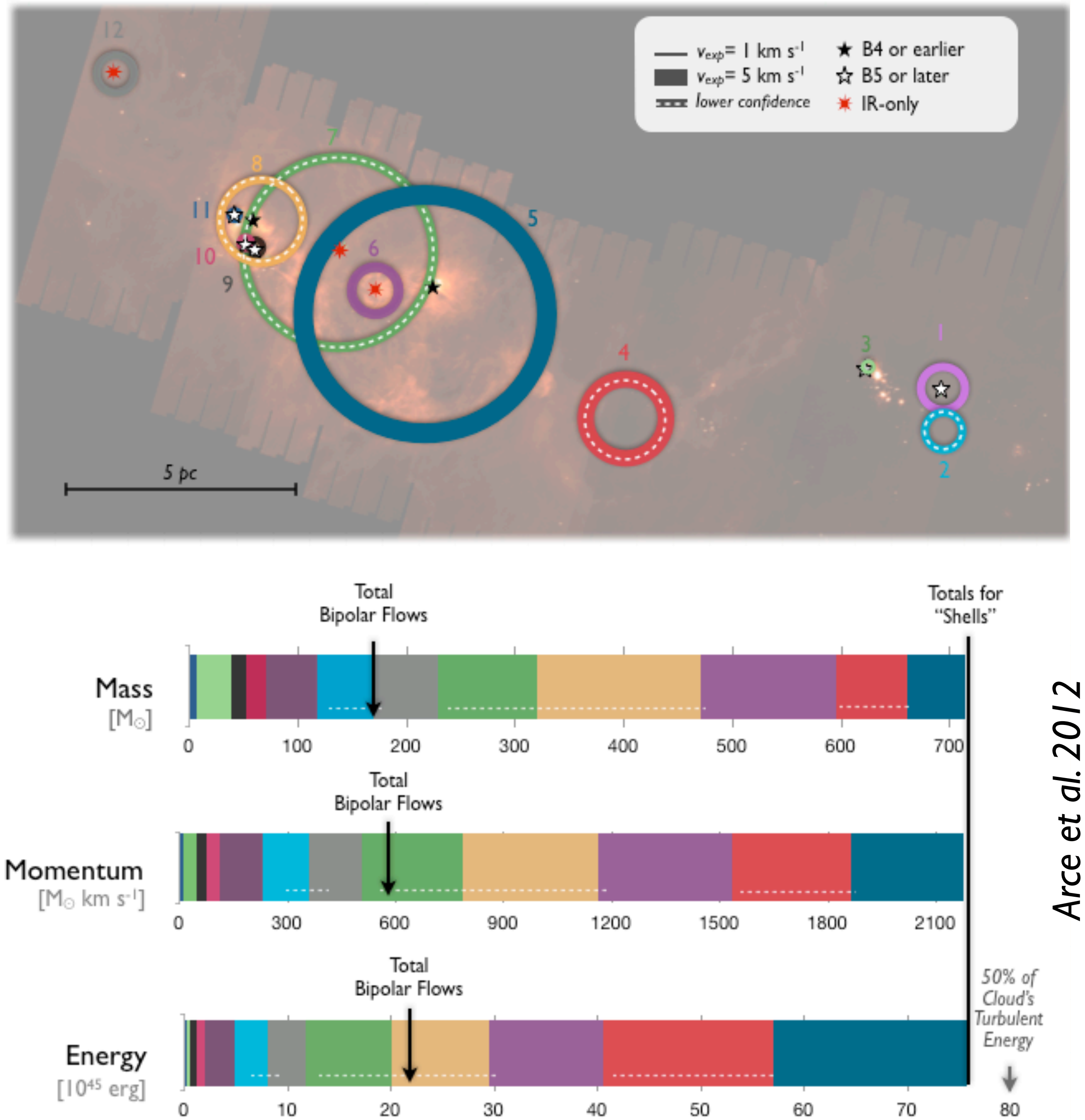


+ "tasty" approaches to answers

Monday, March 12, 2012

# What Stars can do to the ISM

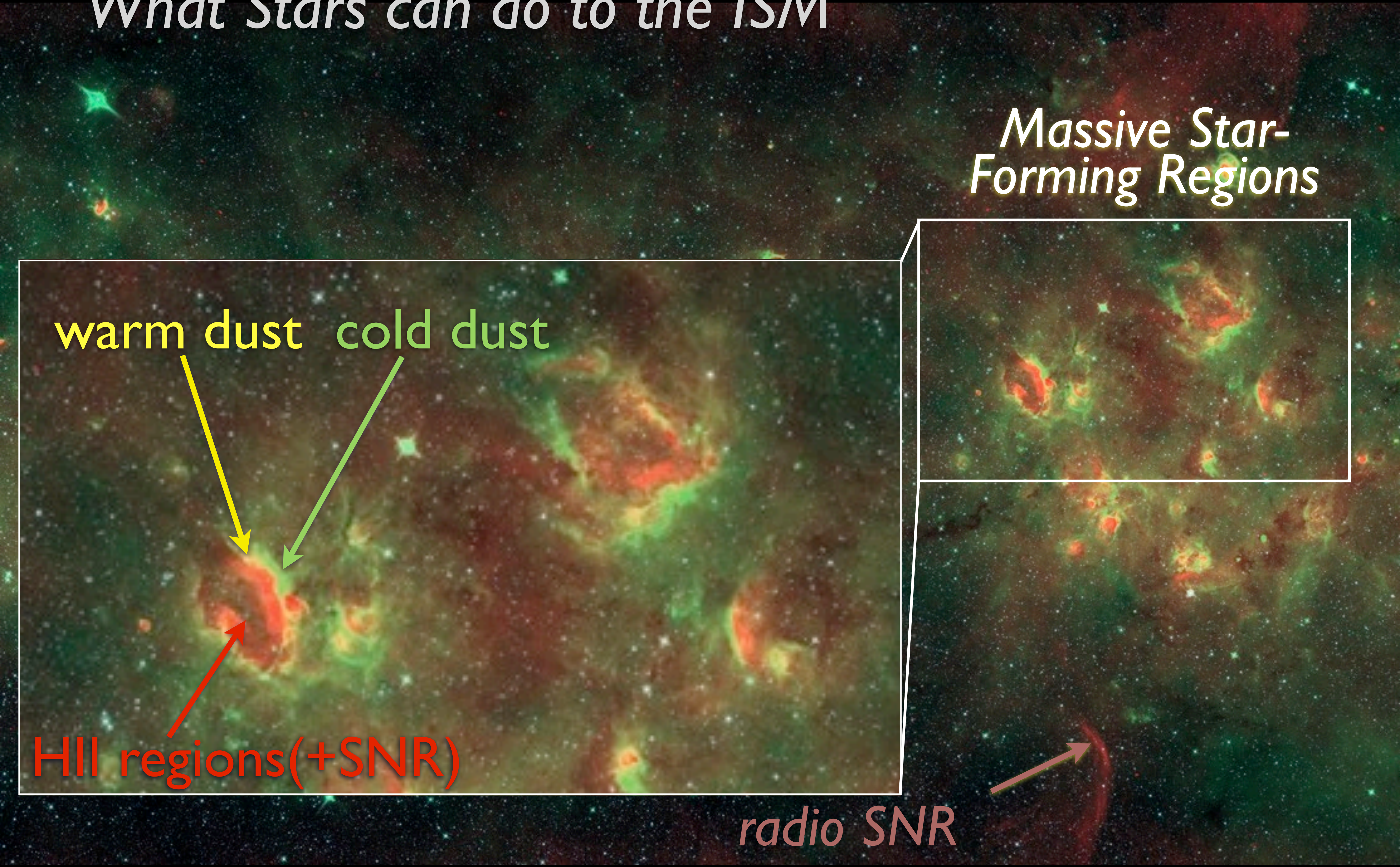


*20 cm VLA from MAGPIS (Helfand et al. 2006) & MIR from Spitzer GLIMPSE (see Churchwell et al.)*
3.6, 4.5, 8.0, 20cm *(Luptonized, see Lupton et al. 2004)*
*image "height" is 1.6 degrees (e.g. 140 pc at 5 kpc)*

# Evolution of an HII Region in a Turbulent Medium

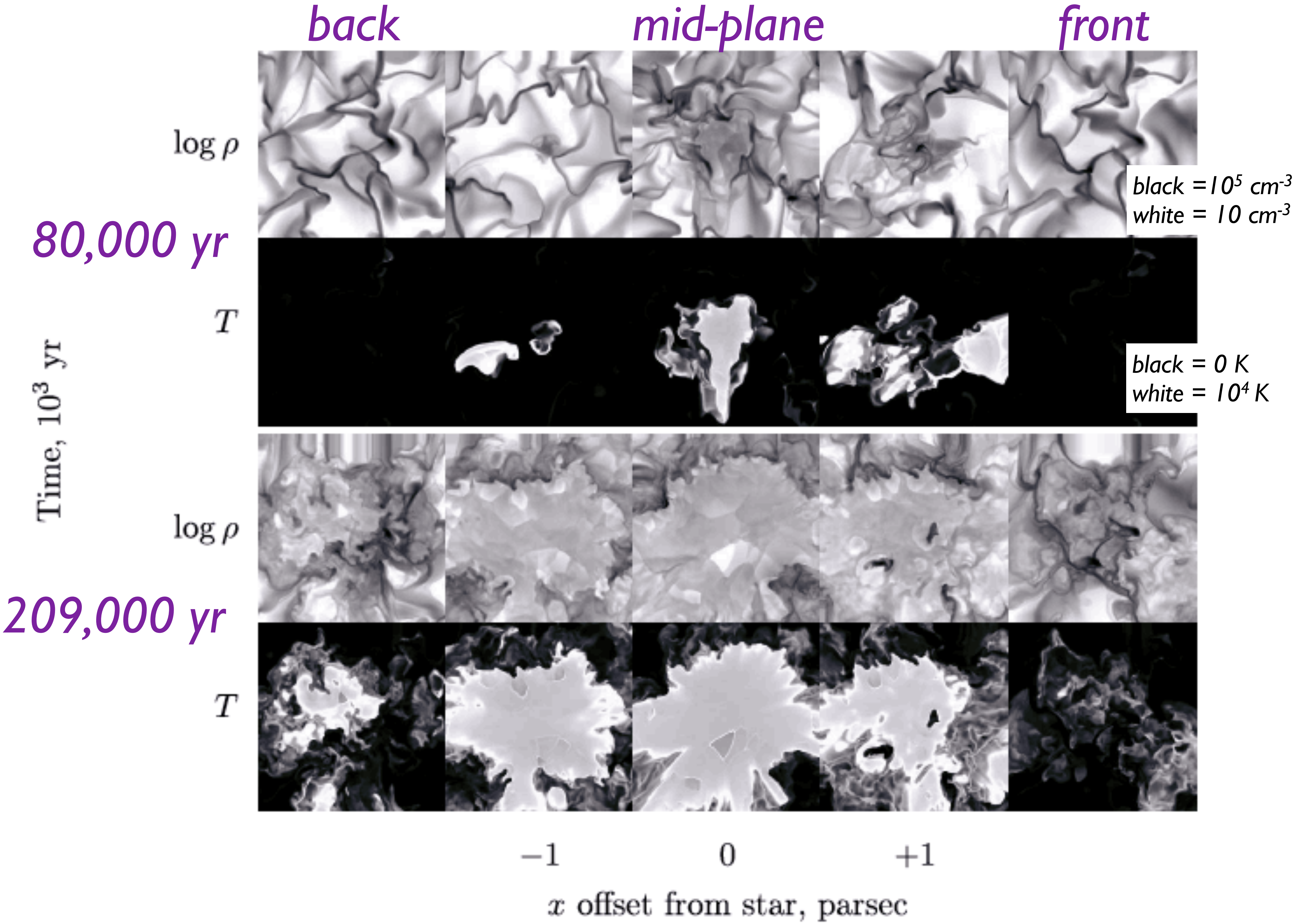


*from S.J.Arthur 2007*

# M17

Hubble image of the Swan Nebula
Photograph courtesy of NASA/STSCI/Jeff Hester, Arizona State University

NATIONAL GEOGRAPHIC

# Tasting "M17"...

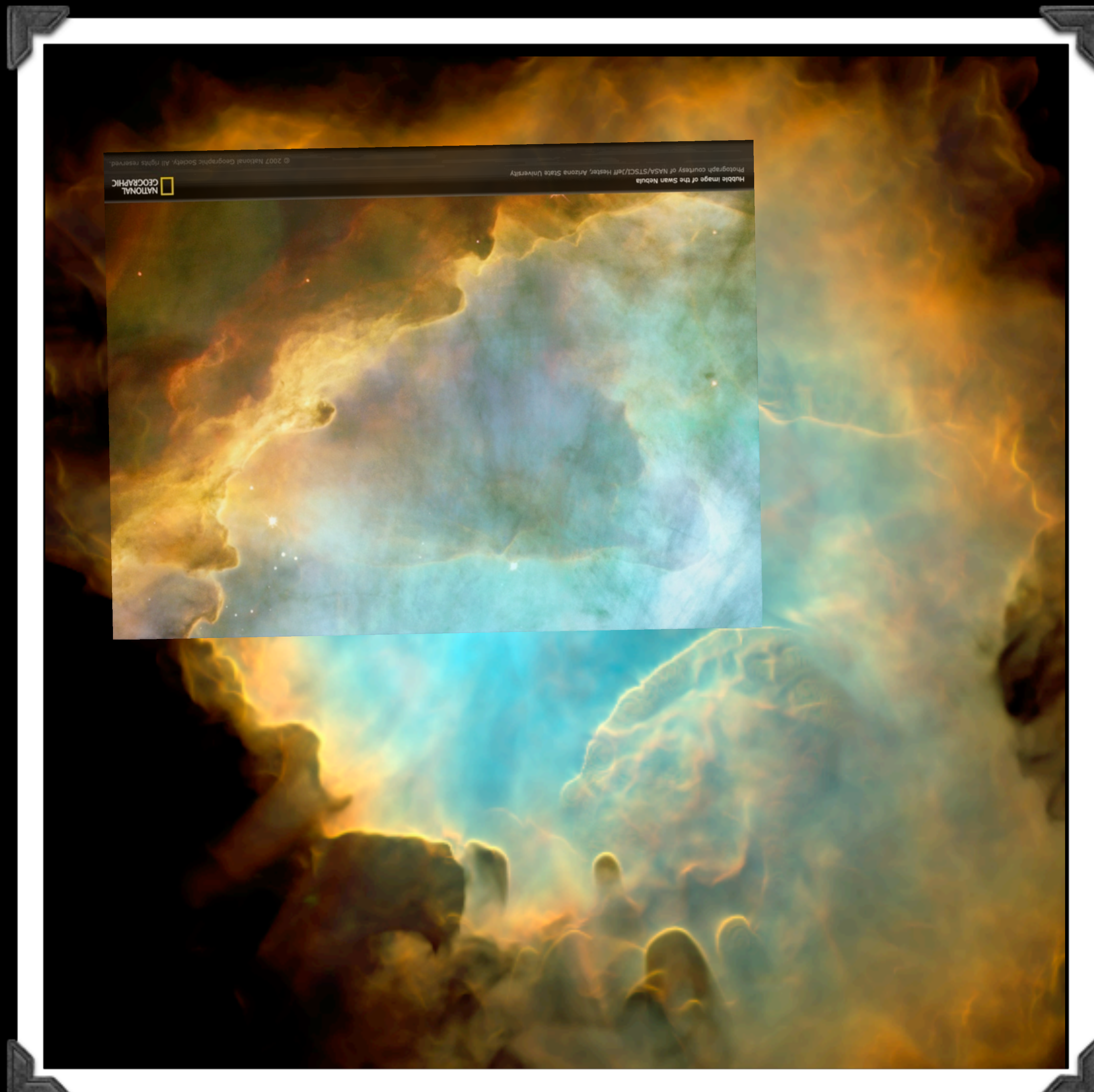

*Synthetic [OIII], Hα and [NII] emission-line image from a $512^3$ numerical simulation: Mellema, Henney, Arthur & Vàzquez-Semadeni 2009*

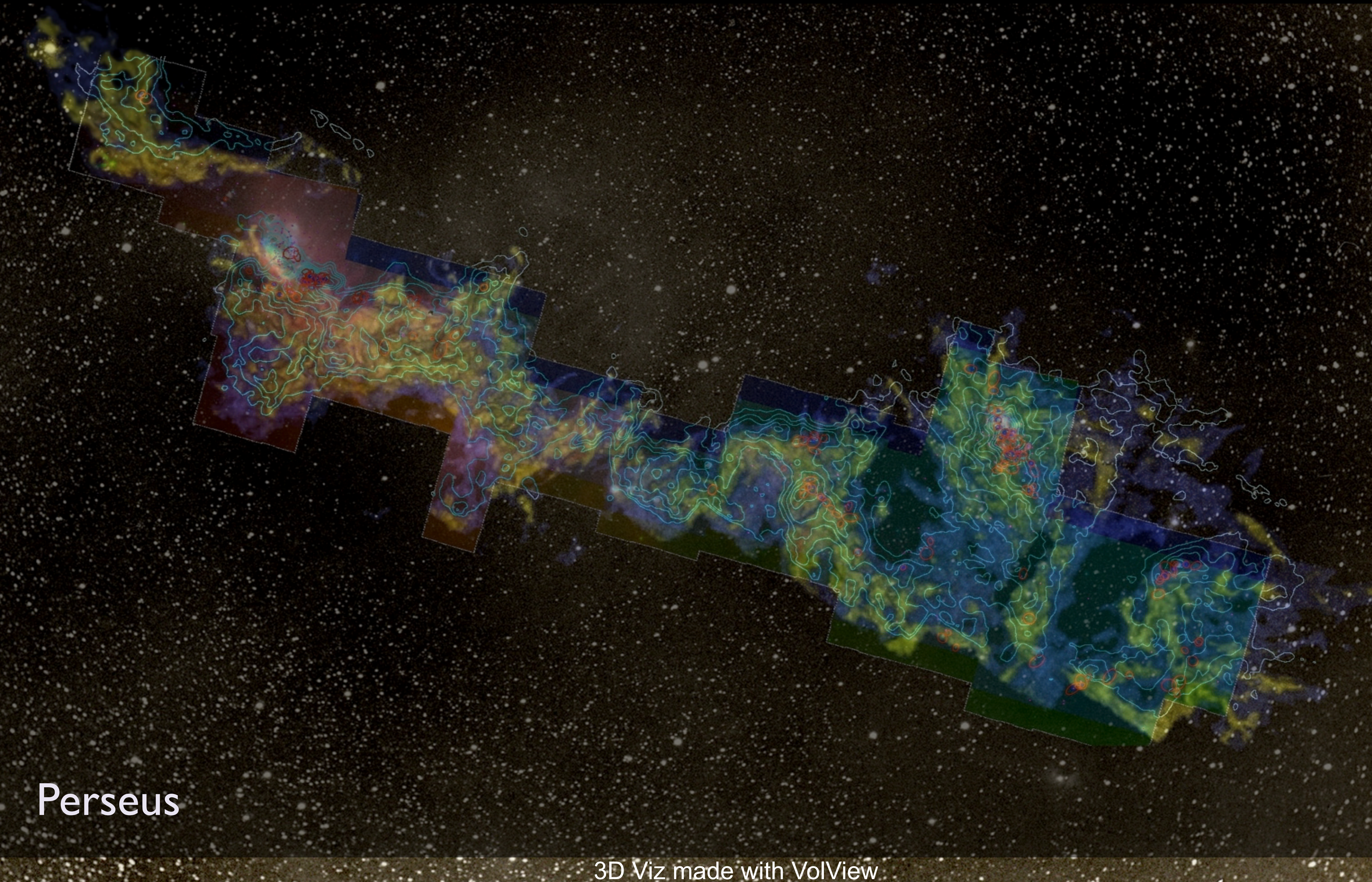
Perseus
3D Viz made with VolView

# “CPOCs”

## **C**OMPLETE **P**erseus **O**utflow **C**andidates

*Note: I did not make up that name!*

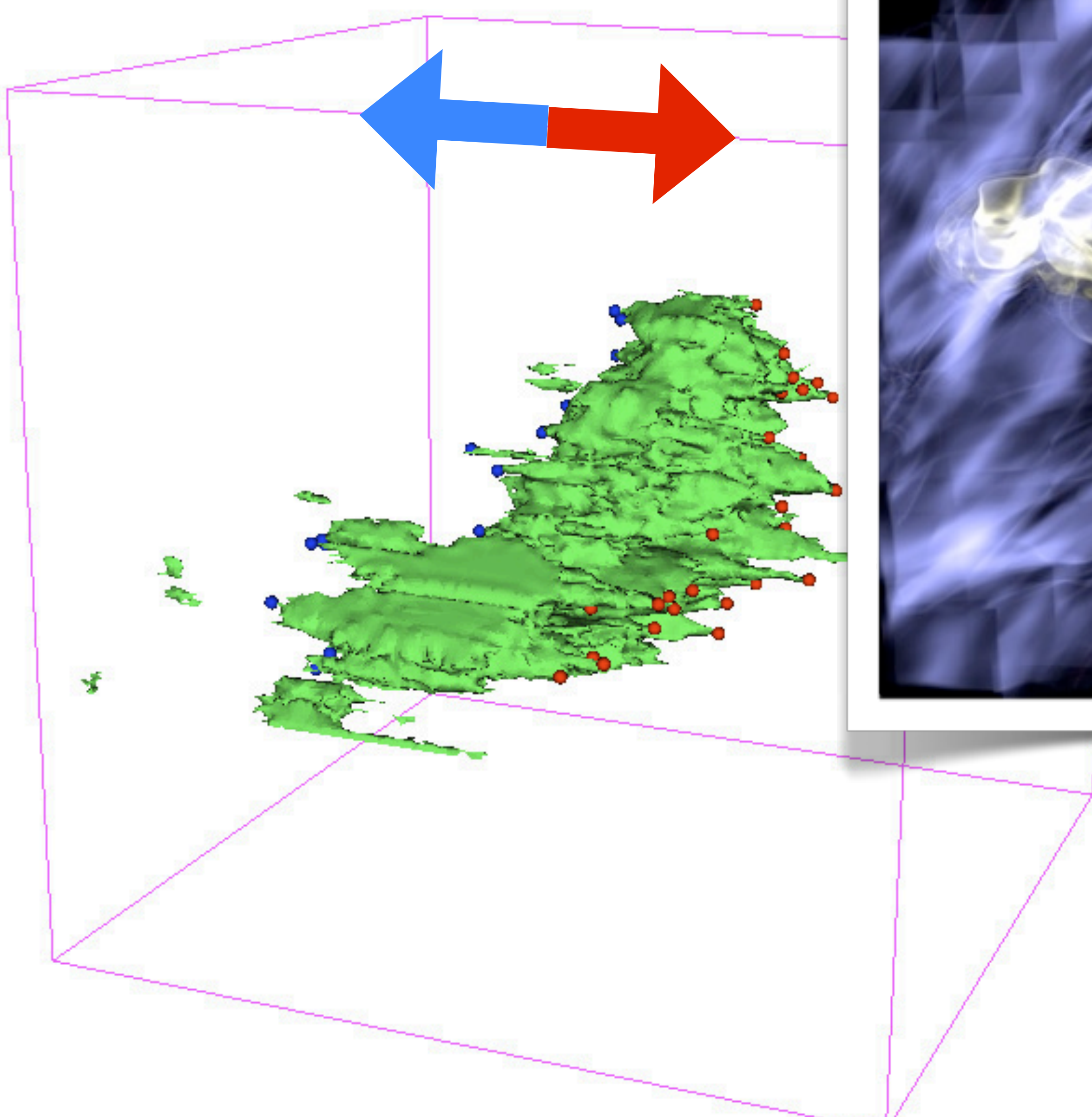

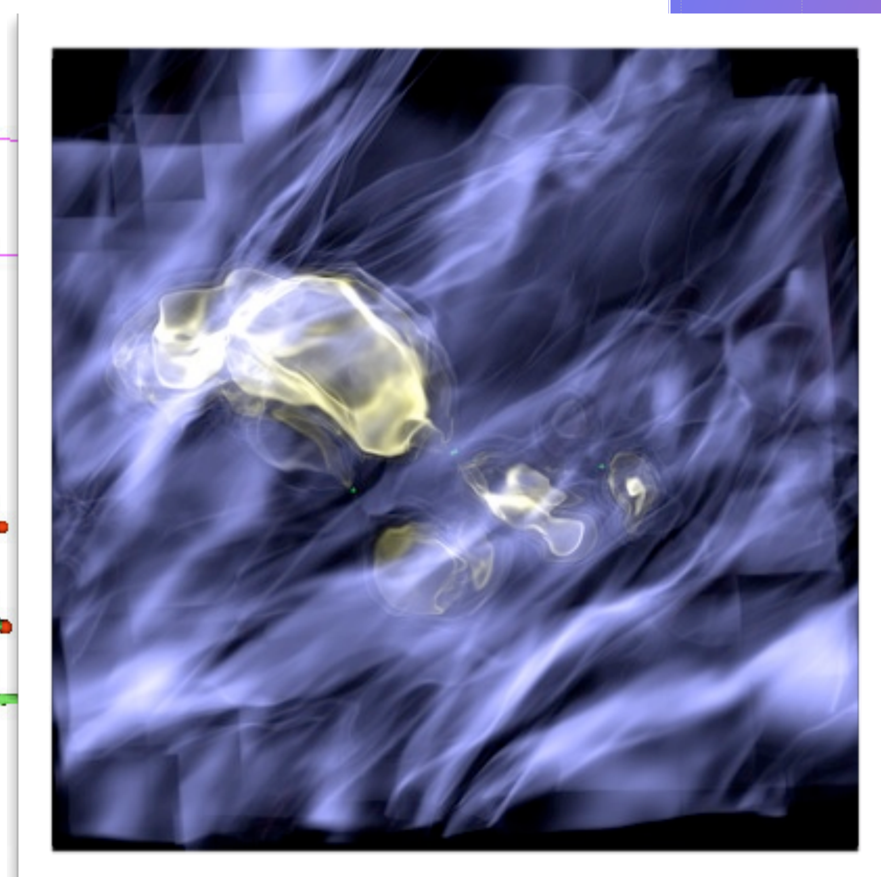

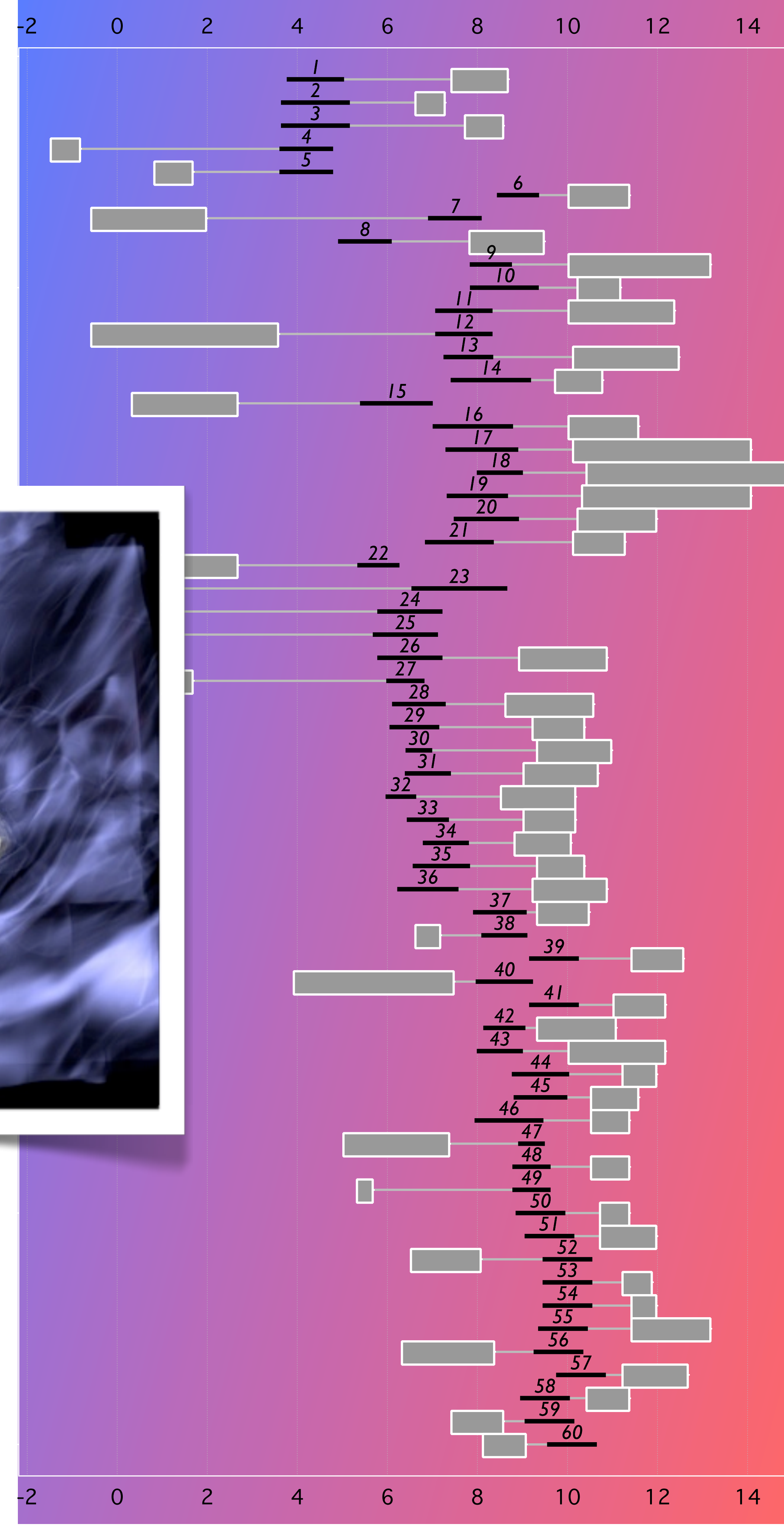


*Arce et al. 2010; inset based on Offner et al. 2011*

# Perseus Bipolar Outflows

*Arce et al. 2010a*

**Table 5**
Physical Parameters of Active Star-forming Regions in Persesus

| Name | $M_{reg}$[a] ($M_\odot$) | $R_{reg}$[b] (pc) | $\Delta v$[c] (km s$^{-1}$) | $T_{ex}$[d] (K) | $v_{esc}$[e] (km s$^{-1}$) | $E_{grav}$[f] ($10^{46}$ erg) | $E_{turb}$[g] ($10^{45}$ erg) | $t_{diss}$[h] ($10^5$ yr) | $L_{turb}$[i] ($10^{32}$ erg s$^{-1}$) |
|---|---|---|---|---|---|---|---|---|---|
| L1448 | 150 | 0.6 | 1.9 | 10 | 1.5 | 0.3 | 2.9 | 2.6 | 3.6 |
| NGC 1333 | 1100 | 2.0 | 2.2 | 13 | 2.2 | 5.2 | 28.8 | 5.7 | 15.9 |
| B1-Ridge | 210 | 0.7 | 1.9 | 13 | 1.6 | 0.5 | 4.1 | 3.1 | 4.1 |
| B1 | 430 | 0.9 | 2.1 | 13 | 2.0 | 1.8 | 10.2 | 2.9 | 11.2 |
| B5 | 420 | 1.4 | 1.5 | 12 | 1.6 | 1.1 | 5.1 | 7.6 | 2.1 |
| IC 348 | 620 | 0.9 | 1.8 | 15 | 2.4 | 3.7 | 10.9 | 3.0 | 11.4 |

**Notes.**
[a] Mass of star-forming region, obtained using the procedure described in Section 5.1.
[b] Radius estimate of the region obtained from the geometric mean of minor and major axes of the extent of the $^{13}$CO integrated intensity emission.
[c] Average velocity width (FWHM) of the $^{13}$CO(1–0) line in the region.
[d] Average excitation temperature of region.
[e] Escape velocity, given by $\sqrt{2GM_{reg}/R_{reg}}$.
[f] Gravitational binding energy given by $GM_{reg}^2/R_{reg}$.
[g] Turbulence energy given by $\frac{3}{16 ln2} M_{reg} \Delta v^2$.
[h] Turbulence dissipation time, see Section 5.2.1.
[i] Turbulence energy dissipation rate give by $E_{turb}/\tau_{diss}$.

**Table 7**
Quantitative Assessment of Outflow Impact on Star-forming Regions

| Name | $E_{flow}/E_{turb}$ | $r_L = L_{flow}/L_{turb}$ | $E_{flow}/E_{grav}$ | $M_{esc}$[a] ($M_\odot$) | $M_{esc}/M_{reg}$ |
|---|---|---|---|---|---|
| L1448 | 0.41 | 2.1 | 0.40 | 15 | 0.10 |
| NGC 1333 | 0.30 | 3.4 | 0.17 | 76 | 0.07 |
| B1-Ridge | 0.24 | 1.5 | 0.20 | 14 | 0.07 |
| B1 | 0.30 | 1.7 | 0.17 | 21 | 0.05 |
| IC 348 | 0.14 | 0.8 | 0.04 | 23 | 0.04 |
| B5 | 0.80 | 12.4 | 0.37 | 98 | 0.23 |

**Note.** [a] Escape mass, given by $M_{esc} = P_{out}/v_{esc}$ (see Section 5.2.3).

**Table 6**
Total Outflow Mass, Momentum, Energy, and Luminosity in Star-forming Regions

| Name | $M_{flow}$[a] ($M_\odot$) | $P_{flow}$[a] ($M_\odot$ km s$^{-1}$) | $E_{flow}$[a] ($10^{44}$ erg) | $L_{flow}$[b] ($10^{32}$ erg s$^{-1}$) |
|---|---|---|---|---|
| L1448 | 1.0/5 | 3.1/21.7 | 1.2/12 | 8 |
| NGC 1333 | 5.0/25 | 17.4/121.8 | 6.9/69 | 44 |
| B1-Ridge | 1.1/5.5 | 3.2/22.4 | 1.0/10 | 6 |
| B1 | 1.5/7.5 | 6.2/43.4 | 3.1/31 | 20 |
| IC 348 | 4.2/21 | 7.7/53.9 | 1.5/15 | 10 |
| B5 | 12.8/64 | 22.3/156.1 | 4.1/41 | 26 |

**Notes.**
[a] Values before and after the slash are the original estimates and the estimates adjusted by the correction factor, respectively (see Section 5.1).
[b] Outflow luminosity, $L_{flow} = E_{flow}/\tau_{flow}$, obtained using the value of the total outflow kinetic energy adjusted by the correction factor and using an average outflow timescale of $5 \times 10^4$ yr.

*Typically 20% binding energy in flows.*

## Bottom line

local influence *significant*,

HOMEWRECKERS *not.*


But, we have other options.
Turns out bipolar outflows are nothing
compared to spherical shells...

# “Cinema Arce”

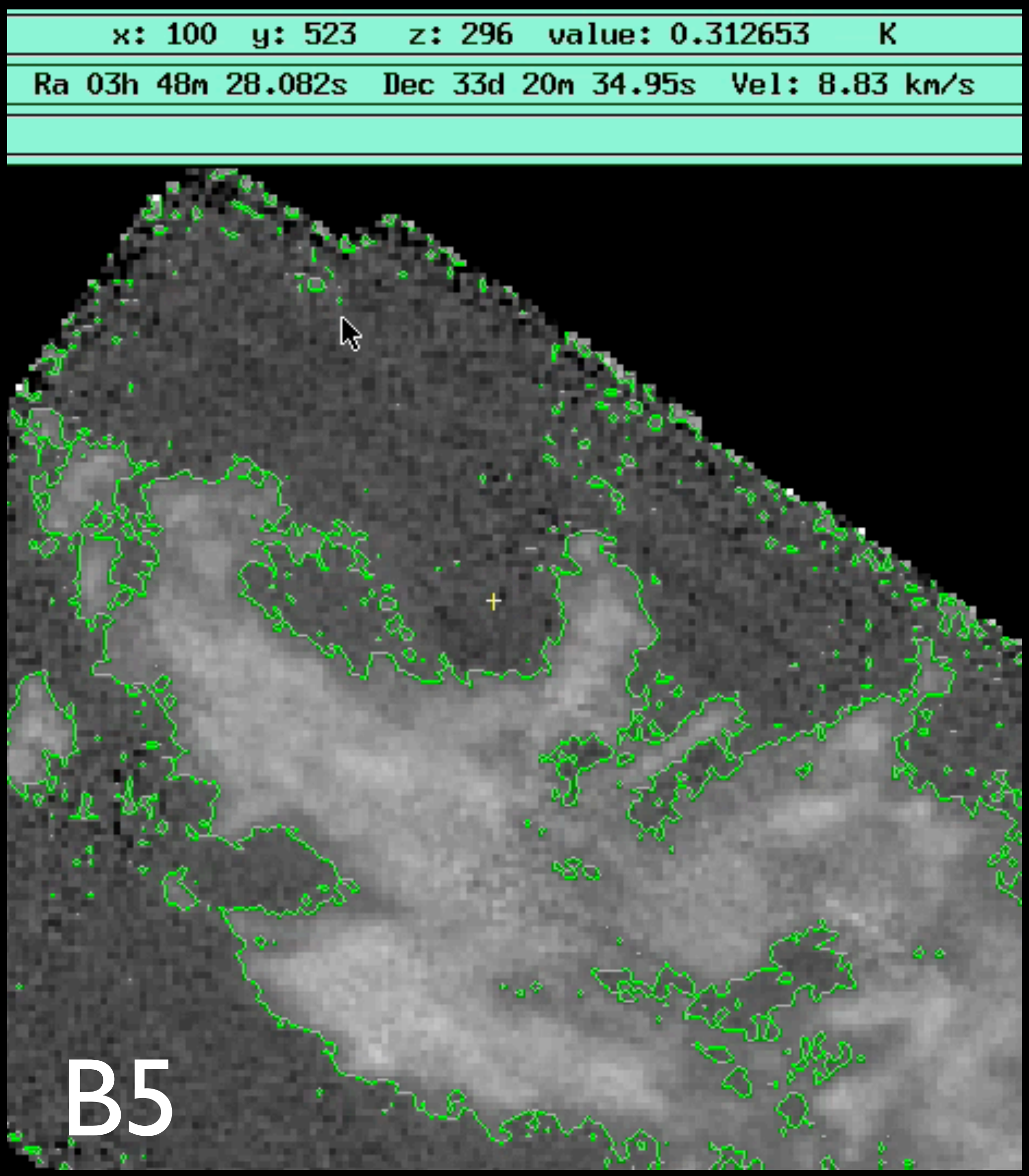
x: 100 y: 523 z: 296 value: 0.312653 K
Ra 03h 48m 28.082s Dec 33d 20m 34.95s Vel: 8.83 km/s
B5

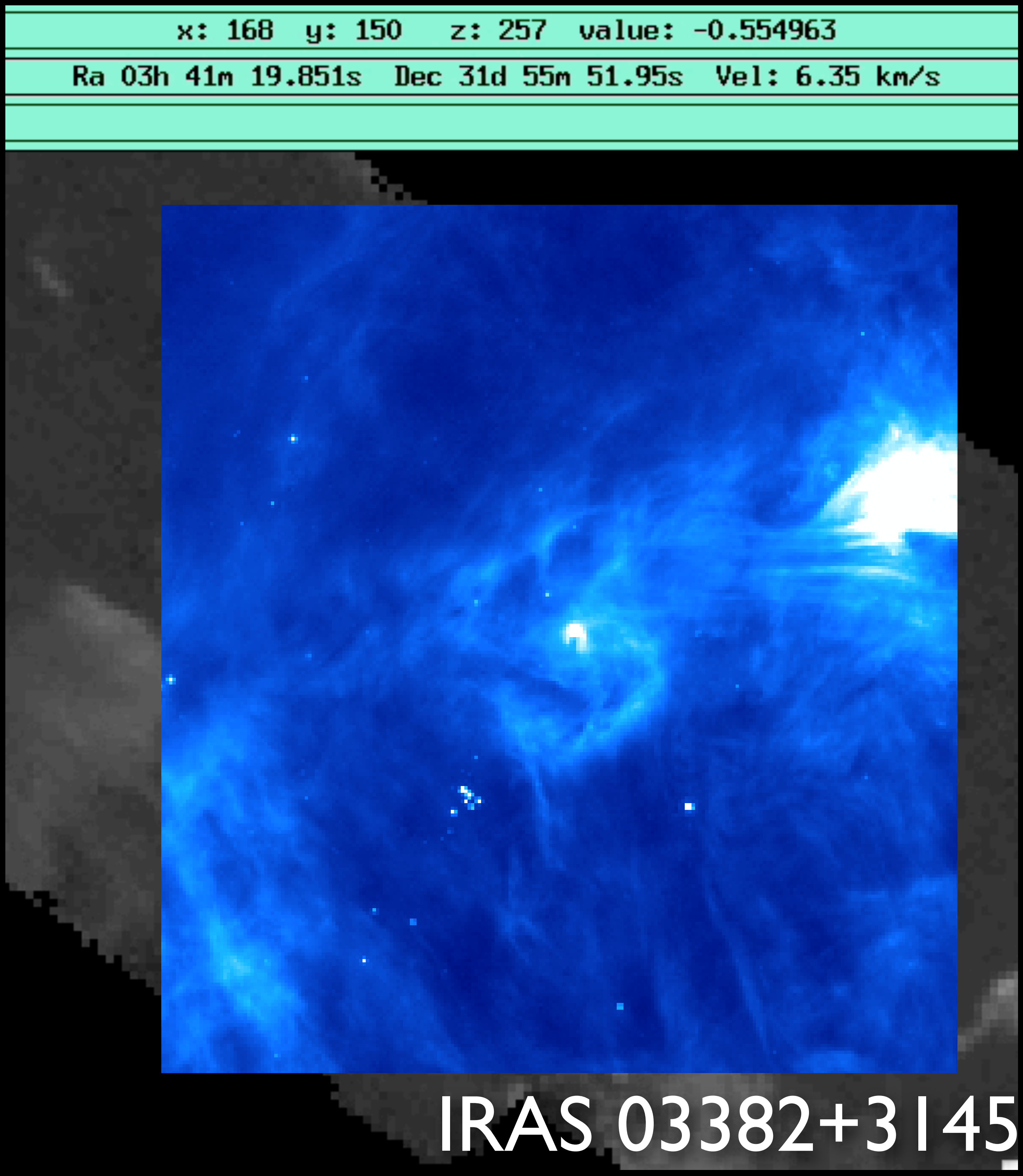
x: 168 y: 150 z: 257 value: -0.554963
Ra 03h 41m 19.851s Dec 31d 55m 51.95s Vel: 6.35 km/s
IRAS 03382+3145

# “Spherical” Outflows

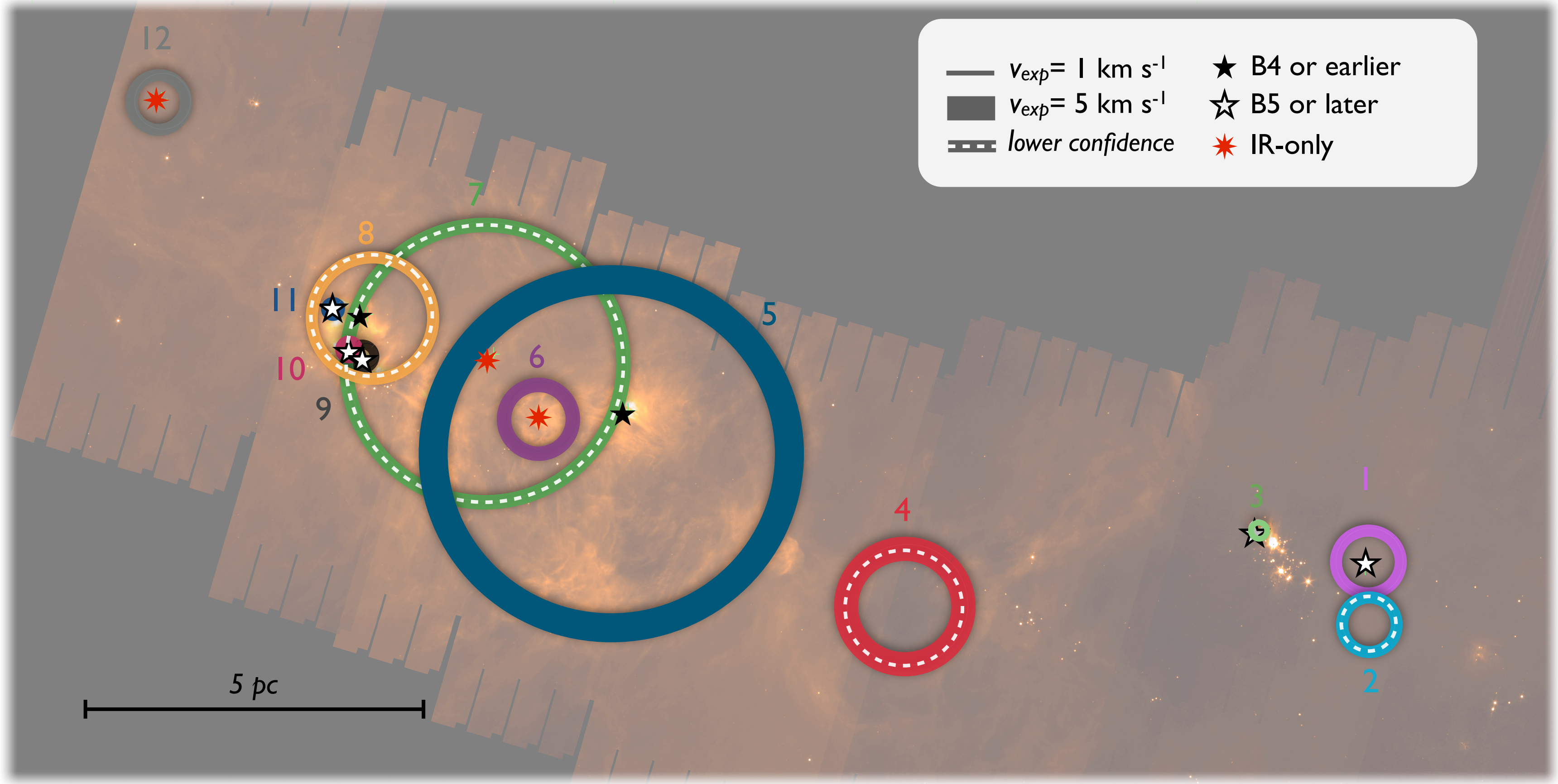


**News Flash**
Spherical shells from young-ish stars may stir molecular clouds (much) MORE than bipolar flows, and B-stars may matter much.

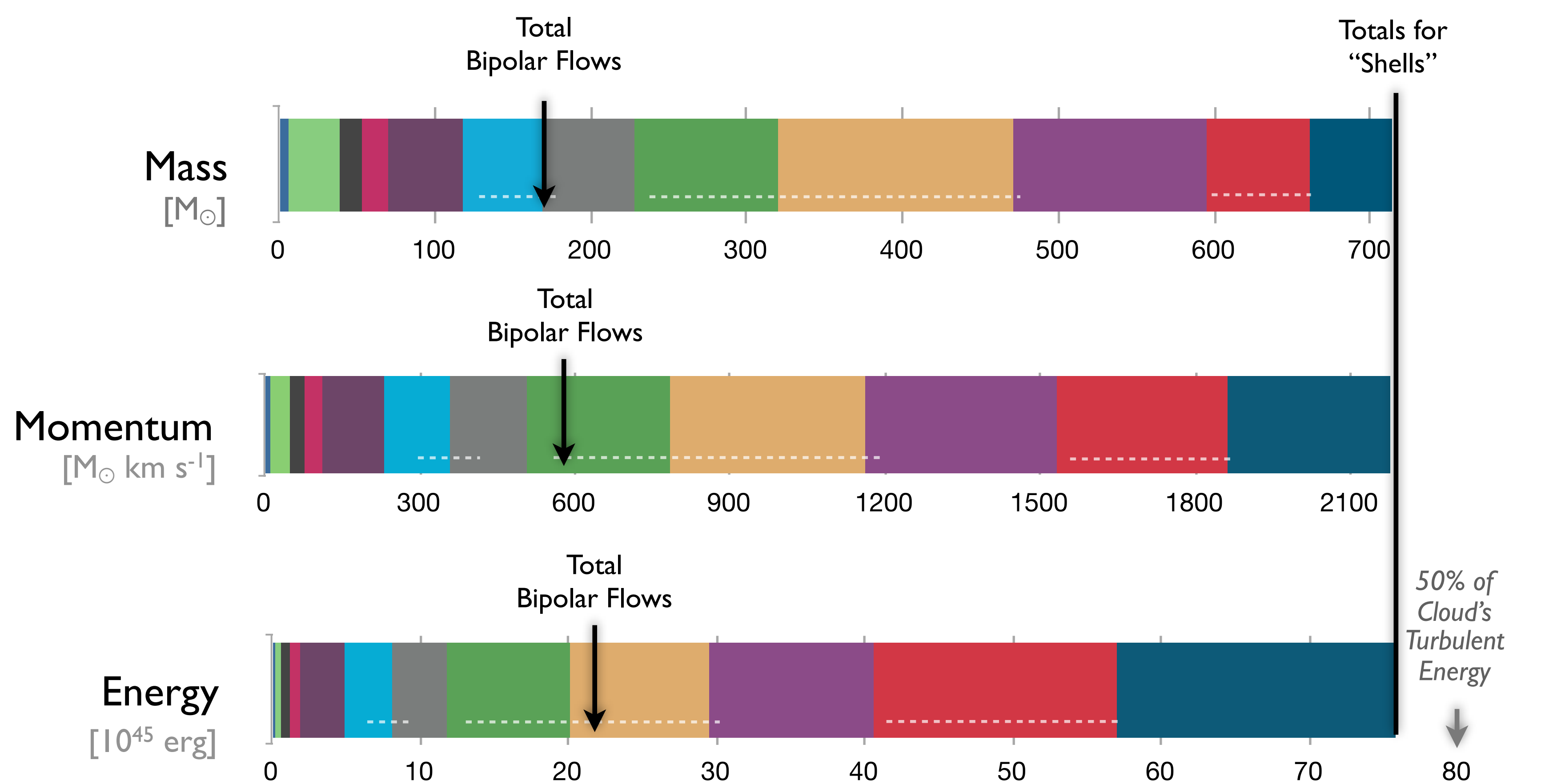


*Arce et al. 2011*

# 3 Questions

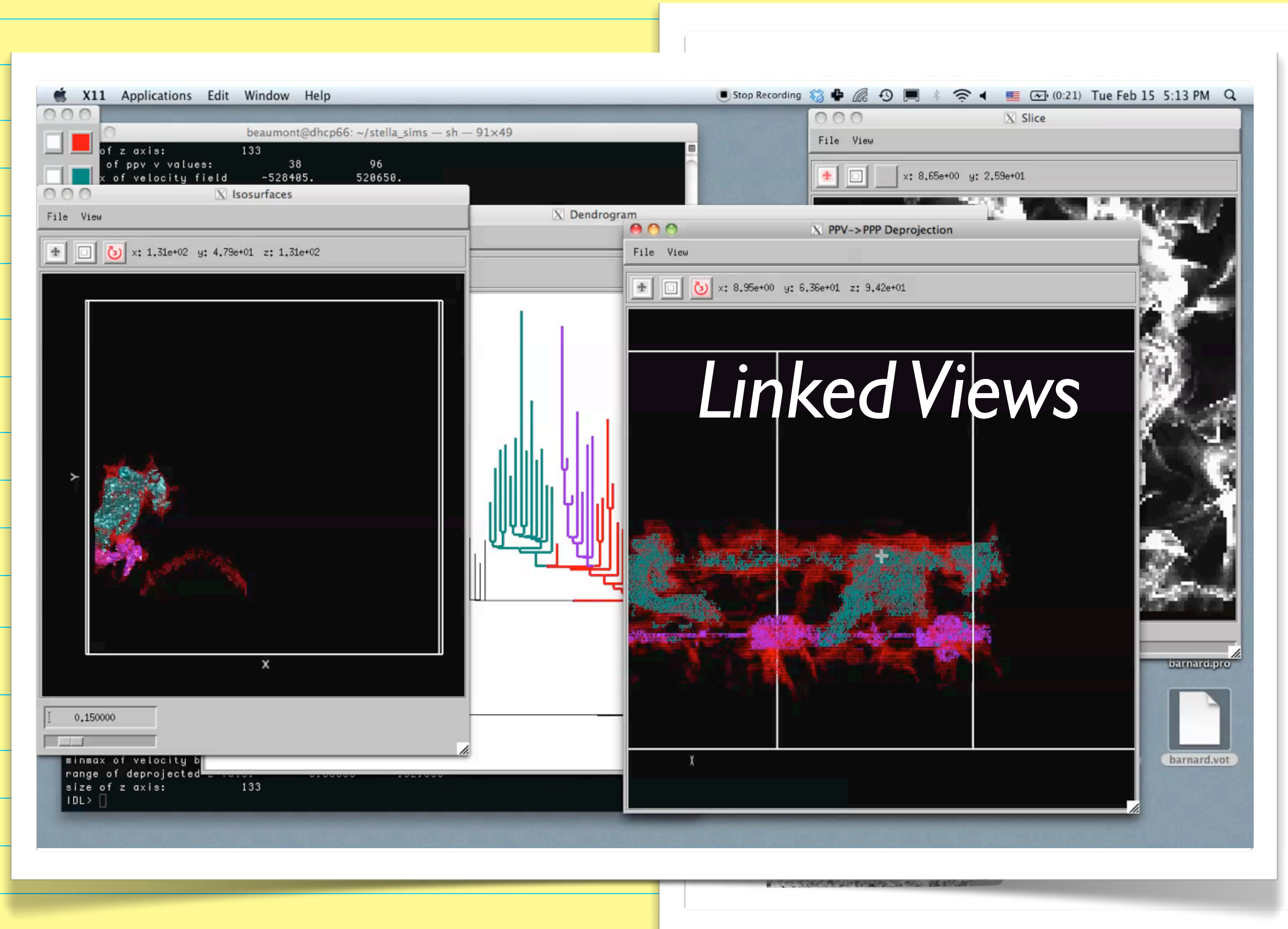


+ "tasty" approaches to answers

# (p-p-v) Case Study

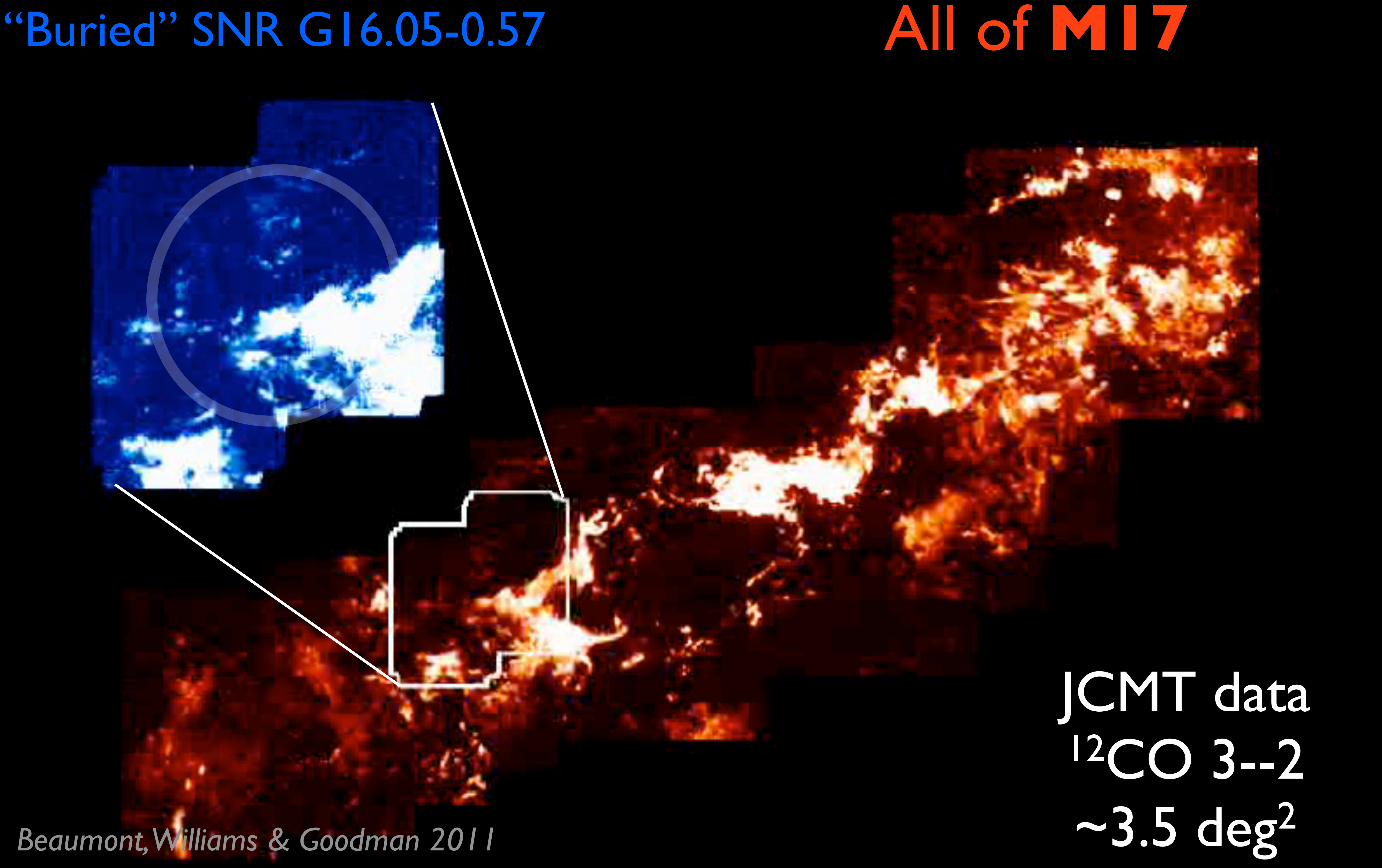

# Support Vector Machines in One Minute (SVM is a kind of "Machine Learning")

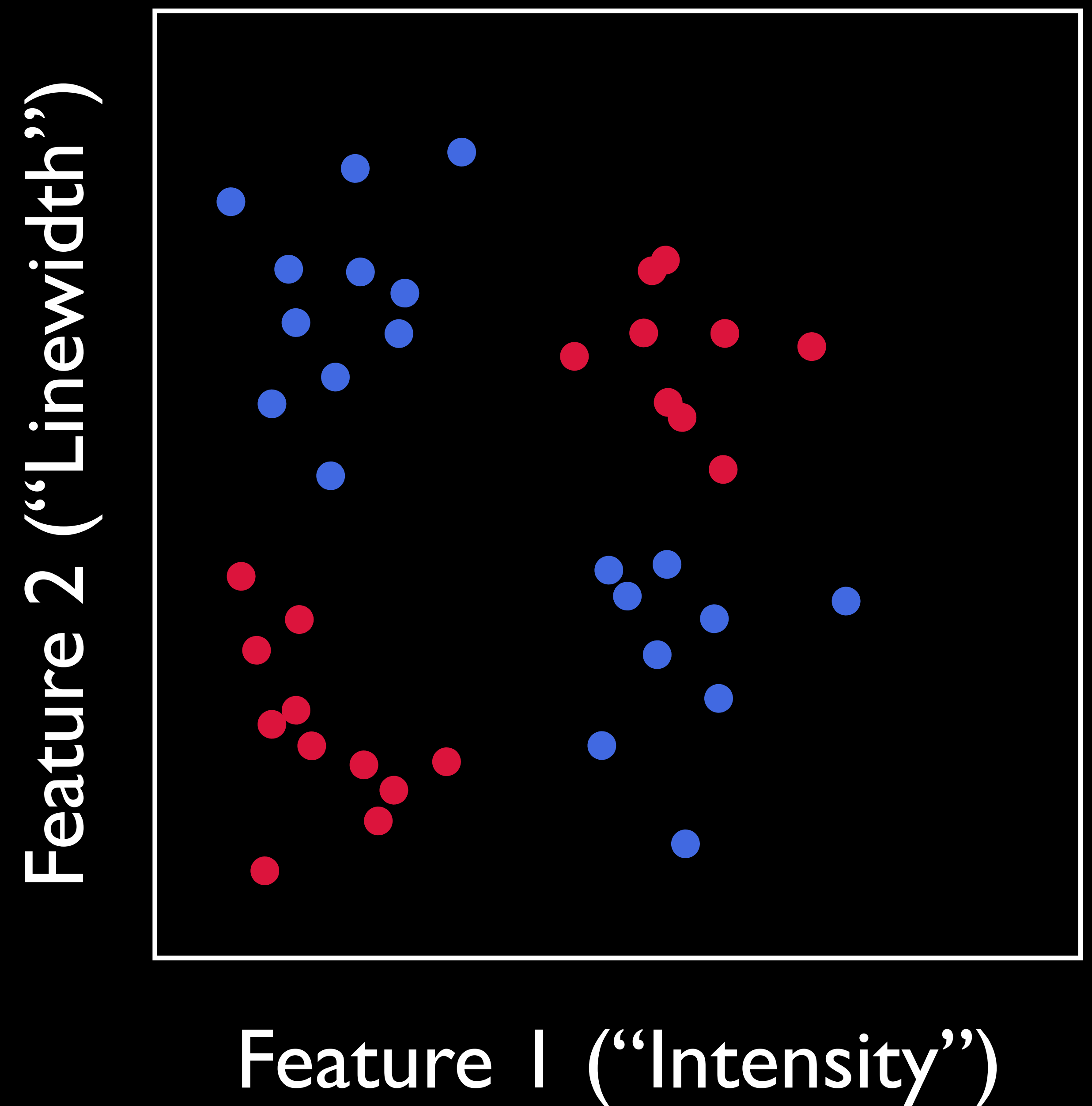

# Support Vector Machines in One Minute

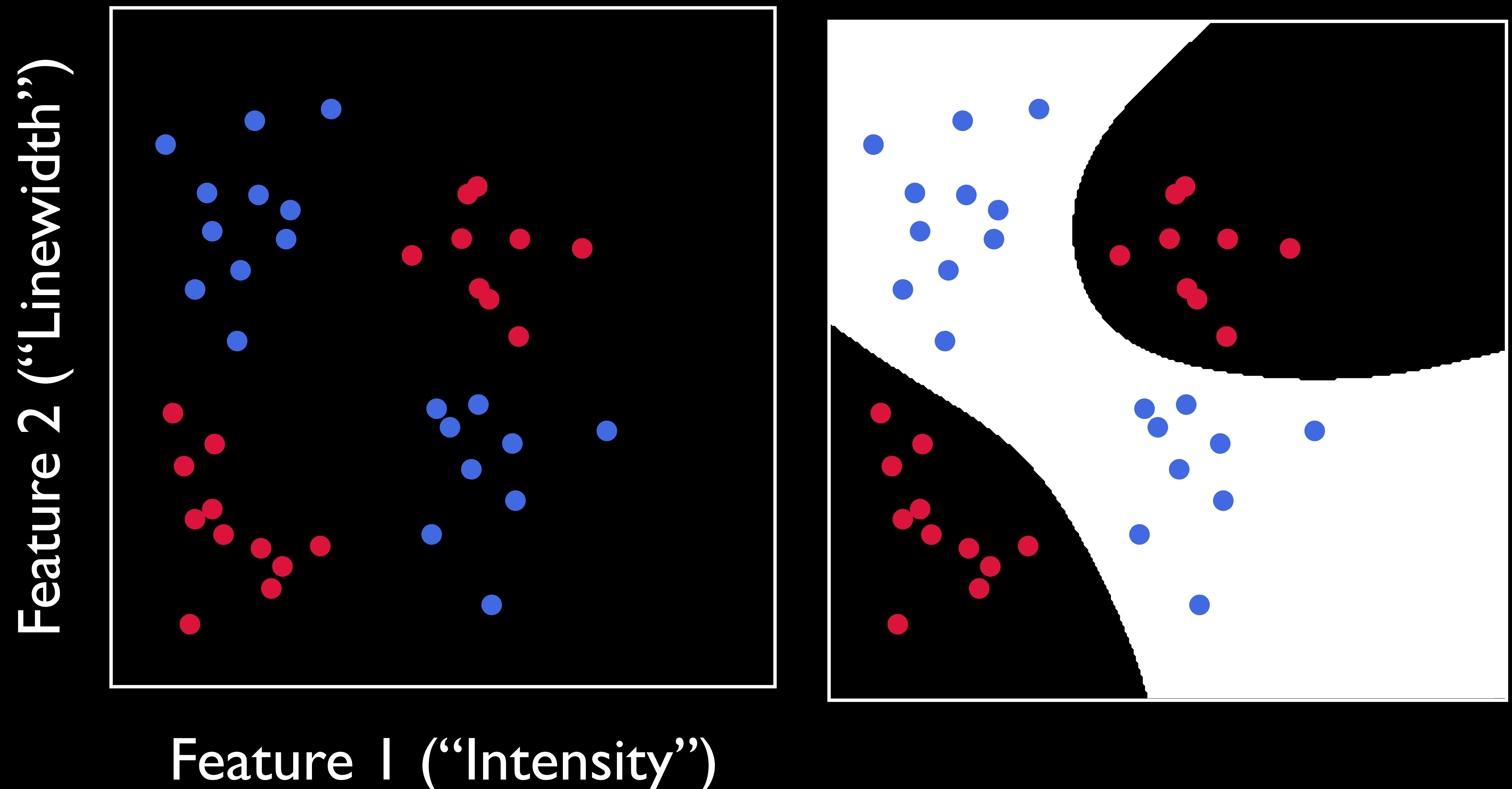

# Training Set

Slice


Cloud

Supernova

(regions defined via rectangles and contours)

Classification

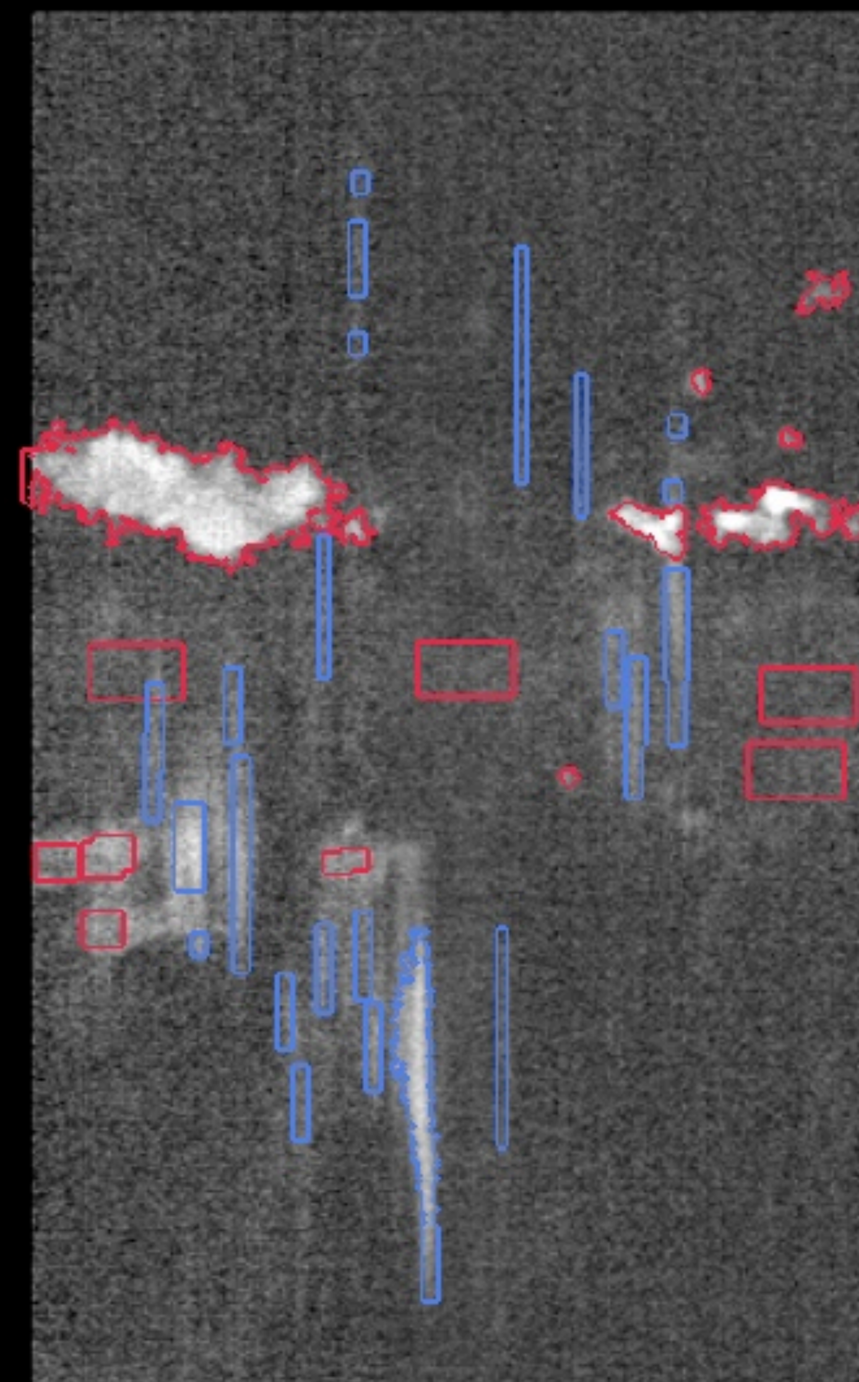

# Results

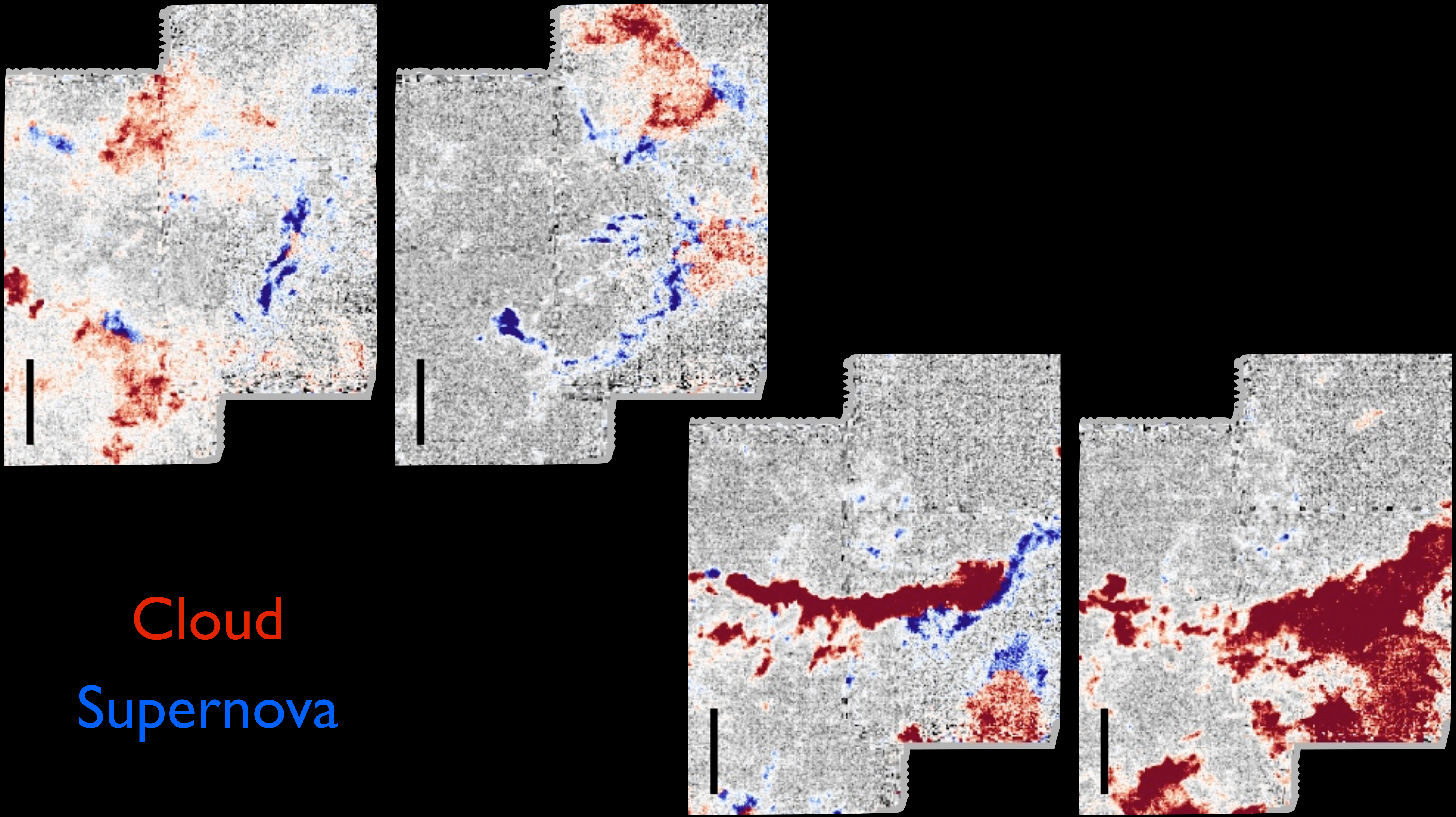

Cloud
Supernova

# Results

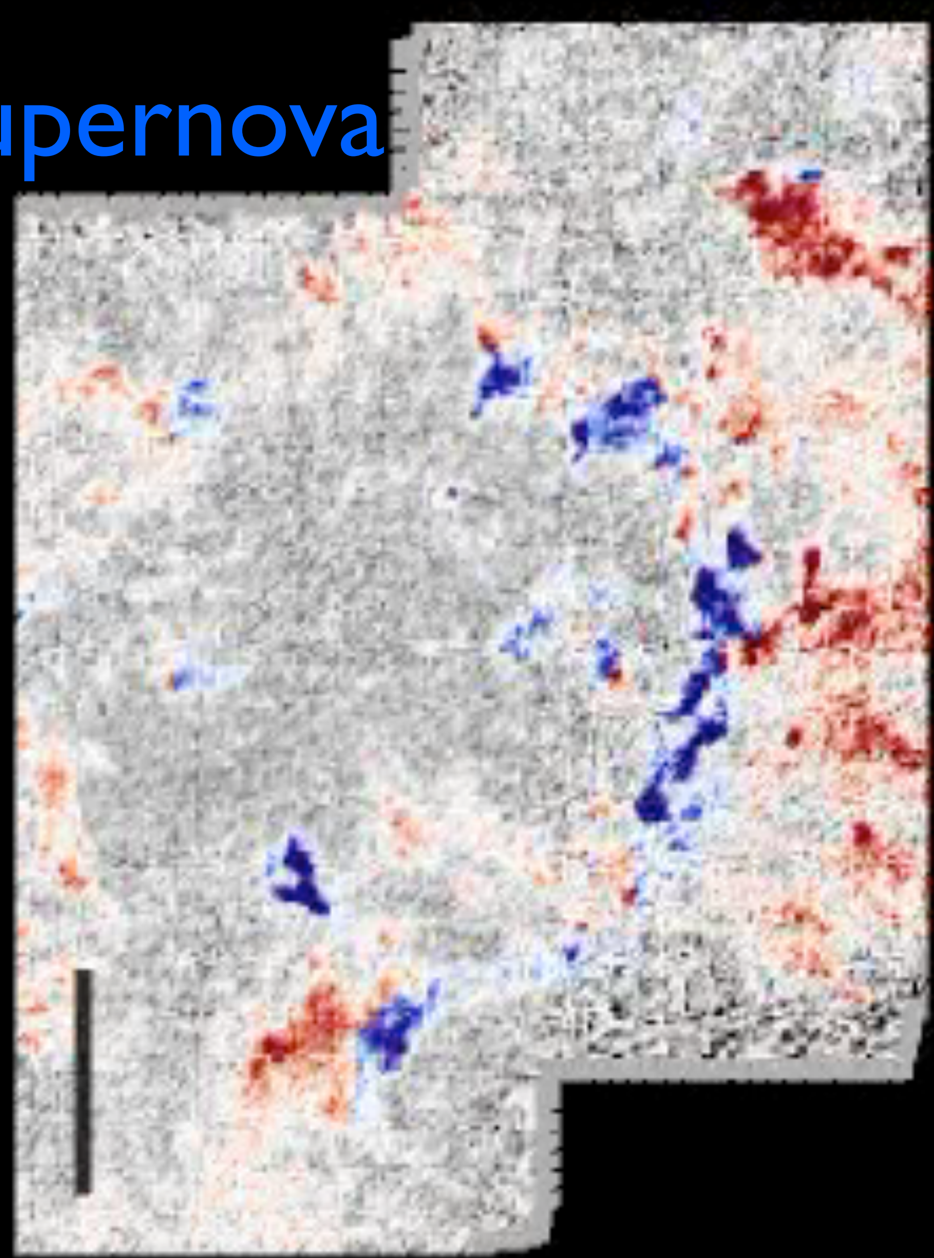
Cloud
Supernova

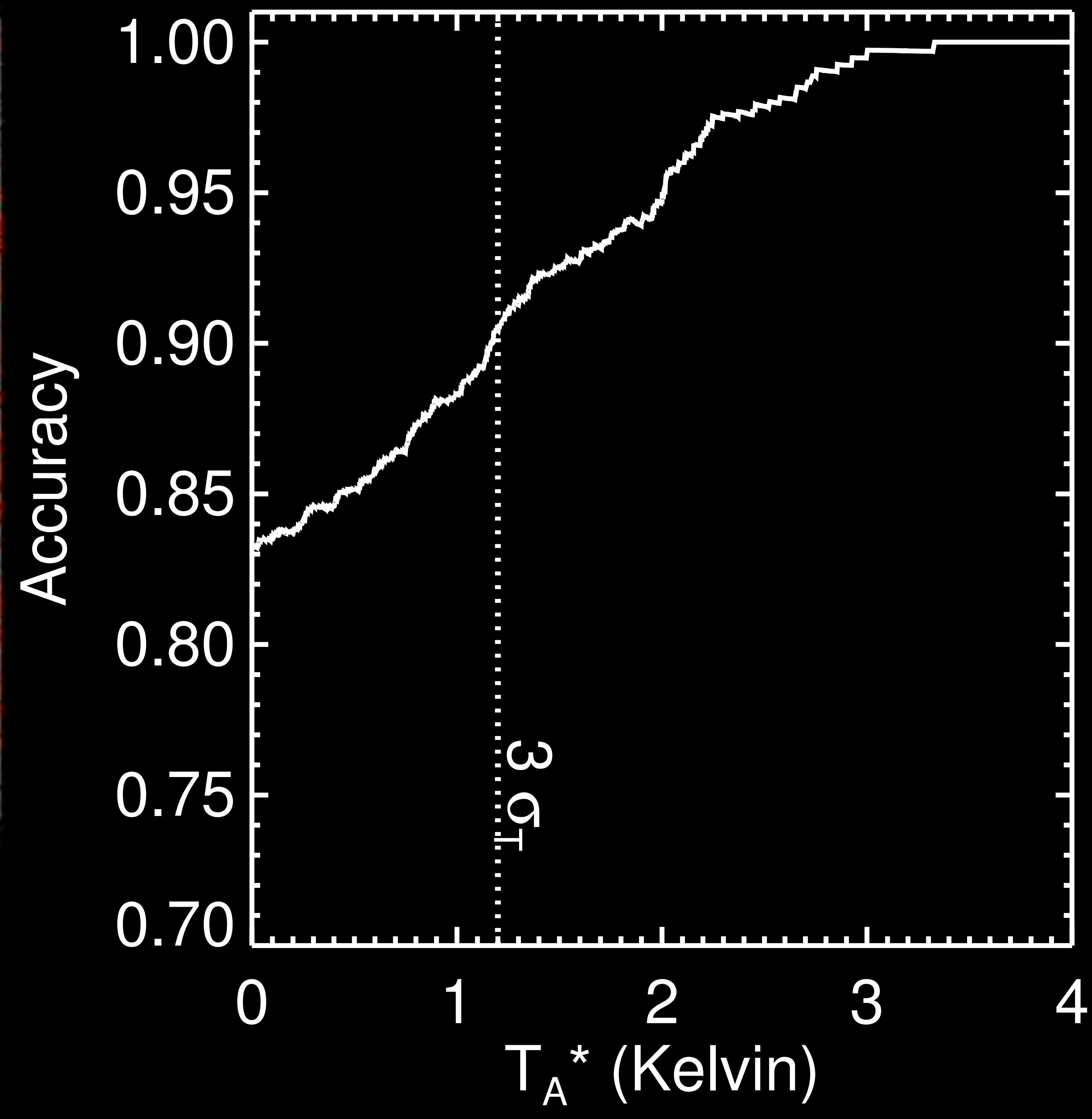
1.00
0.95
0.90
0.85
0.80
0.75
0.70
Accuracy
3 σ_T
0
1
2
3
4
T_A* (Kelvin)

# Linked Dendrogram Views in IDL (I)

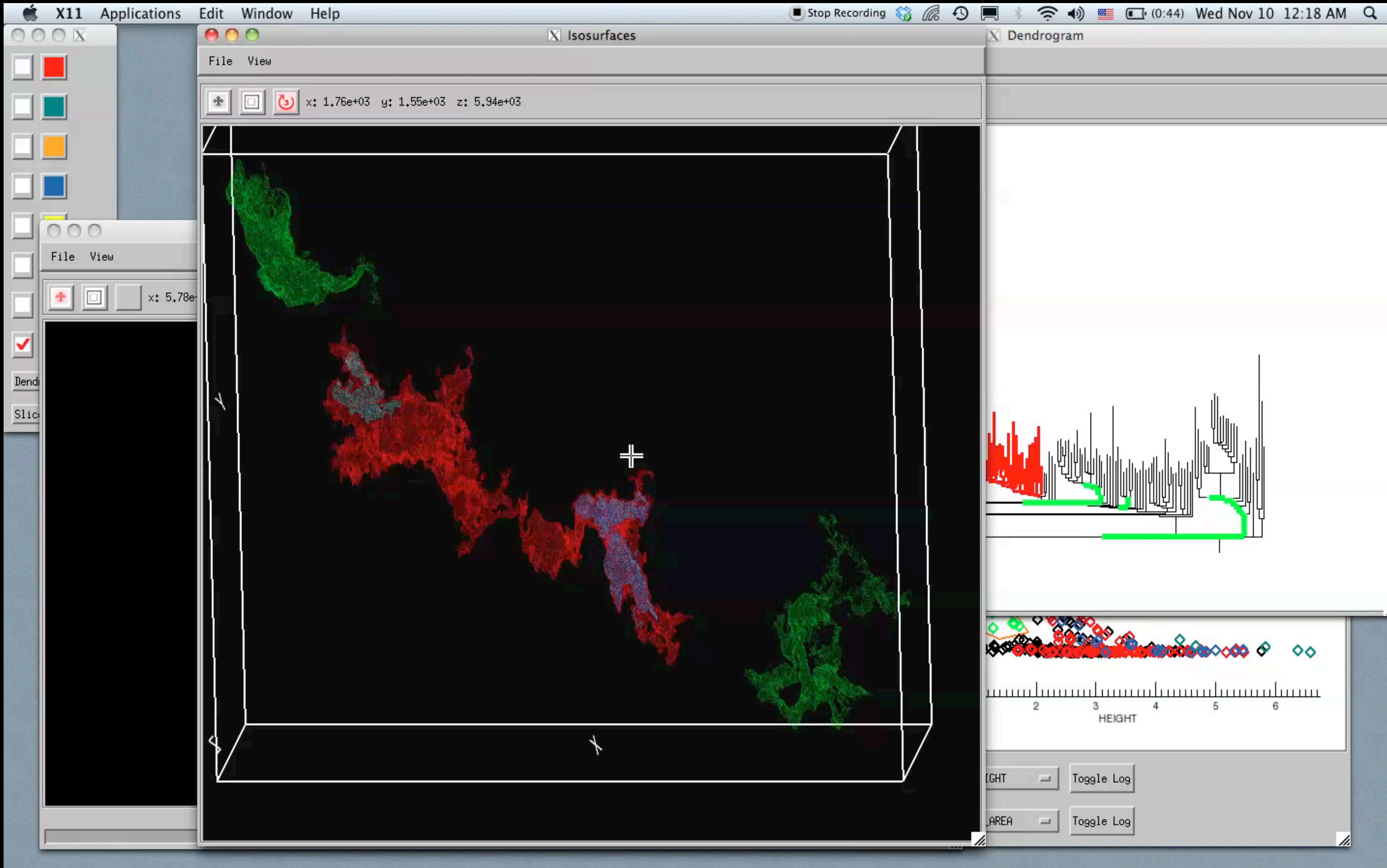


*Video & implementation: Christopher Beaumont, CfA/UHawaii;*
*inspired by AstroMed work of Douglas Alan, Michelle Borkin, AG, Michael Halle, Erik Rosolowsky*

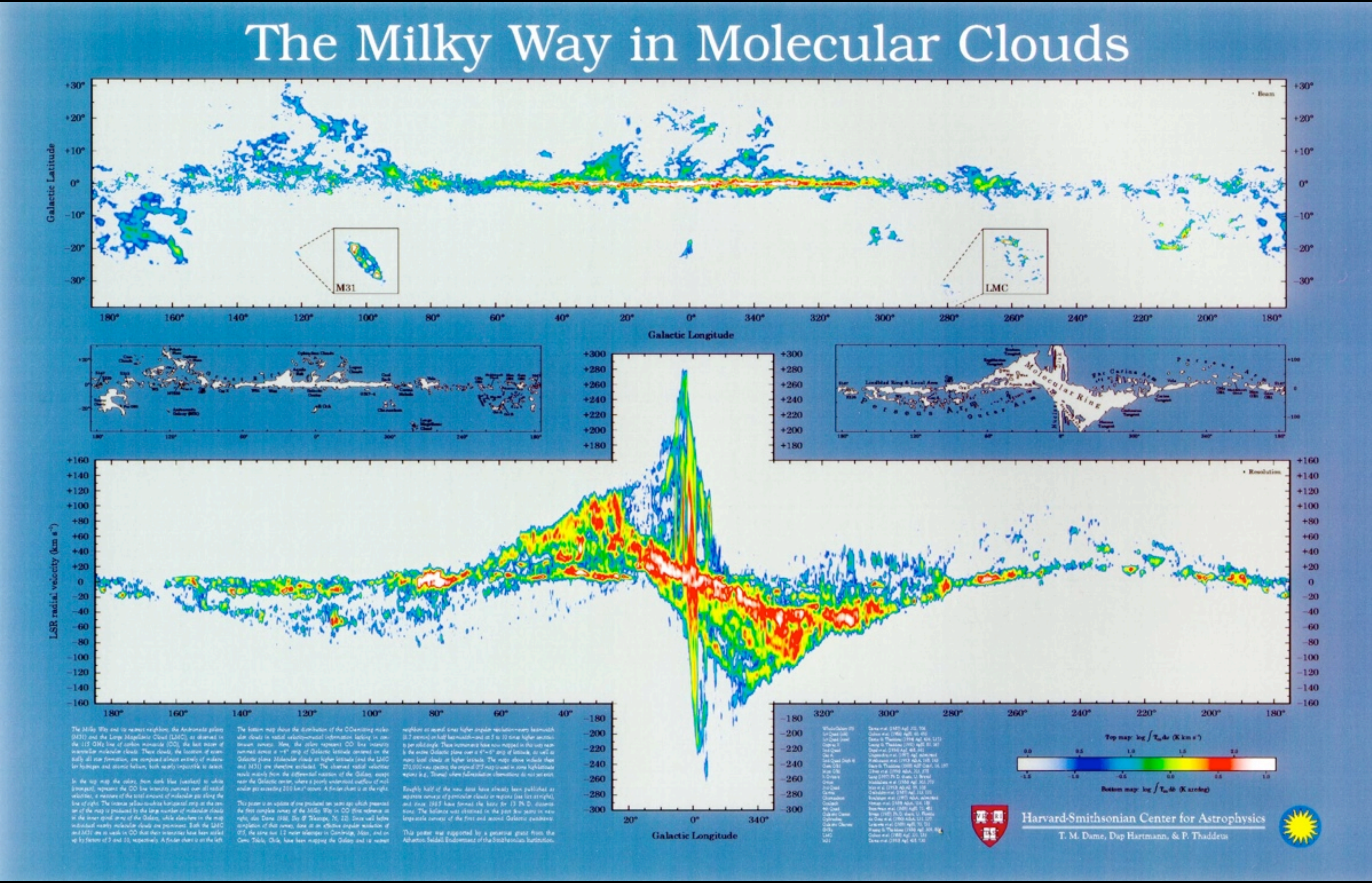


Dame et al. 2001 1.3-m "Mini" Telescope Survey of the Milky Way in CO

# Hot off the Press

## Nearby Star Forming Regions in The Milky Way

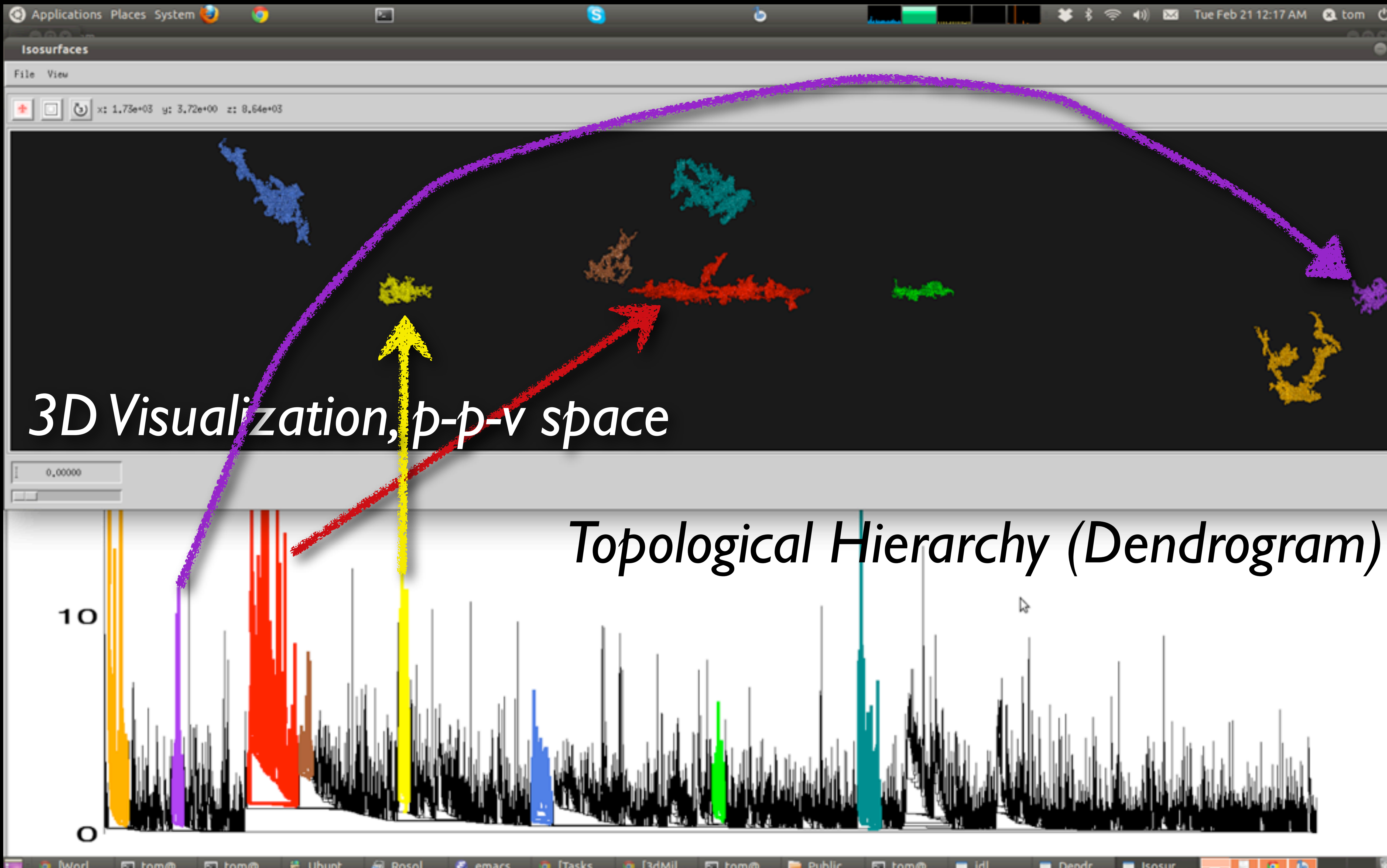


2012 Senior thesis of Tom Rice, Harvard, in collaboration with AG, Chris Beaumont & Tom Dame
(data from Dame et al. 2001 1.3-m "Mini" Telescope Survey of the Milky Way in CO)

# Large (100 pc) Scales:
# Does Gravity *Define* GMCs?

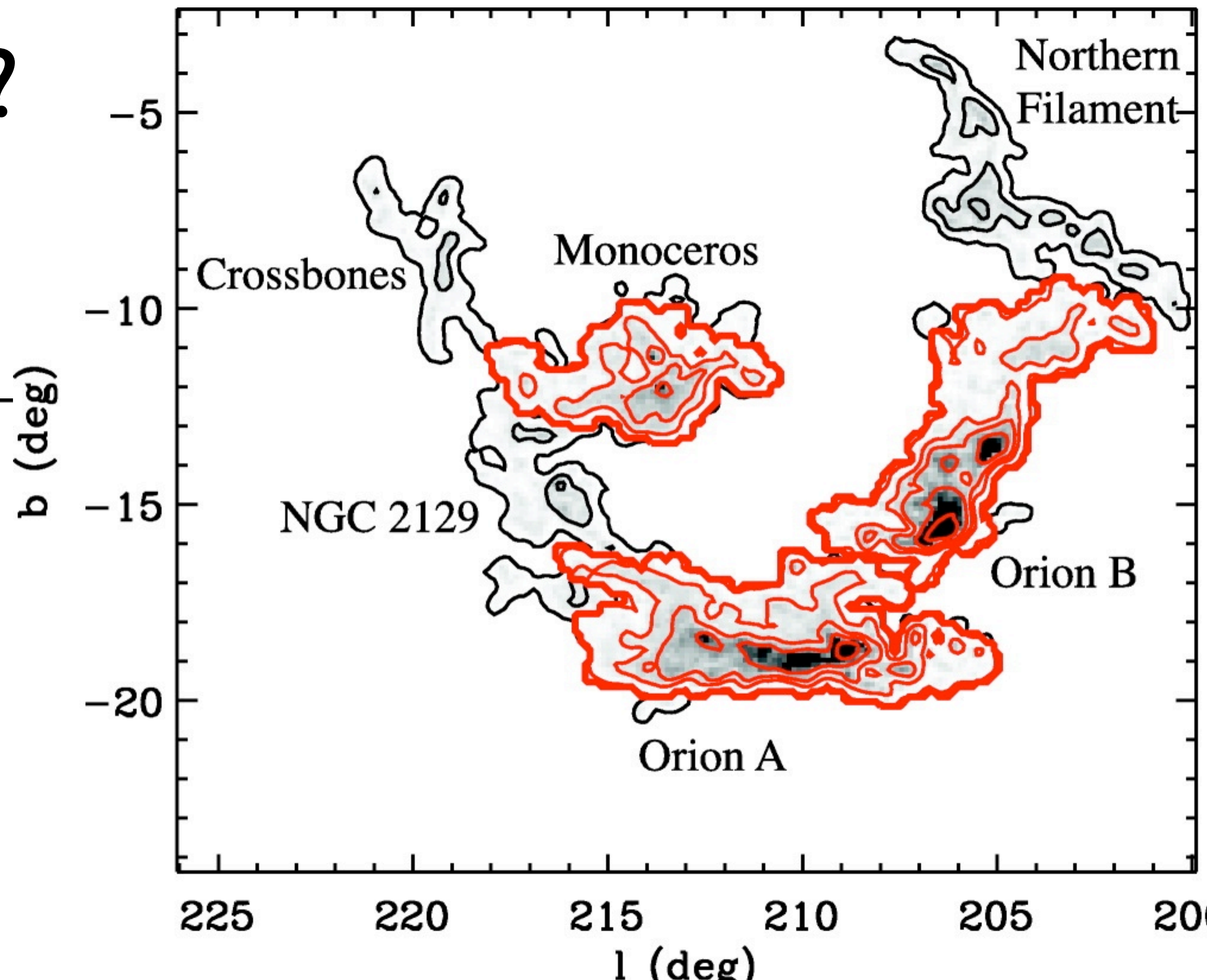


*"Dendrogram" of Orion*

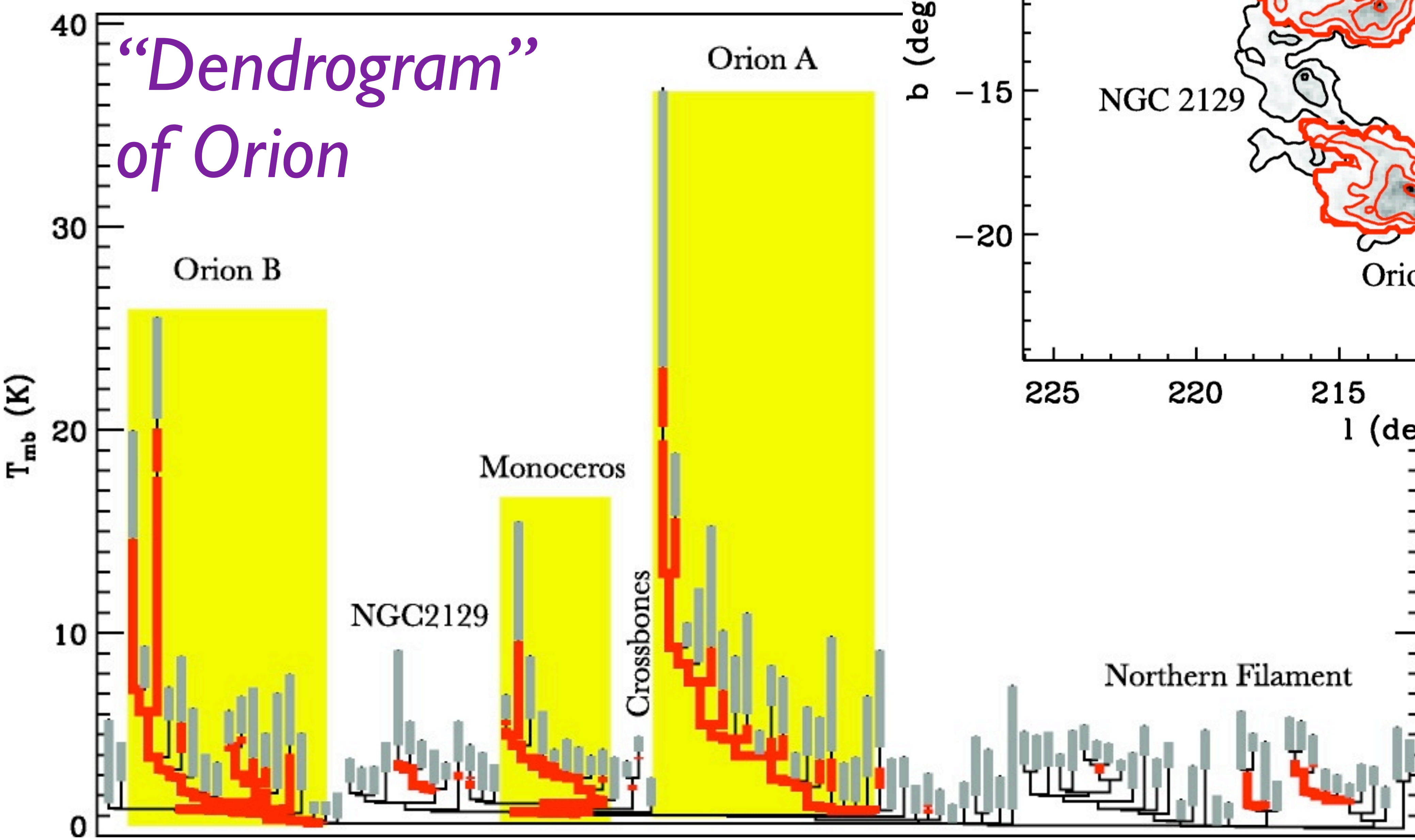


*Figures from Rosolowsky et al. 2008*

# The dream scenario...

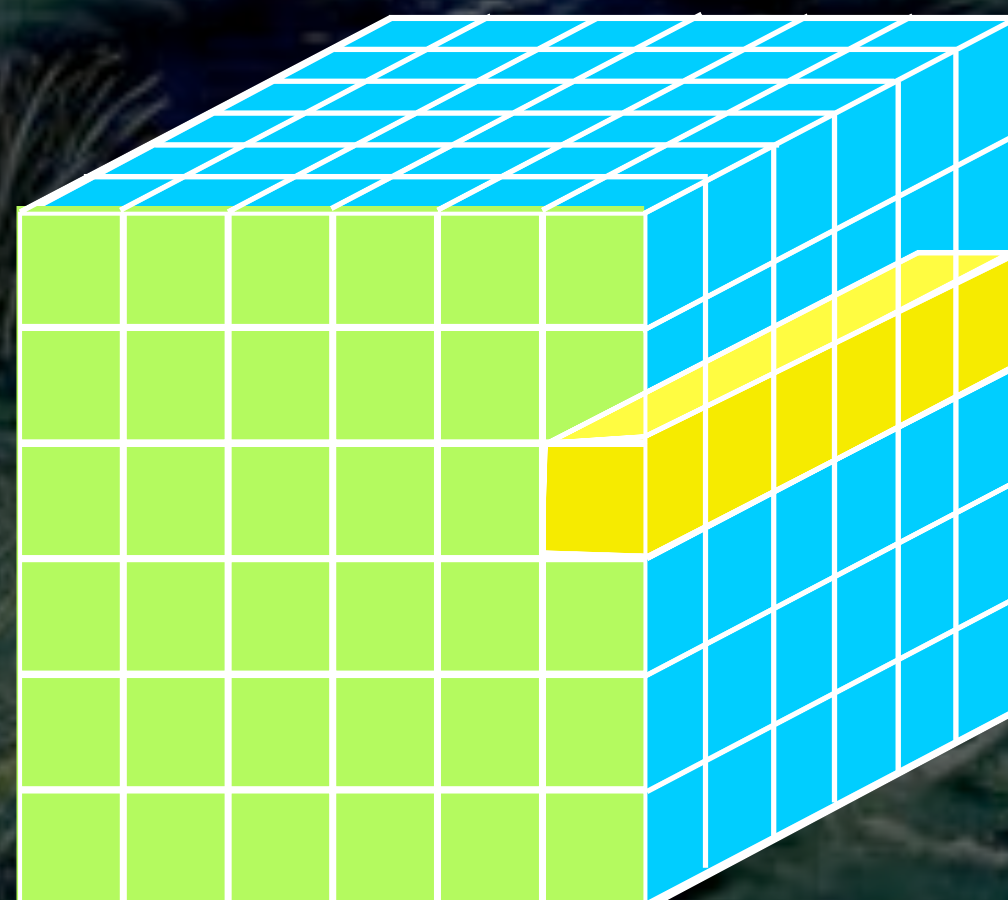

# "Astronomers" Saving Lives?

# "Astronomers" Saving Lives?


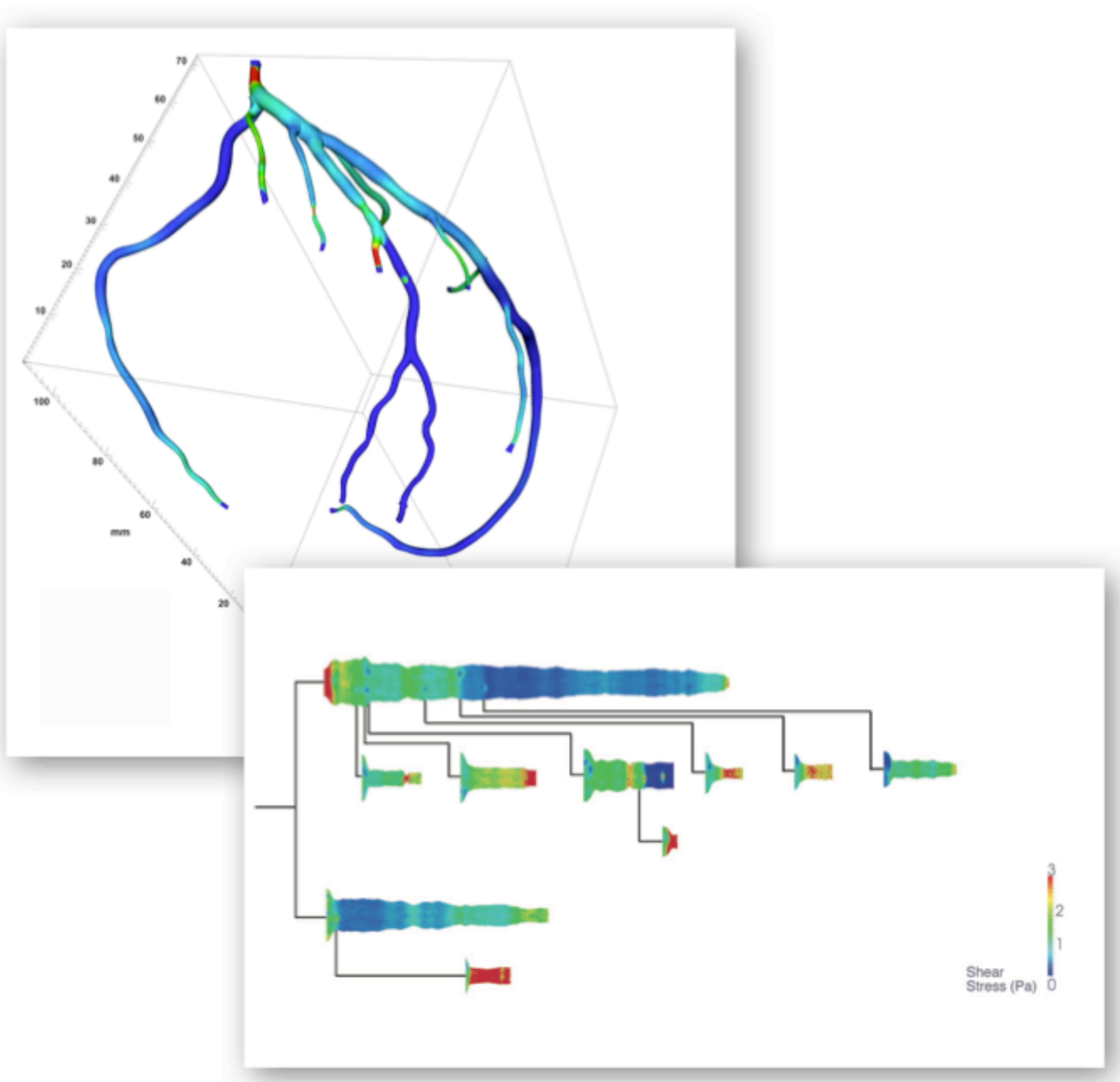


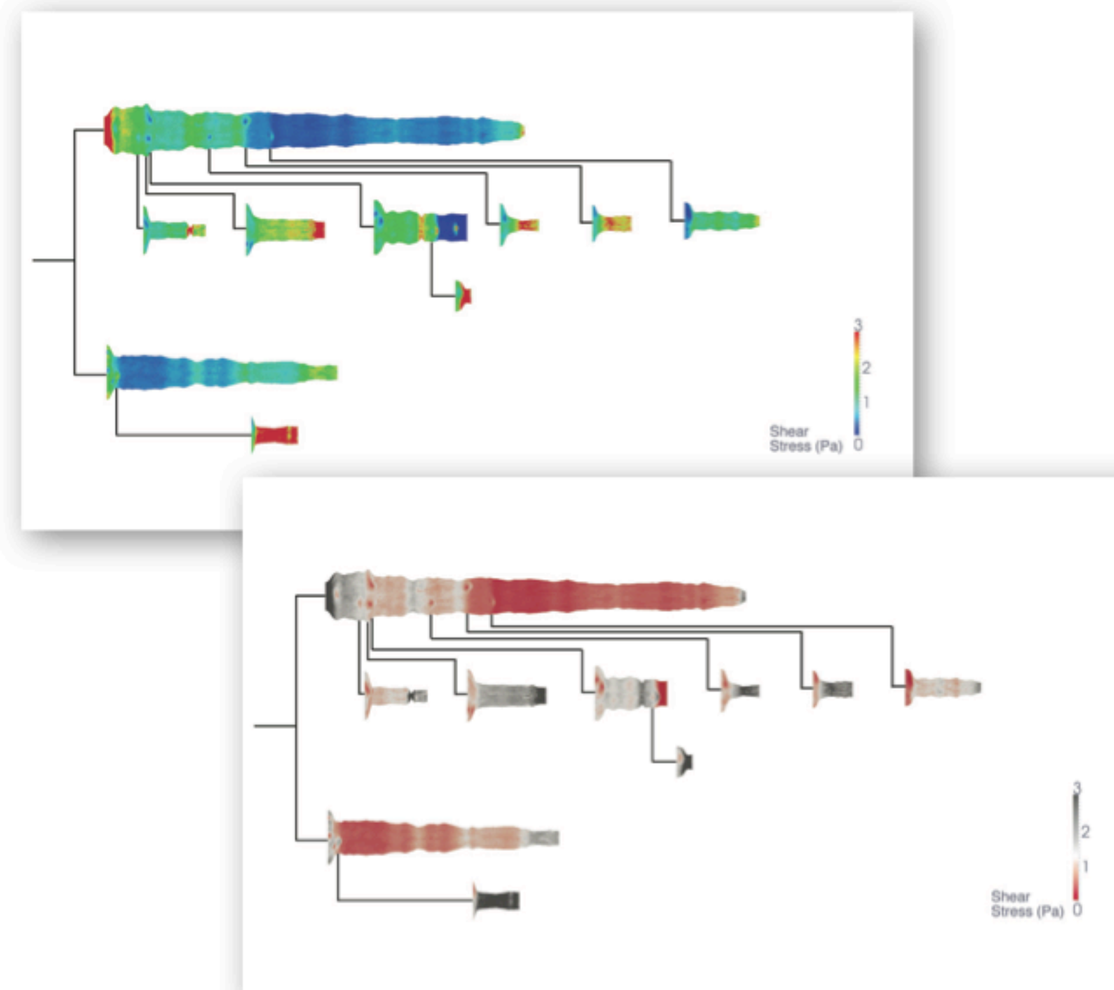


*The Future of "Astronomical Medicine"...*

# Watching Stars Form

*(or "The Importance of p-p-v Data and Linked Views in Understanding Star Formation")*

Alyssa A. Goodman
*Harvard-Smithsonian Center for Astrophysics*

*Modern Hydrodynamic AMR Simulation, (B=0), courtesy Stella Offner*

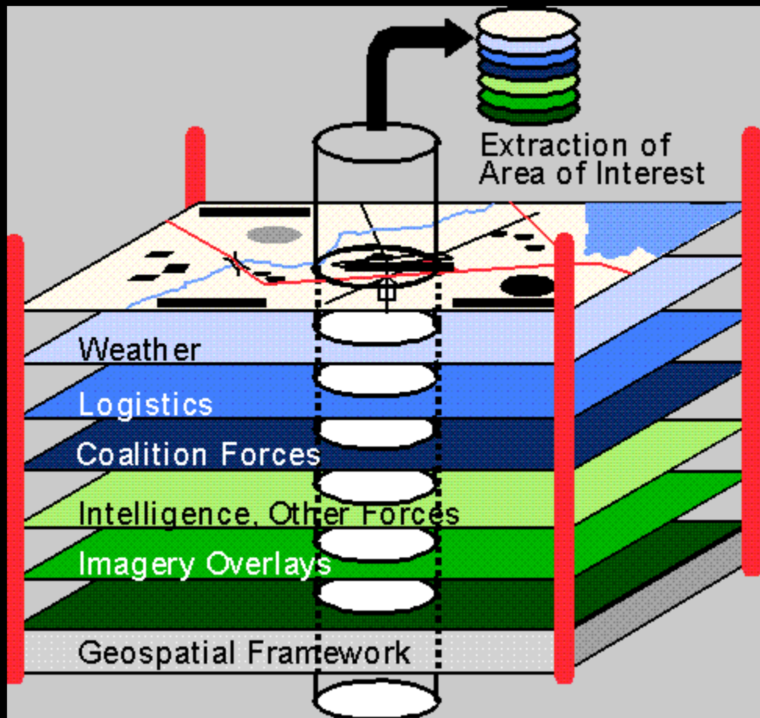


# COMPLETE


## COMPLETE Data Available

Center on Perseus | Center on Ophiuchus | Center on Serpens

**Full-Cloud Data (Phase I, All Data Available)**

| Dataset | Show | Perseus | Ophiuchus | Serpens | Link |
|---|---|---|---|---|---|
| GBT: HI Data Cube | ☑ | √ | √ | Ø | Data |
| IRAS: Av/Temp Maps | ☑ | √ | √ | √ | Data |
| FCRAO: 12CO | ☑ | √ | √ | √ | Data |
| FCRAO: 13CO | | √ | √ | √ | Data |
| JCMT: 850 microns | ☑ | √ | √ | Ø | Data |
| Spitzer c2d: IRAC 1,3 (3.6,5.8 μm) | ☑ | √ | √ | √ | Data |
| Spitzer c2d: IRAC 2,4 (4.5,8 μm) | ☑ | √ | √ | √ | Data |
| CSO/Bolocam: 1.2-mm | ☑ | √ | Ø | Ø | Data |
| Spitzer MIPS: Derived Dust Map | ☑ | √ | Ø | Ø | Data |
| **Targeted Regions (Phase II, Some Data Not Yet Available)** | | | | | |
| CTIO/Calar Alto: NIR (J,H,Ks) | ☑ | √ | √ | Ø | Data |
| IRAM 30-m: N2H+ and C18O | ☑ | √ | Ø | Ø | Data |
| IRAM 30-m: 1.1-mm continuum | ☑ | √ | Ø | Ø | Data |
| Megacam/MMT: r,i,z images | ☑ | √ | Ø | Ø | Data |
| **Catalogs & Pointed Surveys** | | | | | |
| NH3 Pointed Survey | ☐ | √ | Ø | Ø | Data |
| YSO Candidate list (c2d) | ☐ | √ | √ | √ | Data |

# Seamless Astronomy

*Alberto Accomazzi, Doug Burke, Alberto Conti, Carol Christian, Mercé Crosas, Raffaele D'Abrusco, Rahul Davé, Christopher Erdmann, Jonathan Fay, Jay Luker, Alyssa Goodman, Michael Kurtz, Gus Muench, Alberto Pepe, Curtis Wong*

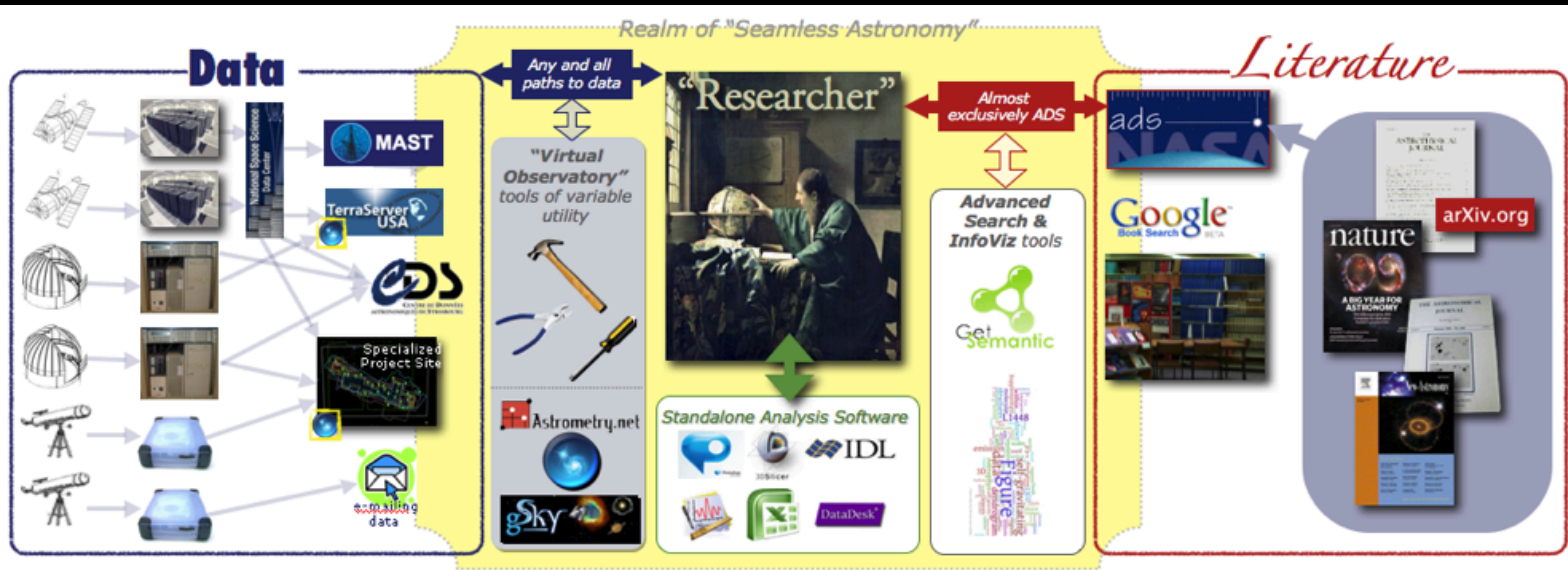

# Microsoft® Research WorldWide Telescope

*Experience WWT at* **worldwidetelescope.org**

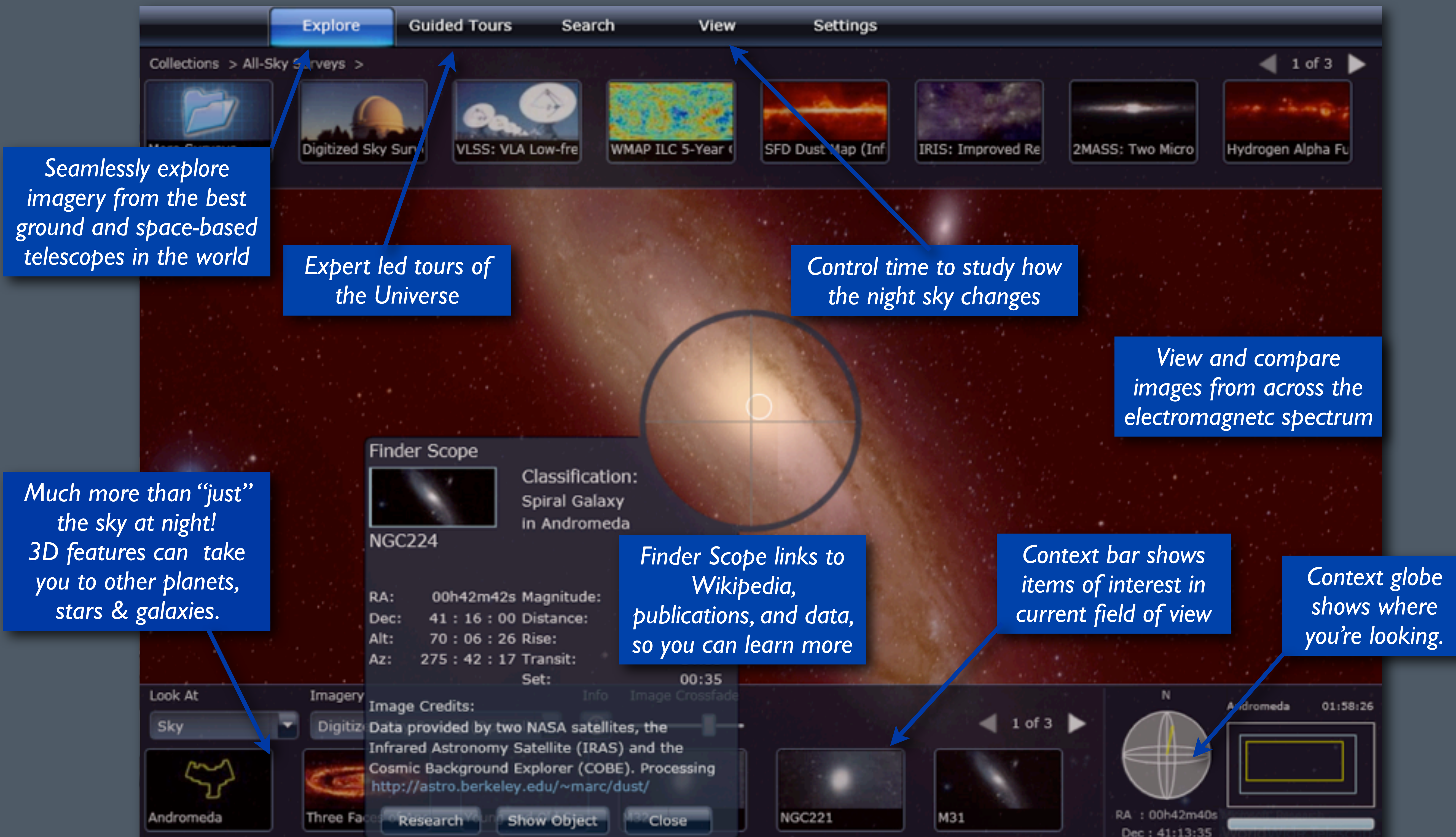

# The dream scenario...

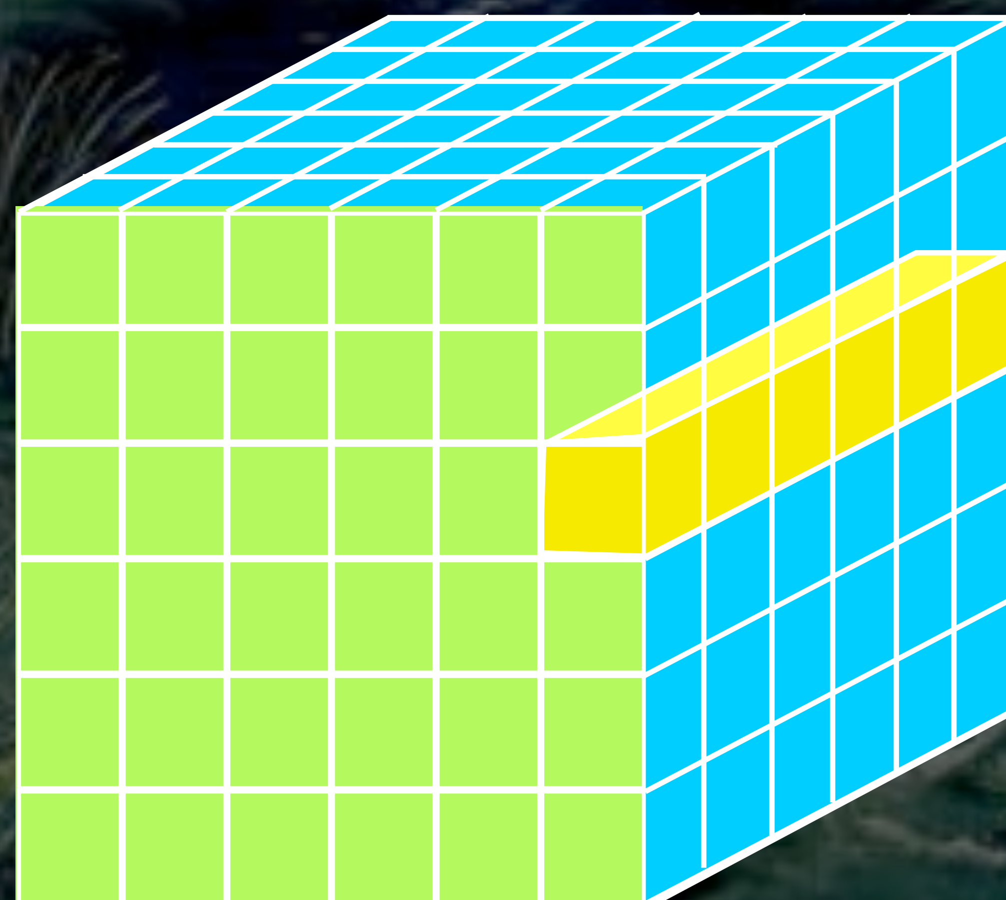

# Challenge #1: 3D Selection

Wh

How

How on?

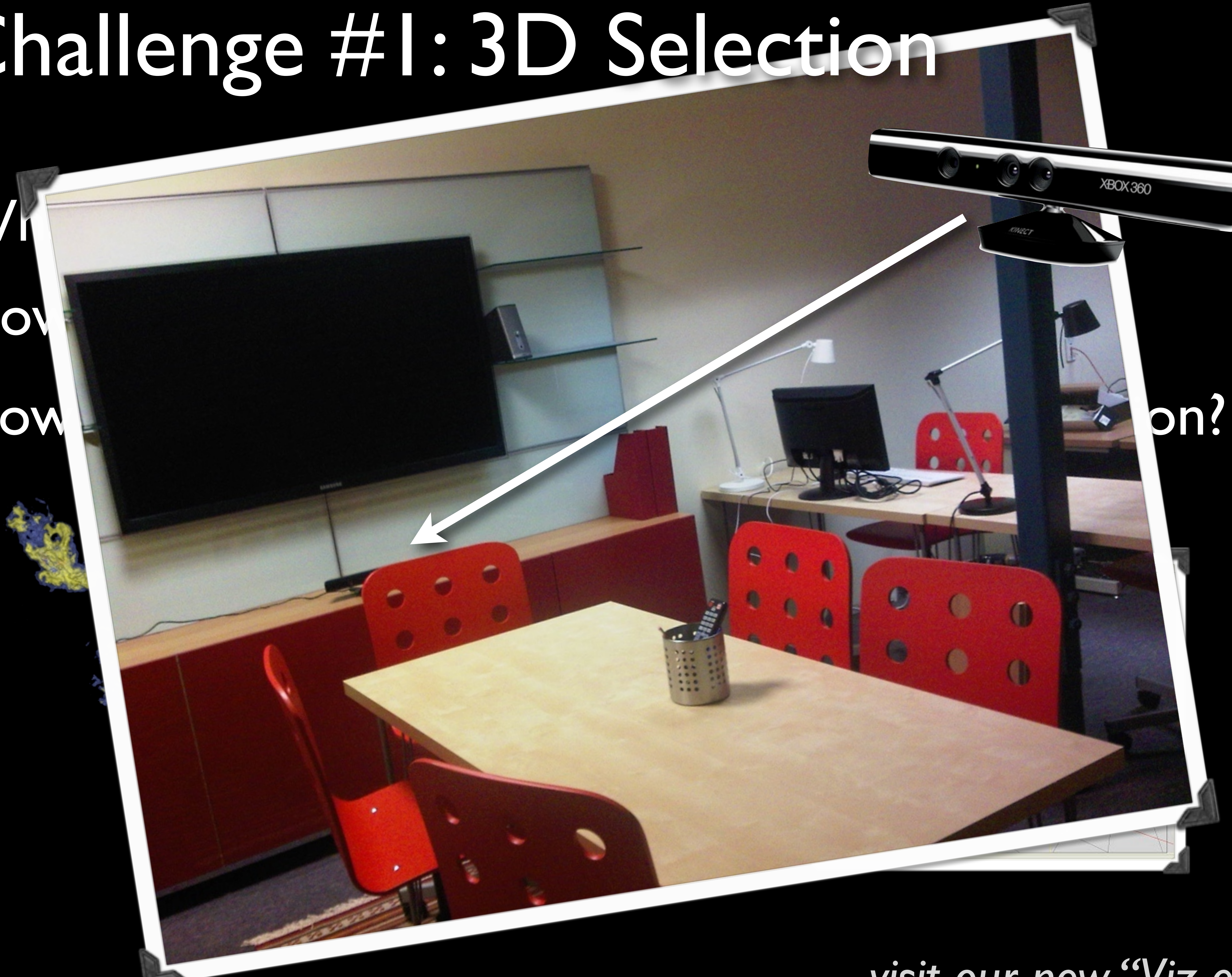


*visit our new "Viz-e-Lab"!*

# Challenge #2: Too many windows...

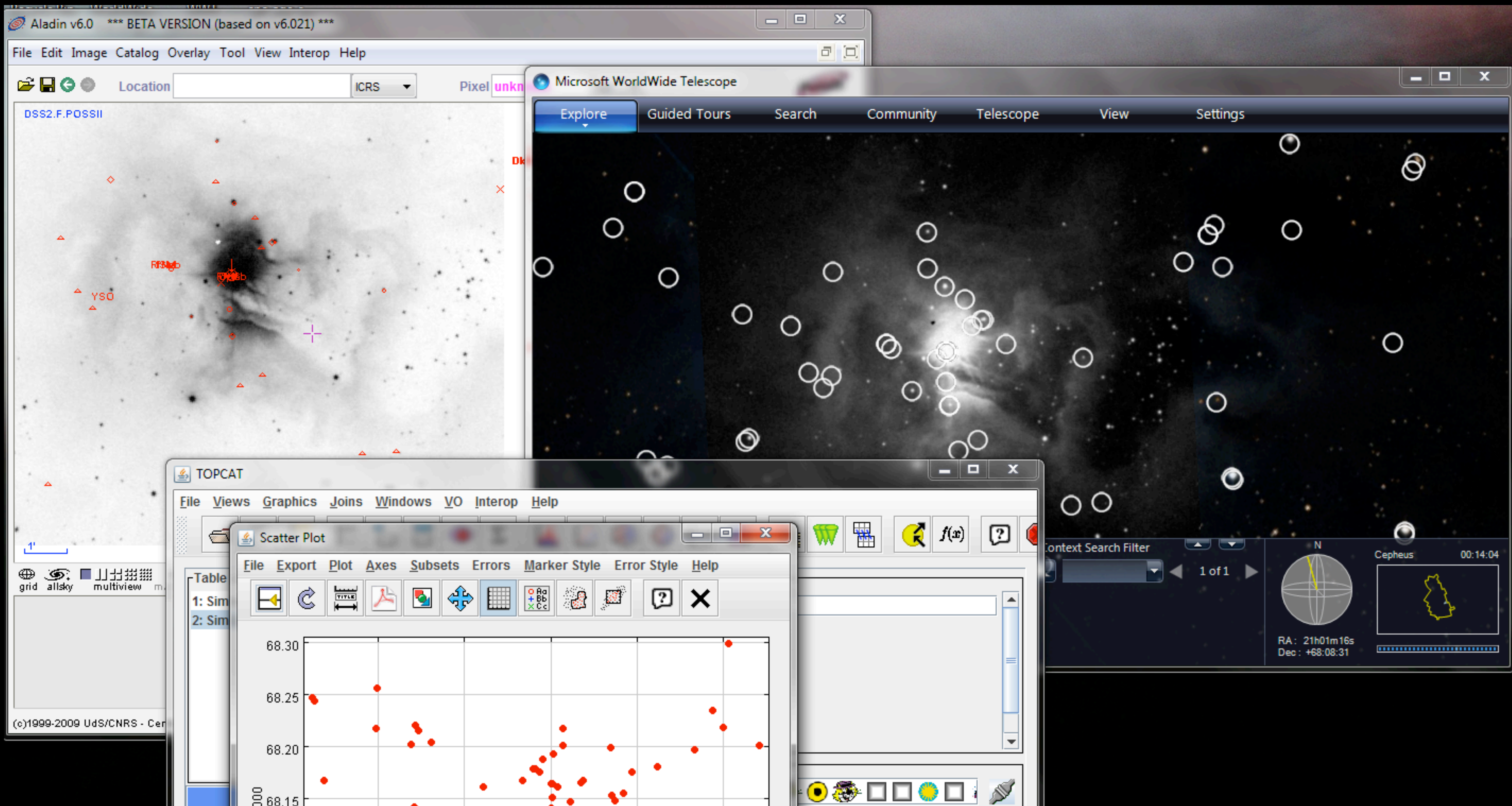

# Challenge #3:

## What does “Publication-Quality” Graphics Mean in an Interactive 3D World?

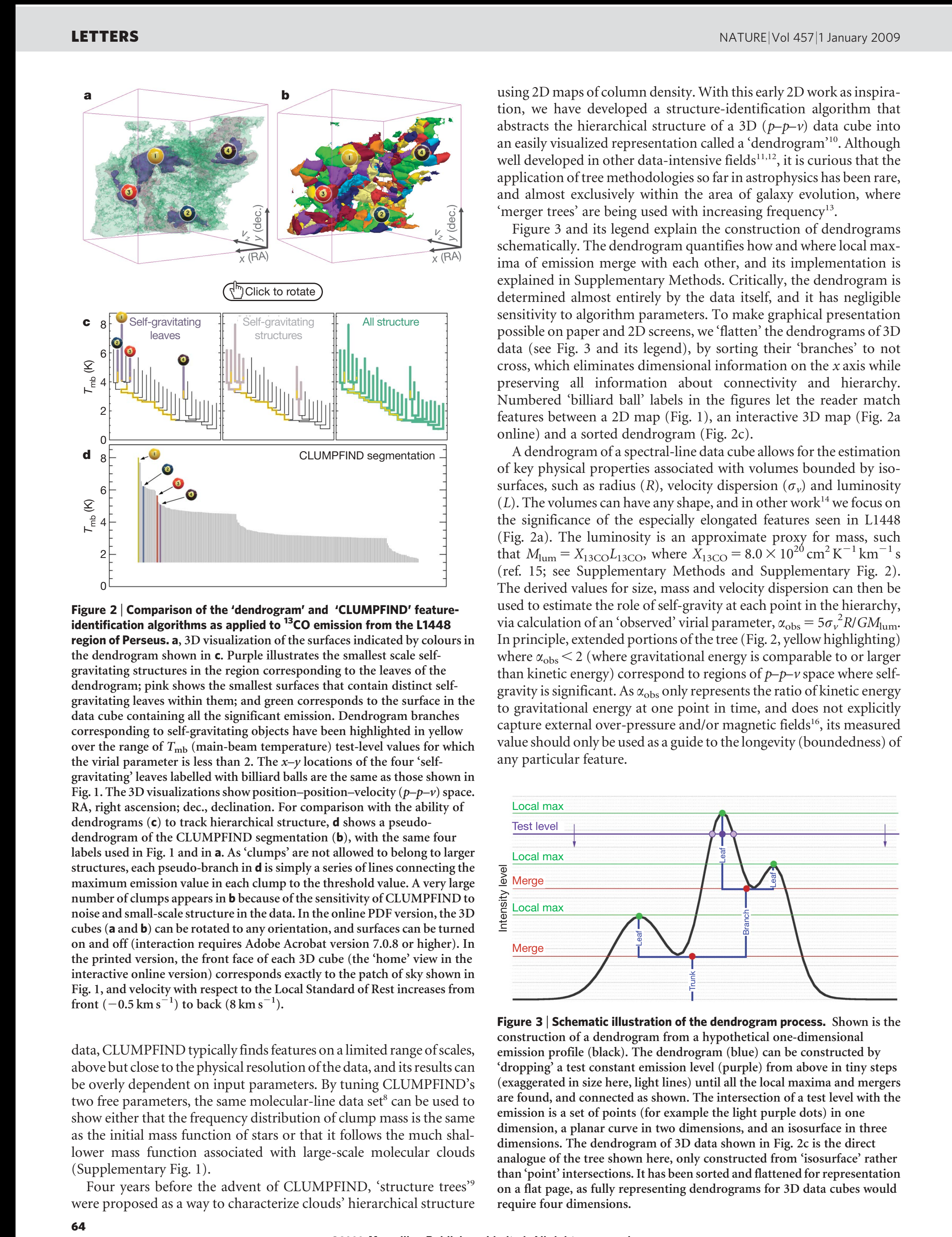




**Figure 2 | Comparison of the ‘dendrogram’ and ‘CLUMPFIND’ feature-identification algorithms as applied to $^{13}CO$ emission from the L1448 region of Perseus. a**, 3D visualization of the surfaces indicated by colours in the dendrogram shown in **c**. Purple illustrates the smallest scale self-gravitating structures in the region corresponding to the leaves of the dendrogram; pink shows the smallest surfaces that contain distinct self-gravitating leaves within them; and green corresponds to the surface in the data cube containing all the significant emission. Dendrogram branches corresponding to self-gravitating objects have been highlighted in yellow over the range of $T_{mb}$ (main-beam temperature) test-level values for which the virial parameter is less than 2. The $x$–$y$ locations of the four ‘self-gravitating’ leaves labelled with billiard balls are the same as those shown in Fig. 1. The 3D visualizations show position–position–velocity ($p$–$p$–$v$) space. RA, right ascension; dec., declination. For comparison with the ability of dendrograms (**c**) to track hierarchical structure, **d** shows a pseudo-dendrogram of the CLUMPFIND segmentation (**b**), with the same four labels used in Fig. 1 and in **a**. As ‘clumps’ are not allowed to belong to larger structures, each pseudo-branch in **d** is simply a series of lines connecting the maximum emission value in each clump to the threshold value. A very large number of clumps appears in **b** because of the sensitivity of CLUMPFIND to noise and small-scale structure in the data. In the online PDF version, the 3D cubes (**a** and **b**) can be rotated to any orientation, and surfaces can be turned on and off (interaction requires Adobe Acrobat version 7.0.8 or higher). In the printed version, the front face of each 3D cube (the ‘home’ view in the interactive online version) corresponds exactly to the patch of sky shown in Fig. 1, and velocity with respect to the Local Standard of Rest increases from front ($-0.5\,km\,s^{-1}$) to back ($8\,km\,s^{-1}$).

data, CLUMPFIND typically finds features on a limited range of scales, above but close to the physical resolution of the data, and its results can be overly dependent on input parameters. By tuning CLUMPFIND’s two free parameters, the same molecular-line data set[8] can be used to show either that the frequency distribution of clump mass is the same as the initial mass function of stars or that it follows the much shallower mass function associated with large-scale molecular clouds (Supplementary Fig. 1).

Four years before the advent of CLUMPFIND, ‘structure trees’[9] were proposed as a way to characterize clouds’ hierarchical structure using 2D maps of column density. With this early 2D work as inspiration, we have developed a structure-identification algorithm that abstracts the hierarchical structure of a 3D ($p$–$p$–$v$) data cube into an easily visualized representation called a ‘dendrogram’[10]. Although well developed in other data-intensive fields[11,12], it is curious that the application of tree methodologies so far in astrophysics has been rare, and almost exclusively within the area of galaxy evolution, where ‘merger trees’ are being used with increasing frequency[13].

Figure 3 and its legend explain the construction of dendrograms schematically. The dendrogram quantifies how and where local maxima of emission merge with each other, and its implementation is explained in Supplementary Methods. Critically, the dendrogram is determined almost entirely by the data itself, and it has negligible sensitivity to algorithm parameters. To make graphical presentation possible on paper and 2D screens, we ‘flatten’ the dendrograms of 3D data (see Fig. 3 and its legend), by sorting their ‘branches’ to not cross, which eliminates dimensional information on the $x$ axis while preserving all information about connectivity and hierarchy. Numbered ‘billiard ball’ labels in the figures let the reader match features between a 2D map (Fig. 1), an interactive 3D map (Fig. 2a online) and a sorted dendrogram (Fig. 2c).

A dendrogram of a spectral-line data cube allows for the estimation of key physical properties associated with volumes bounded by isosurfaces, such as radius ($R$), velocity dispersion ($\sigma_v$) and luminosity ($L$). The volumes can have any shape, and in other work[14] we focus on the significance of the especially elongated features seen in L1448 (Fig. 2a). The luminosity is an approximate proxy for mass, such that $M_{lum} = X_{13CO} L_{13CO}$, where $X_{13CO} = 8.0 \times 10^{20}\,cm^2\,K^{-1}\,km^{-1}\,s$ (ref. 15; see Supplementary Methods and Supplementary Fig. 2). The derived values for size, mass and velocity dispersion can then be used to estimate the role of self-gravity at each point in the hierarchy, via calculation of an ‘observed’ virial parameter, $\alpha_{obs} = 5\sigma_v^2 R/GM_{lum}$. In principle, extended portions of the tree (Fig. 2, yellow highlighting) where $\alpha_{obs} < 2$ (where gravitational energy is comparable to or larger than kinetic energy) correspond to regions of $p$–$p$–$v$ space where self-gravity is significant. As $\alpha_{obs}$ only represents the ratio of kinetic energy to gravitational energy at one point in time, and does not explicitly capture external over-pressure and/or magnetic fields[16], its measured value should only be used as a guide to the longevity (boundedness) of any particular feature.



**Figure 3 | Schematic illustration of the dendrogram process.** Shown is the construction of a dendrogram from a hypothetical one-dimensional emission profile (black). The dendrogram (blue) can be constructed by ‘dropping’ a test constant emission level (purple) from above in tiny steps (exaggerated in size here, light lines) until all the local maxima and mergers are found, and connected as shown. The intersection of a test level with the emission is a set of points (for example the light purple dots) in one dimension, a planar curve in two dimensions, and an isosurface in three dimensions. The dendrogram of 3D data shown in Fig. 2c is the direct analogue of the tree shown here, only constructed from ‘isosurface’ rather than ‘point’ intersections. It has been sorted and flattened for representation on a flat page, as fully representing dendrograms for 3D data cubes would require four dimensions.




*Goodman, Rosolowsky, Borkin, Foster, Halle, Kauffmann & Pineda, **Nature**, 2009*

# Linked Dendrogram Views in IDL (2)

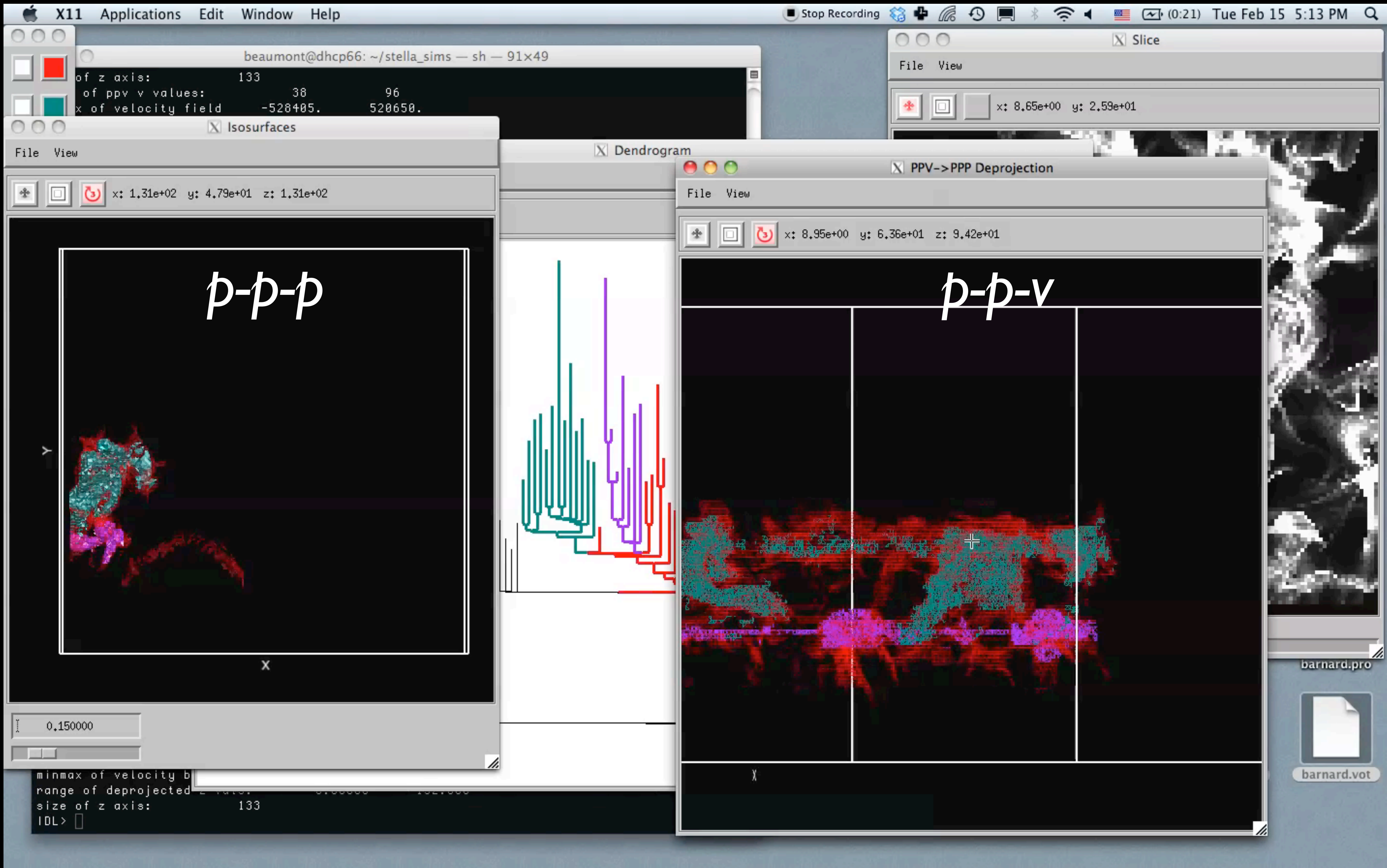


Monday, March 12, 2012

# Linked Dendrogram Views in IDL (3)